LUNDS UNIVERSITET
Lunds Tekniska Högskola

Technische Universität München

Master Thesis

Enzyme engineering of a haloacid dehalogenase-like phosphatase from *Thermotoga neopolitana* for optimization of substrate specificity

Submitted to

Lund University
Faculty of Engineering
Division of Biotechnology

and

Prof. Dr. Volker Sieber
Technische Universität München
Lehrstuhl für Chemie Biogener Rohstoffe

Presented by
Samuel Sutiono
19911006-7759

Lund, May 2016

Performed at:
Technische Universität München, Lehrstuhl für Chemie Biogener Rohstoffe
Wissenschaftszentrum Straubing, Straubing, Germany

Supervised by:
Prof. Dr. Volker Sieber
Technische Universität München
Lehrstuhl für Chemie Biogener Rohstoffe

Co-supervised by:
Dr. Javier A Linares-Pastén
Assistant Lecturer
Lund University
Division of Biotechnology

André Pick, Dipl. Biologie
PhD Student
Technische Universität München
Lehrstuhl für Chemie Biogener Rohstoffe

Examined by:
Prof. Patrick Adlercreutz
Lund University
Division of Biotechnology

Declaration of originality

I hereby declare that this master thesis project was entirely and solely my own independent work and any direct or indirect aids have been faithfully acknowledged. I have also read Lund University policy of plagiarism and fully aware of the consequences of noncompliance.

Lund, May 2016

Place and Date of Submission

Samuel Sutiono

Abstract

Haloacid dehalogenase (HAD)-like hydrolases represent a vast superfamily characterised by their ability to form covalent enzyme-substrate intermediates facilitating the cleavage of C-Cl, C-P, or CO-P bonds. Within this work one member of this superfamily, HAD from *Thermotoga neopolitana* (HADTn) exhibiting a phosphatase (P-O bond cleavage) like activity was investigated in the context of altering the substrate specificity. The enzyme shows different affinities for sugar phosphates, e.g. fructose-6-phosphate (F6P) and glucose-6-phosphate (G6P) at high temperatures, which is of great interest for industrial applications. In this study, HADTn was engineered using semi rational site saturation mutagenesis to increase its specificity toward F6P for use in enzymatic cascade reactions. At first, several mutants were generated to deduce the role of different amino acids. Results suggested that serine at position 166 (S166) played an important role in catalysis, presumably in the positioning of Mg (II). Additionally, glutamic acid at position 47 (E47) was identified to influence substrate recognition. Based on these findings, degenerate primers using an NNK motif were designed to generate libraries for six different amino acid positions (Y19, M8, P46, E47, P110, R117) around the catalytic centre. High-throughput screening of the libraries with two different substrates (F6P and G6P) resulted in an improved variant that had a mutation at position 46 from proline to threonine (P46T). Further characterisation of HADTnP46T was performed for F6P and G6P with respect to the wild type and the results showed almost a two-fold increase in the ratio of the catalytic efficiency (k_{cat}/K_m). Moreover, thermal stability studies revealed that HADTnP46T had a half-life of 392 min at 94ºC; similar to that of the WT. Addition of Mg (II) doubled the half-life for both the enzymes. Fructose and glucose inhibited both enzymes via a noncompetitive mechanism. These findings support the already existing proposal of the presence of a probable fifth loop in the HAD family that plays a pivotal role in substrate specificity.

Keywords: Haloacid dehalogenase-like hydrolase, Enzyme engineering, Catalytic efficiency, Thermal stability, Inhibition

Sammanfattning

Hydrolaser av Haloacid dehalogenase (HAD)-typ utgör en omfattande superfamilj kännetecknad av deras förmåga att bilda kovalenta enzymsubstratsintermediärer som underlättar brytandet av C-Cl P-C eller P-O-bindningar. I detta arbete undersöktes vilken påverkan ett enzym i denna superfamilj, HAD från *Thermotoga neopolitana* (HADTn), har på substratspecificitet. Detta enzym uppvisar en fosfatas-liknande aktivitet och bryter med andra ord P-O-bindningar. Det har olika affinitet för olika sockerfosfater t.ex. fruktos-6-fosfat (F6P) och glukos-6-fosfat (G6P), vid höga temperaturer vilket är av stort intresse för industriella användningar. I studien konstruerades HADTn för att skifta dess specificitet mot F6P för användning i enzymatiska kaskadreaktioner, genom semirationella punktmättnads-mutationer. Först skapades ett flertal mutanter för att undersöka rollen hos olika aminosyror. Resultaten indikerade att serin på position 166 (S166) spelade en viktig roll i katalys, troligen vid positioneringen av Mg (II). Dessutom visades att glutaminsyra på position 47 (E47) påverkade igenkänning av substrat. Grundat på dessa upptäckter designades degenererade primrar, med hjälp av NNK-motif, för att skapa bibliotek för 6 olika aminosyrapositioner (Y19, M8, P46, E47, P110, R117) kring det katalytiska centrat. Högkapacitets-screening av biblioteken med två olika substrat (F6P och G6P) resulterade i en förbättrad variant med en mutation från prolin till treonin på position 46 (P46T). Ytterligare undersökning av HADTnP46T med avseende på F6P och G6P visade en nästan tvåfaldig ökning av det katalytiska effektsförhållandet (k_{cat}/K_m) jämfört med vildtypen. Dessutom visade studier av termisk stabilitet att halveringstiden för HADTnP46T var 392 min vid 94^{o}C, inte långt från vildtypens halveringstid. Addition av Mg (II) fördubblade halveringstiden för båda enzymerna. Fruktos och glukos inhiberade båda enzymerna via en icke-kompetitiv mekanism. Dessa resultat stödjer den redan existerande modellen av förekomsten av en femte loop, med stor betydelse för substratspecificitet, i HAD-familjen.

Nyckelord: Hydrolaser av Haloacid dehalogenase (HAD)-typ, Enzymteknik, katalytiska effektivitet, Termisk stabilitet, Inhibition

Zusammenfassung

Halosäure-Dehalogenase-ähnliche (HAD) Hydrolasen repräsentieren eine vielseitige Überfamilie, welche durch die Ausbildung eines kovalenten Enzym-Substrat Komplexes im Verlauf des katalytischen Zyklus in der Lage sind C-Cl, P-C oder P-O Bindungen zu spalten. In dieser Arbeit wurde ein Enzym aus dieser Familie, HAD von *Thermatoga neopolitana* (HADTn), welches eine Phosphatase-ähnliche (P-O-Spaltung) Aktivität aufweist, in Bezug auf einer Optimierung der Substratspezifität eingehend untersucht. Das Enzym zeigt unterschiedliche Affinitäten für Zuckerphosphate, z.B. Fruktose-6-Phosphat (F6P) und Glukose-6-Phosphat (G6P), bei hohen Temperaturen, was für industrielle Anwendungen von großem Interesse ist. In dieser Studie wurde HADTn durch *halb rationale ortsgerichtete* Mutagenese verändert, um seine Spezifität zu F6P für enzymatische Kaskadereaktionen zu erhöhen. In einem ersten Schritt wurden mehrere Mutanten generiert, um die Rolle verschiedener Aminosäuren im aktiven Zentrum des Enzyms für die Substraterkennung zu bestimmen. Die Ergebnisse wiesen auf eine wichtige Rolle des Serin in Position 166 (S166) für die Katalyse hin, vermutlich für die Mg (II) Positionierung. Außerdem wurde der Einfluss der Glutaminsäure in Position 47 auf die Substraterkennung identifiziert. Basierend auf diesen Erkenntnissen wurden mit Hilfe von degenerierten Primern (NNK Triplet Motiv) Bibliotheken für sechs verschiedene Aminosäurepositionen (Y19, M8, P46, E47, P110, R117) erstellt. Ein Hochdurchsatz-Screening der Bibliotheken mit zwei verschiedenen Substraten (F6P und G6P) führte zur Identifizierung einer verbesserten Variante, bei der Prolin an Position 46 zu Threonin (P46T) ausgetauscht war. Die anschließende Charakterisierung von HADTnP46T für die Substrate F6P und G6P zeigte eine nahezu zweifache Erhöhung der Rate der katalytischen Effizienz für F6P bezogen auf den Wildtyp (V_{max}/K_m). Außerdem zeigten thermale Stabilitätsstudien, dass HADTnP46T eine Halbwertszeit von 392 min bei 94 °C aufweist, welche ähnlich zu der des Wildtyps ist. Der Zusatz von Mg (II) verdoppelte die Halbwertszeit für beide Enzyme. Die Produkte Fruktose und Glukose hemmten beide Enzyme durch einen nicht-kompetitiven Mechanismus. Die Identifizierung von Position 46 in Bezug auf die Substraterkennung unterstützt Erkenntnisse für die Präsenz eines fünften Loops in der HAD Familie, welcher eine zentrale Rolle für die Substratspezifität spielt.

Schlüsselwörter: Halosäure-Dehalogenase-ähnliche Hydrolasen, Enzymengineering, katalytische Effizienz, Thermostabilität, Inhibition

Acknowledgements

"I was taught that the way of progress was neither swift nor easy."
Marie Skłodowska Curie (1867 – 1934)

I am genuinely grateful for this exciting period in my life. I give thank for being able to learn state-of-the-art of protein engineering and acquire know-how from the experts in this field. I could not be any luckier to get the opportunity to study this particular topic further. Nothing is possible without the supports of some people, at whom I want to thank cordially.

At first, I would like to thank Prof. Dr. Volker Sieber for having allowed me to conduct my thesis in his research group as well as for his direct and indirect supervision. I am also deeply thankful for the opportunity and trust from him such that I can continue working in his group after my Master studies.

Second, I would like to thank Prof. Patrick Adlercreutz for his encouragement to me to pursue a PhD and his invaluable comments regarding this work. Further to Dr. Javier Linares-Pastén for the share of his knowledge and his time to correct my thesis as well as his assistance for organising my defence in Lund University.

I also want to show deep appreciation to my supervisor and also my friend, André Pick for his assistance in planning the experiments, his shrewd ideas to tackle problems during the experiments, and for the possibility of testing my own ideas. I also want to thank him for his time and patience in correcting my thesis as well as his tremendous support and example to always work hard and give 110% for research.

Without neglecting the importance of personal supports I also would like to thank all friends at Lehrstuhl für Chemie Biogener Rohstoffe for their friendliness and enthusiasm, in particular to Jörg Carsten for invaluable discussions, to Michael Loscar, Daniel Bauer, and Herbert Goldinger for always staying late, and to Alfiya Wohn for her help in molecular biology. Special thanks to Sumanths Ranganathan for proof-reading, to Lisa Steiner, Anja Schmidt, and Edilberto Medina for warm atmosphere in the office. Further thanks to all friends in Lund for great companionship, to Erik Karlström for his help in translating my abstract to Swedish, and to Franziska Olm for her help in rewriting my abstract in German. Last but not least is to my family who always supported me unconditionally to do what I love.

Finally, I have to thank Swedish Institute for academic and financial supports during my studies in Sweden. Its scholarship not only gave me the opportunity to earn a Master's degree from the prestigious Lund University, but also helped me broaden my horizons toward openness and sustainability. Further, I want to acknowledge Lund University's Erasmus Traineeship program for the additional stipend to perform this work.

Table of Contents

List of Tables

List of Figures

List of Abbreviations

F6P	Fructose-6-phosphate
G6P	Glucose-6-phosphate
V_{max}	Maximum rate
K_m	Michaelis-Menten constant
min	Minute
h	Hour
SD	Standard deviation
Avg	average
HAD	Haloacid Dehalogenase
PCR	Polymerase Chain Reactions
QC	QuikChange™ Site-Directed Mutagenesis
WT	Wild type

1 Introduction

The demand to replace fossil fuels with greener resources is increasing in the last decades. Application of green chemistry for industrial processes is also urged since its introduction in 1990 (Centi & Perathoner, 2009). Re-utilisation of catalysts is one of the 12 principles described in ~~the~~ green chemistry (Anastas & Warner, 1998). However, conventional chemical catalysts are not biodegradable and are sometimes toxic (Greimel, et al., 2013). Application of these catalysts for food and pharmaceutical industries are not advised. Enzymes, on the other hand, have been gaining more interest recently due to their biodegradability and activity that are similar to chemical catalysts. They are regarded as safe thus application in food and pharmaceutical industries are encouraged (Illanes, 2008). However, not all enzymes can be directly compatible for industrial application. Several improvements need to be done to make these enzymes able to compete with chemical catalysts in terms of productivity. There are two major strategies that are being implemented. The first strategy is to discover new enzymes to cater to the needs of the industry, while the second strategy is to engineer an enzyme with a known function to increase its characteristics. The second approach is applied in this work.

1.1 Enzyme as biocatalyst

Most biochemical reactions cannot occur fast enough without any catalyst to sustain life due to a large energy barrier. Enzymes are the natural counterpart to chemical catalysts and indispensable for biochemical reactions. Similar to catalysts in chemical reactions, enzymes act by lowering the activation energy and thereby increasing the reaction rate. Enzymes decrease the activation energy by several mechanisms such as substrate activation, stabilisation of the transition state, and providing an alternative route for a reaction to occur (Benkovic & Hammes-Schiffer, 2003). However, enzymes do not change the direction of reactions. Enzymes are not able to catalyse reactions that are by nature not spontaneous (positive Gibbs free energy). In most cases, the kinetics of an enzyme is best described by the Michaelis-Menten model. Although this model is one of the very first models to be proposed, it is still widely used today. In this model, the enzymatic reaction is considered to happen in two steps. Firstly, a reversible step to form an enzyme-substrate complex, followed by a second catalysis step, in which the substrate is converted to a product. According to the model, enzyme activity will increase linearly with an increase of substrate concentration up to a certain point till all the enzymes are saturated, after which, any further increase in substrate concentration will not increase the reaction rate. This model is given below,

$$v = \frac{V_{max} * [S]}{K_m + [S]} \qquad \textit{Equation 1}$$

Two important parameters can be derived from this model, V_{max} and K_m. V_{max} is the maximum rate of enzyme activity and usually has the unit of μmol/min*mg. In addition, K_m has the unit mM and is defined as the concentration of substrate at which the rate (V) is a half of V_{max}. The double reciprocal plot or Lineweaver-Burk plot has been widely used to calculate these two parameters from the model. However, with recent developments in computer software, nonlinear regression is commonly used in research replacing the Lineweaver-Burk plot (Ranaldi, et al., 1999).

Further useful parameters that are widely used to compare enzymes are the turn over number or k_{cat} and catalytic efficiency or k_{cat}/K_m. Turn over number is the amount of product formed by one molecule of an enzymes per second and the formula is described in Equation 2. Reciprocal of k_{cat} can be defined as the time needed to convert one molecule of substrate

into product by one enzyme. Catalytic efficiency is the measure of how efficient an enzyme converts its substrates thus k_{cat}/K_m is also known as specificity constant. Catalytic efficiency is a powerful indicator of the efficiency of an enzyme in converting two or more substrates. Catalytic efficiency, however, should not be used to compare two enzymes acting on the same substrates (Eisenthal, et al., 2007).

$$k_{cat} = \frac{V_{max}}{[E_0]} \qquad \textit{Equation 2}$$

Although many enzymes obey Michaelis-Menten model, some enzymes show a deviation. There are many factors that cause this deviation. The Michaelis-Menten model is based on the assumption that the amount of substrate used is very large compared to the amount of enzyme. This model also assumes that the initial rate of enzyme is the initial rate where substrate and product inhibition have yet to occur. However, some enzymes may be inhibited by their substrates or products. Substrate and product inhibition of enzymes are important and a common mechanisms exist for cells to control their metabolism (Nelson & Cox, 2008). Inhibition in general can be classified into two types, reversible and irreversible inhibition.

- Reversible inhibition
  This type of inhibition can inhibit the enzymes' activity in a reversible way. There are four mechanisms of reversible inhibition. A Lineweaver-Burk plot of each mechanism and the modification of Michaelis-Menten model is presented in Figure 1.1.
  - Competitive inhibition
    Inhibitors from this class compete with substrates to bind to the active site of enzymes resulting in a lower V_{max}. Addition of substrates will rescue the activity, thus the amount of substrate to reach the same activity is higher in the presence of the inhibitors. That results in a decrease of an apparent K_m. The structure of the inhibitors usually resembles the structure of the substrates.
  - Uncompetitive inhibition
    Inhibitors that exhibit uncompetitive mechanism bind to the enzyme-substrate complex, unlike competitive inhibition, the binding site of these inhibitors is not the active site. This results in a decrease of V_{max} and K_m upon the presence of this inhibition due to a decreased amount of the active enzyme-substrate complex. Addition of more substrate does not increase the V_{max}.
  - Noncompetitive inhibition
    In the presence of noncompetitive inhibitors, V_{max} of the reaction decreases but not the K_m. This is because inhibitors from this class bind to the site of enzymes other than the active site. Unlike uncompetitive inhibitors, these inhibitors do not bind to enzyme-substrate complex. Upon inhibitor binding, the active site of the enzymes is unavailable for substrates. This is due to slight conformation changes by the inhibitor, which block the access to the active site.
  - Mixed-type inhibition
    These inhibitors have a similar mechanism as the noncompetitive inhibitors but inhibitors from this class can also bind to the enzyme-substrate complex. This type of inhibition results in a decrease of the apparent the V_{max} and an increase in the apparent K_m. Further addition of substrates will slightly increase the enzyme activity but will not be able to achieve the initial rate.

- Irreversible inhibition
  Covalent modification of enzymes is the common in this type of inhibition. Inhibitors will bind to the active site of enzymes covalently causing a conformation change in the active site of the enzyme rendering the enzymes inactive. This mechanism of inhibition is different than irreversible inactivation of enzymes, e.g. by extreme pH and temperature. The latter has nonspecific effects and destroy the structure of enzymes.

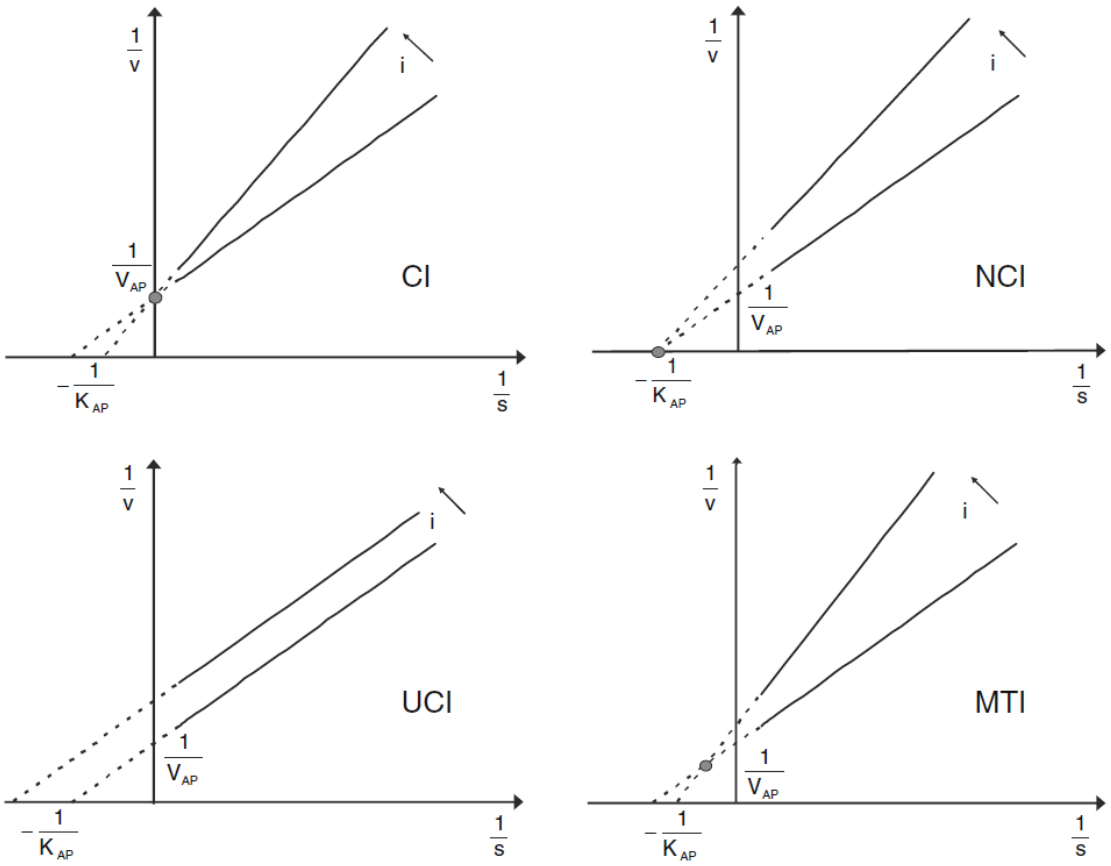

Figure 1.1. Lineweaver-Burk double reciprocal plot of different mechanisms of inhibition. CI is competitive inhibition; NCI is noncompetitive inhibition; UCI is uncompetitive inhibition; MTI is mixed-type inhibition. Adapted from (Illanes, 2008).

Enzymes as biocatalysts also show superiority over chemical catalysts. In general, enzymes show high specificity toward substrates and selectivity of products (stereoselectivity). Some enzymes are able to catalyse very complex reactions under mild conditions that chemical catalysts are incapable of. However, enzymes possess also some drawbacks. Chemical catalysts have benefit by being robust for industrial application in part due to their small size. In many cases it is also cheaper to produce and maintain chemical catalysts than enzymes (Illanes, 2008). Those disadvantages are account for the fact that enzymes are protein. Unlike chemical catalysts, protein is not designed by the nature to be robust for industrial applications, rather it is designed to be active and to sustain life of organisms in the mild conditions.

Activity of an enzyme is determined by several amino acids situated in a small region of an enzyme called the active site. In addition to the active site, the enzyme structure is also

important for enzyme activity. An enzyme's structure can be divided into four levels: primary, secondary, tertiary, and quaternary structures. Intermolecular forces that sustain tertiary and quaternary structures of enzymes (three-dimensional structure) are weaker than covalent bonds in the primary structure. Several parameters can affect the stability of the three-dimensional (3D) structure of enzymes. Stability is not something quantifiable, activity, on the other hand is. As mentioned earlier, the activity of enzymes directly correlates with their stability thus stability at different conditions could be measured by comparing enzymes' activity at those conditions. However, this approach should be understood with attention. Temperature and pH are examples of parameters that influence enzymes' activity independent to the enzymes' stability. Those two parameters also have effects on enzyme stability that will affect enzymes' activity.

As discussed earlier, amino acids in the active site of enzymes play a significant role in enzymes' activity. Some amino acids are influenced by pH while others are less sensitive to a pH fluctuation. Charged amino acids such as arginine (R), histidine (H), lysine (L), aspartic acid (D) and glutamic acid (E) are examples of amino acids that are strongly influenced by pH. Numbers of enzymes have those amino acids in their active site. RNAse, for example, is a class of enzymes that has histidine in their active site with an optimum pH at 5.5 (Thompson & Raines, 1994) and pepsin with pH optimum below 2 uses aspartic acid in its active site to catalyse the hydrolysis of proteins (Antonov, et al., 1978). If the reaction carried out at a suboptimal pH this will result in lower activity but this lower activity is not the result of enzyme destabilisation. In extreme pH conditions, decrease of activity is not reversible. That is the result of an irreversible inactivation of the enzyme. At very high pH (>11), all positively charged amino acids will be deprotonated in the same way as very low pH (<1), where, all negatively charged amino acids will be protonated. Protonation and deprotonation will result in loss of ionic interactions that help stabilise 3D structure of a protein. At high pH, disulphide bridges could also be broken.

However, the effect of temperature is different from the effect of pH. The pattern is similar to that of a chemical reaction; enzymatic reaction is also increased with an increase in temperature. Arrhenius law is widely used to represent the effect of temperature to the rate of reaction. At higher temperature, the kinetic energy of molecules is increased thus the probability of collision between molecules are also increased. In enzymatic reactions, the collision is between the enzyme and its substrate. Kinetic energy does not only represent the movement of molecules in the solution relative to its primary position, it also represents the movements (translational, vibrational, and rotational) of atoms constructing the molecule. For biomolecules like enzymes, movements of atoms of each amino acid are limited to the enzymes' 3D structure. With an increase in temperature, movements of the atoms could be so high such that the intermolecular forces compromising the 3D structure disappear. The effect of temperature on enzyme activity is then a competition of increased activity due to higher probability of collisions and decreased activity due to the denaturation of enzymes. The temperature at which the interaction of these two factors results in the highest possible activity is considered as the optimum temperature (Figure 1.2).

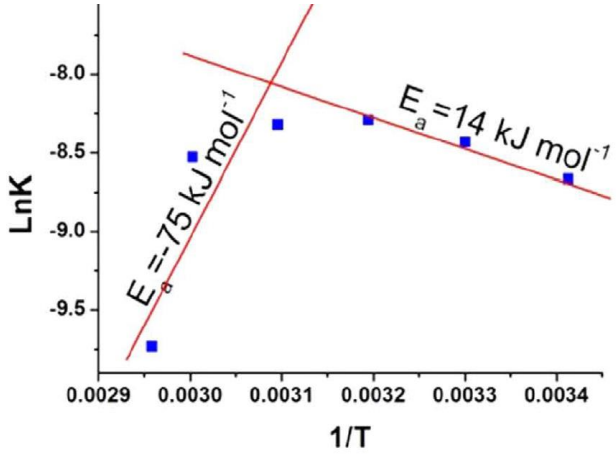

$$K = Ae^{-E_a/RT}$$

$$Ln(k) = Ln(A) - \frac{E_a}{R}\frac{1}{T}$$

Figure 1.2. Arrhenius plot of hydrolysis of pNPP by carbohydrate anhydrase. At lower temperature (1/T > 0.0031), apparent activation energy (Ea) is positive correspond to increase activity with increased temperature. At higher temperature (1/T < 0.0031), deactivation energy (E) is negative marking denaturation of enzyme begins to occur. Optimum temperature is at 50ºC (Vinogradov & Avnir, 2015)

Similar to kinetic characteristics (V_{max} and K_m), optimum conditions for each enzyme are dictated by the nature of the enzymes (the sequence of the amino acids). In general, the enzymes will have optimum conditions similar to the living conditions of the organism producing it. Enzymes from mesophilic bacteria tend to have an optimum temperature between 25 – 40ºC. This means that microorganisms found under extreme conditions will have enzymes that can catalyse reactions under similar conditions of growth. Thermophilic microorganisms are a group of microorganisms that thrive at high temperatures (60 – 80ºC). Enzymes from these microorganisms show activities at high temperatures making these enzymes of great interest. Enzymes that show activities at high temperatures tend to have a higher stability towards other conditions such as pH and the presence of organic compounds than their mesophilic counterparts. These characteristics make enzymes from thermophilic microorganisms more suitable for industrial applications (Andrade, et al., 1999).

1.2 Haloacid Dehalogenase (HAD) Superfamily

Enzymes catalyse a vast range of reactions and are grouped to six classes: oxidoreductases, transferases, hydrolases, lyases, isomerases, and ligases. Hydrolases are the most important and widely used enzymes for industrial applications exceeding by far enzymes from other classes (Nissen, 1982). Enzymes from this class usually accept more than one substrate and it is not uncommon that some enzymes from this class show an extensive substrate range thus forming a distinctive superfamily. One of the superfamilies that show broad substrate range is the haloacid dehalogenase family (HAD). This superfamily encompasses the majority of enzymes with phosphohydrolase activity from all three super kingdoms of life marking the significance of enzymes from this superfamily in sustaining life (Burroughs, et al., 2006).

HAD superfamily not only catalyses the chemical breakdown of haloalkanes, but it also catalyses the breakdown of CO-P (phosphatase), C-P (phosphonatase), CO-P followed by the subsequent transfer of phosphate (phosphoglucomutase) (Allen & Dunaway-Mariano, 2004). This family is characterised by using aspartic acid for catalytic reaction. There are four conserved loops based on a sequence alignment study (Aravind, et al., 1998). A conserved aspartic acid that acts as nucleophile is situated in loop 1 while serine/threonine is positioned in loop 2 and will interact with the phosphate group of the substrate. Loop 3 has a conserved

arginine/lysine to stabilise the intermediate together with serine/threonine from loop 2 (Lahiri, et al., 2002) and motif 4 has two to three aspartic acid responsible for the coordination of Mg (II) (Morais, et al., 2000). Loop 1-4 are organised in such a way that in three-dimensional forming active site of HAD hydrolase. Many members of the HAD family have a second domain (cap domain) besides the main catalytic domain. The cap domain contains an additional loop comprised of helix-loop-helix that is proposed to be involved in the substrate recognition. Glycine is a conserved amino acid found in the fifth loop (Lahiri, et al., 2004).

Most enzymes in this group require Mg (II) for catalysis (Burroughs, et al., 2006). Mg (II) interacts with the negatively charged phosphate whereby facilitating a nucleophile attack by the conserved aspartic acid in the loop 1. During the reaction, an acyl-phosphate is formed between the carboxyl group of the aspartic acid and the phosphate group. This results in the destabilisation of the organophosphate bond thereby cleaving the phosphate and its leaving group. Water will then hydrolyse the acyl-phosphate bond completing the reaction (Caparros-Martin, et al., 2013). The schematic reaction is depicted in Figure 1.3.

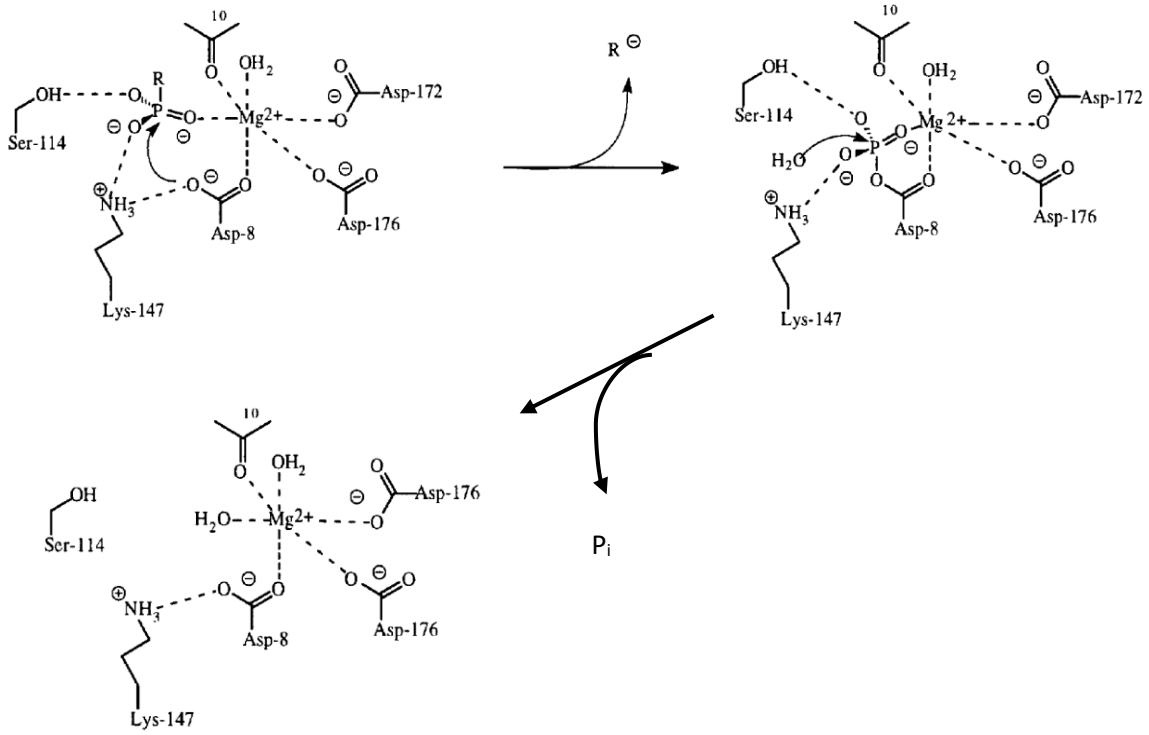

Figure 1.3. Proposed mechanisms of P-type phosphatase member of HAD. R is the leaving group. Asp-8 (D8) is situated in loop 1, S114 is in loop 2, K147 is in loop 3, D172 and D176 are in loop 4. Adapted from (Ridder & Dijkstra, 1999).

Although the HAD family has four conserved loops, possible substrates for individual enzyme from this family cannot be easily predicted. Empirical work has to be done to determine possible substrates. Twelve new enzymes with HAD activity were reported from 23 enzymes characterised from *E. coli* (Kuznetsova, et al., 2006). Most of them show activity towards sugar phosphates. Due to the vast number of substrates a HAD enzyme can catalyse, general enzymatic screens needed to be developed to discover enzymes with new characters (Kuznetsova, et al., 2005). One HAD enzyme from *Thermotoga maritima* (HADTm) (Figure 1.4) is reported to have activity for sugar phosphates (erythorse-4-phosphate / E4P, fructose-6-phosphate / F6P, glucose-6-phosphate / G6P, etc). This enzyme is particularly interesting

since it shows a four times higher activity toward F6P than G6P (Kuznetsova, et al., 2005). Other HAD enzymes reported show higher activity toward G6P than F6P (Kuznetsova, et al., 2006). Further studies of this protein are needed to better understand how HADTm achieves specificity towards F6P. Increasing the specificity of this enzyme towards F6P will be further useful in enzymatic cascade reaction where G6P is present along with F6P while only the reaction toward F6P is desired. Protein engineering is widely used to improve enzyme characteristics.

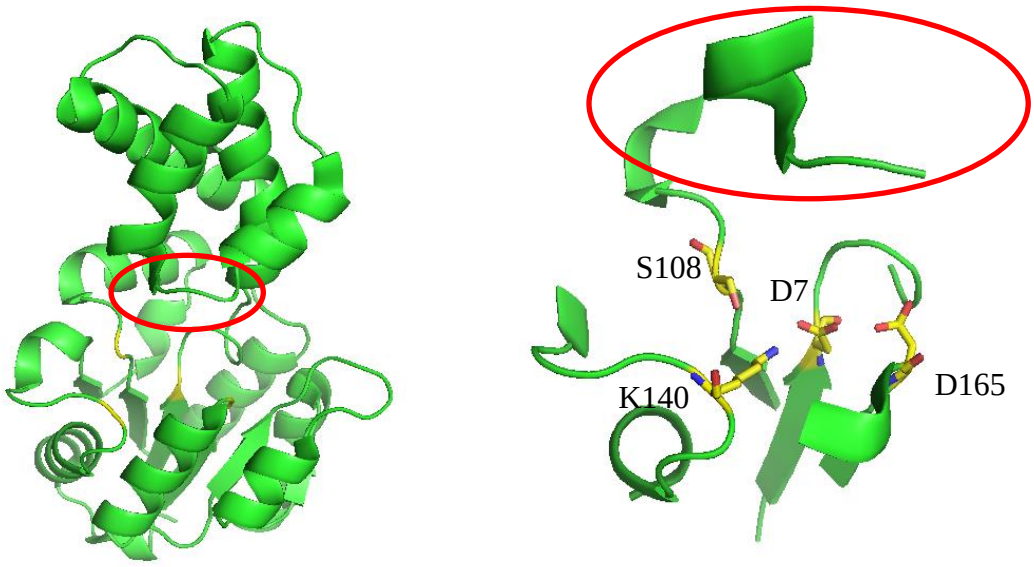

Figure 1.4. Three dimensional structure of HADTm ((PDB entry: 3KBB). Visualisation by PyMol. Red circles show proposed loop 5. Conserved loops with the conserved amino acid are depicted. Loop 1: D7, loop 2: S108, loop 3: K140, loop 4: D165. Right figure is the zoom in of active site from HADTm (left figure).

1.3 Enzyme engineering

Evolution in nature has a great ability to exquisitely develop enzymes enabling them to catalyse certain complex reactions. A similar strategy is adapted *in vitro* to create enzymes with desired characteristics. There are three major strategies to simulate natural evolution *in vitro*: directed evolution, rational design, and a hybrid technique of both.

1.3.1 Directed evolution

This approach mimics the process that occurred in the nature by creating mutants of the enzymes randomly. One report suggests this approach will result in inactivation of the mutants created at least 30 – 40% of the cases (Axe, 2004). It is also necessary to have a very good screening system as large number of variants can be expected. Despite these drawbacks, this method however has proved to be successful in generating desired mutants. Several examples include 10,000 times increase in catalytic activity of glyphosate N-acetyltransferase by DNA shuffling (Castle, et al., 2004), 170-fold increase in stability of Subtilisin E in organic media by error-prone PCR (epPCR) (Chen & Arnold, 1993), and 13-fold improvement of enantioselectivity of epoxide hydrolase by combination of DNA shuffling and epPCR (van Loo, et al., 2004). None of these techniques used require knowledge of enzyme structure and catalytic mechanism. That is one of the reasons directed evolution is still popular today. In addition, directed evolution sometimes can produce mutants that would

not be created by rational design due to unpredictable effects of mutations (Leisola & Turunen, 2007).

1.3.1.1 DNA shuffling

This technique is based on the concept of mutation that happens in the nature. DNA shuffling is performed by cutting the desired DNA using DNAse or defined restriction enzymes creating a library of small DNA fragments. Subsequent PCR is performed without any primers so the small fragments will anneal to each other for sequences that have overlapping regions (natural primers). PCR is then run several times and a final annealing with primers specific to the end sequences of the native DNA to amplify complete DNA (Cohen, 2001). This approach is used to limit the sequence inside the original gene family because random sequences often produce non-functional proteins. A modification of this technique using nonhomologous recombination can increase the performance of DNA shuffling. The modified method using exon for shuffling instead of DNA template (Leisola & Turunen, 2007).

1.3.1.2 Error-prone PCR (epPCR)

This technique is the simplest and commonly used one to create a library based on a single gene. Unlike ordinary PCR, the low fidelity of *Taq* DNA polymerase is used to generate mutations. Several additional modifications are also performed such as using imbalance concentration of dNTPs (Cadwell & Joyce, 1992), addition of $MnCl_2$, or increased extension time (Leung, et al., 1989). Serial dilutions of every fourth PCR cycle are also implemented to enrich single point mutations (McCullum, et al., 2010).

1.3.2 Rational design of enzymes

Although structure and catalytic mechanisms are needed for successful application of this approach, enzymes by design have advantages over directed evolution. A smaller number of variants are generated by this approach so that the screening effort is reduced. High-throughput screening (HTS) is not always possible to implement. There are also more factors to be considered and more importantly, HTS is not a cheap technology (Porter, et al., 2016). There is no single defined protocol for rational designs like DNA shuffling and epPCR in directed evolution. However, rational design is always started by *in silico* analysis as a thorough knowledge of the structure is essential.

The structure of some enzymes has been devised and stored in PDB and for those enzymes, rational design can be started directly. For other enzymes without crystal structures, homology modelling needs to be done prior to rational design. There are various bioinformatics tools that can be used for homology modelling, YASARA is one such tool and was used in this project. In general, 30% of similarity in any sequence is needed to produce a reliable homology model (Sander & Schneider, 1991). YASARA has been designed to perform well in homology modelling with its multi-level optimisation by considering course-grained feature, clipping class costs, and mainly tweaking torsion angles. It is shown to have a comparable performance with related tools, e.g. Rosetta and Undertaker (Krieger, et al., 2009). Depending on the purpose of the rational design, in the case of substrate specificity study, ligand docking may be done. YASARA is also able to execute this task with its default VINA docking. However, this tool is not suitable for protein-protein docking (Trott & Olson, 2010).

Site-directed mutagenesis is the continuation of *in silico* analysis in rational design. QuikChange™ site-directed mutagenesis (QC) represents an improved method compared to conventional PCR based site-directed mutagenesis. QC bypasses the restriction and ligation steps necessary in the conventional method. This method was invented and patented by Stratagene. Two important factors contribute to the success of QC: primer design and DpnI digestion. In the standard QC protocol, plasmid DNA is used as a template and a primer containing the desired mutation is used. During the PCR reaction, linear DNA will be used with staggered end located at mutation point designed. DpnI is used to degrade parental plasmid DNAs that are methylated (Agilent, 2005). Several proposed modifications to the standard QC protocol are reported (Liu & Naismith, 2008; Zheng, et al., 2004). Both of them suggest to use a set of primer that contains non-overlapping regions. This additional modification will give improvement to the standard protocol as it will decrease the likelihood of primer dimer formation and less parental DNA template could be used, thereby reducing the amount of parental DNA not degraded by Dpn1 (Xia, et al., 2014).

1.3.3 Semi-rational site mutagenesis as a hybrid technique

This technique combines the advantages of directed evolution and rational design for generating library sizes that facilitate handling with the precise exchange of a defined amino acid (semi-rational). This approach still needs solid knowledge of protein structure but a much higher quality of the library is generated compared to the directed evolution (Lutz, 2010). This technique is based on the utilisation of degenerate primers to create the library (Figure 1.5).

Degenerate codon	Mixed base sequence	Encoded codons	Stop codons	Encoded amino acids	Properties
NNN	(A,T,G,C) (A,T,G,C) (A,T,G,C)	64	TAA, TAG, TGA	All	Fully randomised codon
NNK	(A,T,G,C) (A,T,G,C) (G,T)	32	TAG*	All	All 20 amino acids
NNS	(A,T,G,C) (A,T,G,C) (G,C)	32	TAG**	All	All 20 amino acids
NDT	(A,T,G,C) (A,T,G) T	12	No	Phe, Leu, Ile, Val, Tyr, His, Asn, Asp, Cys, Arg, Ser, Gly	Mixture of polar, nonpolar, positive and negative charge (Reetz 2008)
NTN	(A,T,G,C) T (A,T,G,C)	16	No	Met, Phe, Leu, Ile, Val	Nonpolar residues
NAN	(A,T,G,C) A (A,T,G,C)	16	TAA, TAG	Tyr, His, Gln, Asn, Lys, Asp, Glu	Charged, larger side chains
NCN	(A,T,G,C) C (A,T,G,C)	16	No	Ser, Pro, Thr, Ala	Smaller side chains, polar and nonpolar residues
RST	(A,G) (G,C) T	4	No	Ala, Gly, Ser, Thr	Small side chains

Figure 1.5. List of degenerate primers commonly used for semi rational site mutagenesis. Adapted from (Currin, et al., 2015)

Successful employment of this method for generating desired mutations have already been reported. Synthetic capacity of γ-humulene to produce different sesquiterpenes is increased by a systematic recombination of the amino acids near the active site (Yoshikuni, et al., 2006). Alcohol dehydrogenase from *E. coli* K-12 was improved in its specificity toward

NADH cofactor over NADPH by degenerate primers containing the NDT triplet modifying amino acids in the binding site of NADPH (Pick, et al., 2014).

1.4 Objective

HAD superfamily is a family known to date to have phosphatase activity more than any phosphatases from different families (Koonin & Tatusov, 1994). Phosphatases together with kinases are the two most important groups in metabolic regulation as 40% of metabolomes have a phosphate functional group (Nobeli, et al., 2003). The significant role of enzymes from the HAD superfamily in metabolism is, however, largely unexplored (Kuznetsova, et al., 2006). Thus more research exploring the potential roles of enzymes from this superfamily needs to done. In this work, one enzyme that belongs to HAD superfamily from *Thermatoga neapolitana* (HADTn) will be studied in respect to its substrate specificity. This enzyme shares 99% sequence similarity with HADTm, a previously studied enzyme that shows four times higher activity toward fructose-6-phosphate (F6P) than glucose-6-phosphate (G6P) (Kuznetsova, et al., 2005). This characteristic is rather unusual because enzymes of the same family from *E. coli* act otherwise (Kuznetsova, et al., 2006). The main focus of this work is to identify amino acids that play a role in substrate specificity in HADTn and to further increase the specificity toward F6P over G6P employing recent technologies in protein engineering. The improved mutants could be used later for different purposes, one of them is in enzymatic cascade reactions that requires enzymes with high substrate specificity.

In silico analysis is the first step that will be used to understand the protein. Homology modelling with HADTm which crystal structure has been devised will be done using YASARA version 15 (Krieger & Vriend, 2014). Sequence alignment and three dimensional structure comparison to other enzymes from the same family will be performed to be done to locate the active site and predict possible catalytic mechanisms. The results will be used to simulate and calculate the effect of the mutations on substrate specificity. Along with *in silico* analysis, the initial characterisation of WT needs be done to determine the optimum condition for the enzyme assay. Possible mutation with improved specificity toward F6P predicted by YASARA will be generated using QuikChange™ site-directed mutagenesis and later purified by FPLC. Turn over number and catalytic activity are the two parameters that will be used to compare the mutants with WT. Based on those findings, gene libraries for several different positions of a particular amino acid will be generated by site-saturation mutagenesis (NNK motif). A high-throughput screening method will be developed to screen large number of the libraries. Final characterisations of improved variants will be carried out to determine the effect of the mutations on the intrinsic characteristic of the enzymes, e.g. substrate specificity, temperature stability, and inhibition mechanism.

2 Materials and Methods

2.1 Materials

Strains of bacteria

Three different strains of bacteria were used during laboratory work. The strains of bacteria and their genotype are described in Table 2.1.

Table 2.1. List of strain of bacteria

Strain name	Genotype	Purposes	References
E. coli XL 10 gold	*Δ(mcrA)183 Δ(mcrCB-hsdSMR-mrr) 173 endA1 supE44 thi-1 recA1 gyrA96 relA 1 lac* tet^R *Hte* {F' proAB* $lacI^qZ\Delta M15Tn10(Tet^R)Amy\ Cam^R\}$.	Library generation	(Greener & Jerpseth, 2004)
E. coli Top 10	F– *mcr*A Δ(*mrr-hsd*RMS-*mcr*BC) Φ80*lac*ZΔM15 Δ*lac*X74 *rec*A1 *ara*D139 Δ(*ara leu*) 7697 *gal*U *gal*K *rps*L (StrR) *end*A1 *nup*G	Library generation	(ThermoFisher, 2015)
E. coli BL21 (DE3)	*fhuA2 [lon] ompT gal (λ sBamHIo ΔEcoRI-B int::(lacI::PlacUV5::T7 gene1) i21 Δnin5) [dcm] ΔhsdS*	Protein expression	(NEB, 2016)

Media

Different media were used for plasmid production and protein production. Their composition is listed in Table 2.2.

Table 2.2. List of media

Name	Composition	Purposes
LB (Lysogeny Broth) with kanamycin 30 mg/l (LB-kanamycin 30)	NaCl 10 g/l, yeast extract 10 g/l, tryptone 10 g/l, kanamycin 30 mg/l	Plasmid production
LB agar with kanamycin 30 mg/l (LB agar-kanamycin 30)	NaCl 10 g/l, yeast extract 10 g/l, tryptone 10 g/l, kanamycin 30 mg/l, agar 15 g/l	Colonies growing
SOC media	Trypton 2%, yeast extract 0.5%, NaCl 0.05%, KCl 2.5 mM, MgCl 10 mM, glucose 20 mM	Recovery of the competent cells after electro-transformation
Auto-induction media	Tryptone 10 g/l, yeast extract 5 g/l, glycerol 5 g/l, glucose 0.5 g/l, α-lactose 2 g/l, $MgSO_4$ 1 mM, $(NH_4)_2SO_4$ 25 mM, KH_2PO_4 50 mM, K_2HPO_4 50 mM, kanamycin 100 mg/l	Protein production
Modified auto-induction media	Tryptone 10 g/l, yeast extract 5 g/l, glycerol 5 g/l,	High-throughput screening

	glucose 0.5 g/l, α-lactose 2 g/l, $MgSO_4$ 1 mM, kanamycin 30 mg/l	

Reagents

List of reagents used together with their manufacturers is presented in Table 2.3 – Table 2.6.

Table 2.3. List of reagents used

Reagents	**Manufacturer**
Ascorbic acid	Carl ROTH GmbH
Ammonium Molybdate	Carl ROTH GmbH
Zinc Acetate	Applichem
1-Butanol	Sigma Aldrich
Ethanol	VWR Chemicals
HEPES	Carl ROTH GmbH
Potassium Hydroxide	Carl ROTH GmbH
Sodium Dihydrogen Phosphate	Carl ROTH GmbH
Disodium hydrogen Phosphate	Carl ROTH GmbH
Sodium Chloride	Carl ROTH GmbH
Imidazole	Sigma Aldrich
Citric Acid	Carl ROTH GmbH
Tris Base	Carl ROTH GmbH
Glycerine	Carl ROTH GmbH
Malachite Green	Alfa Aeser
Chloric Acid Fuming 37%	Carl ROTH GmbH
D-Fructose-6-Phosphate	Merck Millipore
D-Glucose-6-Phosphate	Sigma Aldrich
MOPS	Carl ROTH GmbH
Magnesium Sulphate	Merck
α-D-Glucose	Serva
D(-)-Fructose	ROTH
Agar-Agar, Kobe I	ROTH
Magnesium Chloride	Sigma Aldrich

Disposable goods

Table 2.4. List of disposable goods used

Goods	**Manufacturer**
96 R Bottom Plate	Sarstedt
96 F Bottom Plate	Greiner Bio-One
Pipette Tips (1000, 200, 10, 1 µl)	Brand
PCR Plate	Brand
Falcon Tube (50, 15 ml)	Sarstedt
Filter Paper	Sartorius Stedim Biotech

Molecular Biology

Table 2.5. List of molecular biology reagents

Reagent	Manufacturer
Phusion® GC Reaction Buffer 5x	New England Biolabs
dNTP-Mix-10	Rapidozym
Phusion® HF Polymerase	New England Biolabs
DpnI	New England Biolabs
DNAse	Applichem
Lysozyme	Carl ROTH GmbH
Plasmid Miniprep Kit	Thermo Scientific

Instruments

Table 2.6. List of instruments used

Instrument	Manufacturer
Micro Pulser^{TM}	Biorad
Nanophotometer P330	Implen
Aekta Purifier	GE Healthcare Life Science
pH Meter Five Easy	Mettler Toledo
Microplate Shaker TiMix5	Edmund Buehler GmbH
Thermal Cycler C100^{TM}	Biorad
Centrifuge Hereus Pico 21	Thermo Scientific
Centrifuge RC 6 Plus	Sorva
Scale AW 320	Shimadazu
Colony picker: CP-7200	Norgren Systems
Electrophoresis SDS	Bio Rad
Microplate spectrophotometer Multiskan®	Thermo scientific
Microplate dispenser Microflo Select	Biotek

2.2 Methods

2.2.1 Computational methods

2.2.1.1 In silico analysis of mutants

Structure modelling of wild type enzyme haloacid dehalogenase from *Thermotoga neopolitana* (HADTn) was carried out using YASARA version 15 (sequence of the enzyme is presented in Appendix 1A and B) (Krieger & Vriend, 2014). Putatative β-phosphoglucomutase (PDB entry: 3KBB) was used as a template. Sequence alignment with other phosphatases from HAD family from literature was carried out using Clustal Omega (EMBL-EBI, 2016) to identify amino acids that participate in the catalytic reaction. Ligands, glucose-6-phosphate (G6P) and fructose-6-phosphate (F6P), were generated using YASARA. Docking (dock_run) to HADTn wild type was run for every ligand using YASARA. Twenty-five runs based on VINA docking (Trott & Olson, 2010) were performed for each docking. Energy minimisation of ligands was always employed prior to dockings. Amino acids that showed interactions with ligands from the docking calculation but seemed to not be conserved amino acids for catalytic activity based on sequence alignment study were chosen to build new mutant with single or double mutation. New mutants were developed using the

same template (3KBB). Docking of ligands was performed under exactly the same conditions as for wild type. Mutations were analysed based on binding energy and dissociation constant calculated by YASARA.

2.2.1.2 Primers designs

Several sets of primers were designed to develop mutants based on the analysis of calculations performed by YASARA. Primers were ordered from Biomers.net GmbH (Ulm, Germany). It was suggested that the primers have length between 25 to 45 bases and should terminate in either G or C. Melting temperature (Tm) should also be higher than 78^{o}C (Agilent, 2005). Several modifications to enhance performance of the original QuikChange^{TM} protocol developed by Stratagene in regard to the primer design have been reported. Instead of complete overlapping primers, it was suggested that the primers have at least 8 non-overlapping bases (Liu & Naismith, 2008; Zheng, et al., 2004)/ At least each primer designed contained ten or more non-overlapping bases. For insertion mutation, primer design followed the suggestion by (Liu & Naismith, 2008). Tm for each primer was calculated by the online program, Primertemp developed by (Kim, 2015). Other primer properties such as Gibbs free energy (ΔG) for individual primers, ΔG for cross dimer between forward and reverse primers, and numbers of overlapping base pairs, were calculated by OligoAnalyzer 3.1 (Integrated DNA Technologies, Inc, 2015). ΔG for cross dimer was kept as low as possible compared to individual primer so as the numbers of overlapping base pairs.

2.2.2 Molecular biology methods

2.2.2.1 Electrocompetent cells preparation

One colony of a cell strain was inoculated to 30 ml LB-low media and incubated overnight at 37^{o}C. The culture was transferred to 270 ml of LB-low media and incubated at 37^{o}C until optical density at 600 nm (OD600) reached 0.5 – 0.6. The culture was divided into 6 Falcon tubes and centrifuged at 4600 x g at 4^{o}C for 20 min. The supernatant was decanted and each cell pellet was resuspended using 50 ml sterile ddH_2O and then centrifuged again at 4600 x g at 4^{o}C for 20 min. After supernatant was decanted, 50 ml of sterile 10% (w/v) glycerine was used to resuspend the cell pellet. The tubes were centrifuged at 4600 x g at 4^{o}C for 20 min. After the supernatant was decanted, cell pellets from each Falcon tube were resuspended with 25 ml of sterile 10% (w/v) glycerine and two volumes were combined into one Falcon tube followed by centrifugation at 4600 x g at 4^{o}C for 25 min. After discarding the supernatant, the remaining solution in each Falcon tube was used to resuspend every cell pellet and thereupon they were combined into one Falcon tube. Sterile 10% (w/v) glycerine was used to dilute the solution until OD600 = 50. The solution was aliquoted (70 µl) into microtubes and subsequently frozen in liquid nitrogen. Competent cells were stored at -80^{o}C.

2.2.2.2 QuikChangeTM site-directed mutagenesis (QC)

QuikChange^{TM} was performed in two steps using the protocol descried by Wang & Malcom (1999). The first step was to run a reaction with each primer in 50 µl volume for 4 cycles. The second step was to combine 25 µl of each PCR mix containing primer set into a new tube making 50 µl reaction volume, the PCR was then continued for 18 cycles. PCR mix contains 10 µl Phusion® 5x HF, 50 pmol primer, 10 nmol dNTPs, 75 ng template plasmid DNA (plasmid construct can be seen in Appendix 1C), 100 units (U) Phusion polymerase, and autoclaved ddH_2O up to 50 µl. PCR was done as follows:

- Firstly, the lid temperature was set at 105°C and hot start was at 98°C for 3 min.
- This was followed by denaturation at 98°C for 30 s, and then by annealing at 50 – 55°C for 30 s.
- Elongation was carried out at 72°C for 210 s.
- The final step was set at 70°C for 5 s.

Fifteen units of DpnI was added to PCR product to remove methylated DNA (wild type) and the mix was incubated at 37°C overnight, additional 10 U of Dpn was added for at least 5 hours. Plasmid was purified by adding 1 ml butanol from -20°C and centrifuged for 20 min at 4°C, 21,100 x g. After decanting supernatant, 1 ml of 70% ethanol from -20°C was added and centrifuged for 20 min at 4°C, 21,100 x g. After decanting supernatant and drying at 50°C, 10 µl of ddH_2O was added and incubated at room temperature for 30 min.

2.2.2.3 Plasmid transformation (Electroporation)

Competent cells (*E. coli* XL 10 gold or Top 10) were thawed on ice. Four microliter of purified QC product were transferred to the competent cells and mixed gently. The competent cells were transferred to an electroporation cuvette (2 mm) and placed in the electroporator (2.5 kV). 1 ml SOC media preincubated at 37°C was transferred subsequently to the cuvette. The solution was transferred to a microtube and incubated at 37°C, 150 rpm for 1 hour. Serial dilutions with LB were made to achieve desired number of colonies (< 400) per one plate and 100 µl of each of them was plated on LB agar-kanamycin 30 and incubated overnight at 37°C.

2.2.2.4 Plasmid production, purification and sequencing

One colony from LB agar-kanamycin 30 was inoculated to LB-kanamycin 30 and incubated at 37°C, 150 rpm overnight. The culture was transferred to a 2 ml microtube and centrifuged at 17,000 x g and supernatant was removed. Plasmid was purified using GeneJET Plasmid Miniprep Kit (Thermo Fisher Scientific). After purification, plasmid concentration was measured using IMPLEN nanophotometer prior to sequencing by GATC GmbH (Cologne, Germany).

2.2.3 Biochemical methods

2.2.3.1 Protein production and purification

Mutant plasmids were transformed to *E. coli* BL21 (DE3) followed the same protocol described previously. One colony from LB agar-kanamycin was transferred to 20 ml LB-kanamycin 30 and incubated at 37°C, 150 rpm overnight. Twenty millilitre of the culture were transferred to 200 ml auto-induction media and grown 48 hours for enzyme production. The cells were harvested by centrifugation at 10.000 g, at room temperature for 20 minutes. After supernatant decantation, binding buffer (HEPES-K buffer 100 mM pH 7.5, NaCl 500 mM, imidazole 20 mM, glycerine 10%) was used to resuspend the cells. Cell lysis was performed by sonication using a Hielscher sonicator (amplitude 10, cycle 0.5 s) for 30 min with constant cooling of the cell solution in an ice bath. Twenty millimolar of Mg (II) and 10 µg/ml of DNAse were added to the solution and centrifuged at 10.000 x g, room temperature for 20 minutes. The Supernatant was filtered using a 0.45 µm syringae filter and purified with ÄKTA purifier 10 GE Healthcare. His Trap™ FF crude 5 ml was used to capture the histidine containing enzyme. After washing with binding buffer, elution buffer (HEPES-K buffer 100

mM pH 7.5, NaCl 500 mM, imidazole 500 mM, glycerine 10%) was applied to elute the enzyme. Desalting was performed using the same instrument but Hi Prep^{TM} 26/10 Desalting column and the elution buffer was Tris-HCl 50 mM pH 7.5.

2.2.3.2 Phosphate assays

Three different assays were employed. The first assay (P I assay) is based on complexation of phosphate, molybdate, and malachite green (Hoenig, et al., 1989). The second assay (P II assay) is based on reduction of phosphate-molybdate complex with ascorbic acid (Drueckes, et al., 1995). The third assay (P III assay) is the modification of second method for high throughput screening. All three phosphate assays are end point assay.

P I assay: 20 µl of sample was incubated with 180 µl reagent containing reagent A : reagent B 36:1. Reagent A consisted of sodium molybdate 2.6% w/v: HCl 2.5 N 1:1. Reagent B consisted of malachite green 0.126% w/v. Incubation was performed for 120 s at 30^{o}C and final absorbance was read with Multiskan at 620 nm.

P II assay: 30 µl of sample was incubated with 125 µl reagent containing reagent C : reagent D 1:4. Reagent C contained Zn Acetate 15 mM, ammonium heptamolybdate 10 mM pH 5 while reagent D contained ascorbid acid 10% (prepared fresh daily) pH 5. Incubation was performed for 10 minutes at 30^{o}C and final absorbance was read with Multiskan at 850 nm. Reagent C is stable for six months when it is stored at 4^{o}C (Drueckes, et al., 1995).

P III assay: exactly the same procedure for P II assay was followed. The only modification was pH for ascorbic acid was not adjusted making the final pH of the mixture between reagent C and D become 2.5

2.2.3.3 Initial wild type characterisation

Wild type enzyme 0.05 mg/ml was incubated in reaction buffer (HEPES-K 50 mM pH 7.5, Mg (II) 5 mM) containing different G6P (0.1, 0.25, 0.5, 0.75, 1, 5, 10, 25, 50 mM) and incubated in PCR tube at 70^{o}C. This reaction buffer followed suggestion by (Kuznetsova, et al., 2005). Enzyme activity was measured by following the release of phosphate in a time course of 0, 15, 30, 45 minutes. P I assay was used to determine phosphate produced from G6P concentration up to 1 mM while P II assay was used to determine phosphate produced from higher G6P concentration. Maximum rate (V_{max}) and Michaelis constant (K_m) were calculated using SigmaPlot.

Different buffers (citrate, MES, Bis-Tris, Tris-HCl, MOPS, HEPES-K) 50 mM and pH (6 – 9) were used to test enzyme activity. Enzyme activity tests were performed by incubating 0.05 mg/ml wild type enzyme in buffer solution containing Mg (II) 5 mM and G6P 5 mM for 1 hour at 70^{o}C

Different concentrations of Mg (II) and Mn (II) were tested after optimum buffer and pH had been determined. Enzyme activity was performed by incubating 0.05 mg/ml wild type enzyme in HEPES-K 50 mM pH 7 containing G6P 5 mM for 1 hour at 70^{o}C.

For kinetic characterisation, six to seven different concentrations of F6P or G6P were used fordetermination of enzyme activities. The concentrations were 1, 2.5, 5, 7.5, 10, 15, 25 mM for both substrates. The assay was performed in PCR plates containing HEPES-K 50 mM pH 7, Mg (II) 5mM at 70^{o}C (standard condition). Activity was followed at time 0, 15, 30 min. Phosphate production was measured using P II assay.

2.2.4 High throughput screening

2.2.4.1 High throughput screening development

Eighty-four colonies of *E. coli* BL21 (DE3) containing wild type enzyme were inoculated randomly into a 96 deep well plate containing 1.2 ml modified auto-induction media. Eight *E. coli* BL21 (DE3) containing empty pET28 plasmid were also inoculated to the 96 well plate for negative control to see basal activity of indigenous phosphatase. Four remaining wells containing the media were used to check if there was any contamination. All colonies were inoculated using Colony picker (Norgern System) and plates were filled with the media using Microplate dispenser (Biotek). Incubation was performed at 37^{o}C and 1000 rpm for 24 hours (Micorplate Shaker TiMix5, Edmund Bühler GmbH). After incubation, 50 µl culture from each well was transferred to F bottom plate for OD_{600} measurement. OD_{600} measurement was performed in Microplate spectrophotometer Multiskan® after diluting the sample 5 times using NaCl 0.85%. In addition, the other 100 µl culture from each well was transferred to R bottom plate and subsequently centrifuged at 4,600 x g) for 30 minutes at 4^{o}C. Following centrifugation, supernatant was decanted and the plate containing cell pellets was kept at -20^{o}C overnight to improve lysis. Lysis procedure followed the protocol described by (Pick, et al., 2014) with some slight modification. The plate from -20^{o}C was incubated at 37^{o}C for 1 hour. Fifty microliter solution containing DNAse 10 µg/ml, lysozyme 100 µg/ml, Mg (II) 5 mM, HEPES-K 50 mM pH 7 was transferred to the R bottom plate and followed by incubation in the Micorplate Shaker at 37^{o}C, 1200 rpm for one hour. One hundred microliter solution containing HEPES-K 50 mM pH 7 and Mg (II) 5 mM was transferred to each well prior to centrifugation at 4,600 x g for 30 minutes at 4^{o}C.

For wild type landscape and Z' determination, 15 µl of supernatant was transferred to PCR plate containing 135 µl of HEPES-K 50 mM, pH 7 and Mg (II) 5 mM (reaction solution) with different substrate concentration (0.1, 0.5, and 1 mM). The enzyme assay was performed in a thermal cycler at 70^{o}C.Sampling time was 0, 15, 60 and minutes. Z' value was obtained by average of two independent plates. P III assay was used for determining phosphate concentration. The effect of incubation time, substrate concentration, and OD_{600} toward Z' value was calculated.

2.2.4.2 High throughput screening for library

Six microliter of purified QC product was transformed to *E. coli* BL21 (DE3) following previously described protocol. *E. coli* BL21 (DE3) colonies on LB agar-kanamycin 30 were inoculated to 96 deep-well plate containing modified auto-induction media. As a positive control *E. coli* BL21 (DE3) bearing wild type enzyme (inoculated randomly in 8 wells) used was. Negative controls were *E. coli* BL21 (DE3) bearing empty pET28 plasmid (4 wells) and media only (4 wells). Other steps were performed the same as previous described, but in addition to the transfer of 50 µl and 100 µl culture to F and R bottom plate, additional 50 µl of the expression cultures were transferred to 50% glycerol (in 384 deep well plate) and stored at -80^{o}C. Lysis procedure was performed exactly the same as well as the assay.

The screening procedure consisted of three rounds following the protocol described by Pick, *et al*. (2014). The first screening round was performed to screen library developed from transformation of QC product. Improved variants characterised by 20% higher activity than average plus one-time standard deviation of controls were picked for second screening (detail of criteria are presented in Result. Second screening was performed by transferring 10 µl of

glycerol stock of variants that appeared to belong to group A, B, or C from first screening to 1 ml modified auto-induction media in 96 deep well plate (three replicates were made). Sampling, lysis step, and enzymatic assay were performed the same as first screening. Several variants that showed behaviour that appeared to belong to group A, B, or C from second screening glycerol stock were inoculated to LB-kanamycin 30 for plasmid production. Plasmid was purified using GeneJET Plasmid Miniprep Kit (Thermo Fisher Scientific) and transformed to *E. coli* BL21 (DE3) according to previously described protocol. Third screening round was done by inoculating six to eight colonies of each variant to 1 ml modified auto-induction media in 96 deep well plate. Incubation, lysis, and activity assays were performed exactly the same as previously described. Best variants were determined and their plasmids were sent for sequencing.

2.2.5 Final characterisation

Mutant obtained from library screening as well as WT enzyme were produced and purified according the same protocol previously described. Mutant and wild type enzymes were characterised to determine their kinetic parameters, effect of product inhibition, and their stability at elevated temperatures. For determination of kinetic parameters, the experiment was performed as described in the Initial Characterisation.

Product inhibition was studied by incubating 0.01 mg/ml enzyme in reaction solution with two combinations of substrate and inhibitor. Fructose (0, 100, 200, 300 mM) was added to every reaction solution containing F6P (1, 5, 10 mM). Glucose (0, 500, 1000, 1500 mM) was added to every reaction solution containing G6P (1, 5, 10 mM). Phosphate produced was followed every 10 minutes and measured using P II assay. Activity was determined by calculating the slope of phosphate produced over time.

Thermal inactivation of the mutant and wild type enzymes was studied by incubating 1.7 mg/ml of the enzyme in Tris-HCl 50 mM pH 7.5 (desalting solution) at 70, 80, 90, 94^{o}C. Magnesium 100 mM was added to half of the incubation buffers. An aliquot of the enzyme was sampled after 30, 60, 120, 240, 480, 1440 minutes of incubation and transferred to the reaction solution containing 5 mM of G6P or F6P to measure its remaining activity. The activity was determined after 15 minutes of incubation in the reaction solution. Phosphate released was measured with P II assay.

3 Results

3.1 Sequence alignment and in silico analysis for possible mutations

Sequence alignment studies were carried out using Clustal omega (EMBL-EBI, 2016) in order to identify the amino acids that may play a pivotal role in the catalytic reaction and the result is shown in Appendix 1D. Four proteins that are reported to have phosphatase like activity were used for sequence alignment. This study revealed that there were at least seven conserved amino acids for the wild type enzyme (WT) (Table 3.1). Conserved amino acids were identified by considering sequence alignment and 3D structures of each reported protein.

Table 3.1. Conserved amino acids in HAD family

Location	WT	P-type ATPase[1]	P-type ATPase[2]	Phosphatase (*T. maritima*)[3]	Phosphoserine phosphatase[4]
Motif I	D7	D10	D8	D8	D11
	D9			D10	D13
	G10		G10	G11	
	T15	T14	T12		
Motif II	S108	S118	S114	S41	S99
Motif III	K140	K151	K147	K191	K144
Motif IV	E164				
	D165	D176	D172	D214	D167
		D180	D176	N217	D171

[1] (Aravind, et al., 1998). [2] (Ridder & Dijkstra, 1999). [3] (Shin, et al., 2003). [4] (Wang, et al., 2001)
Grey marks represent there are no comparable amino acids found based on sequence alignment and comparison of 3D structure

Using YASARA software, several dockings were performed for the ligands G6P and F6P with the wild type enzyme (WT) in order to understand the ligand-binding pattern. The dockings resulted in several conformations (Figure 3.1 and Appendix 1E). Each conformation differed to the other by a factor of at least 5 Å heavy atom RMSD (default setting in YASARA). With each possible conformation, several amino acids were also identified that interacted with the respective ligands. The results of sequence alignment (Table 3.1) were used to consider the docking conformation produced by YASARA and are shown in Figure 3.1, which has the highest possibility of being the actual conformation of the enzyme and ligands *in vitro*.

The sequence alignment and YASARA docking studies further confirm that D7 (WT) may act as a nucleophile towards the phosphorous atom (Aravind, et al., 1998; Shin, et al., 2003; Wang, et al., 2001). S108 and K140 may be interacting with the phosphate to increase its electrophilicity (Shin, et al., 2003; Wang, et al., 2001). Moreover, magnesium may be coordinated by D165 along with D7 and phosphate (Ridder & Dijkstra, 1999). Additionally, the amino acid D9, may also play a role in the stabilisation of Mg (II) (Wang, et al., 2001)

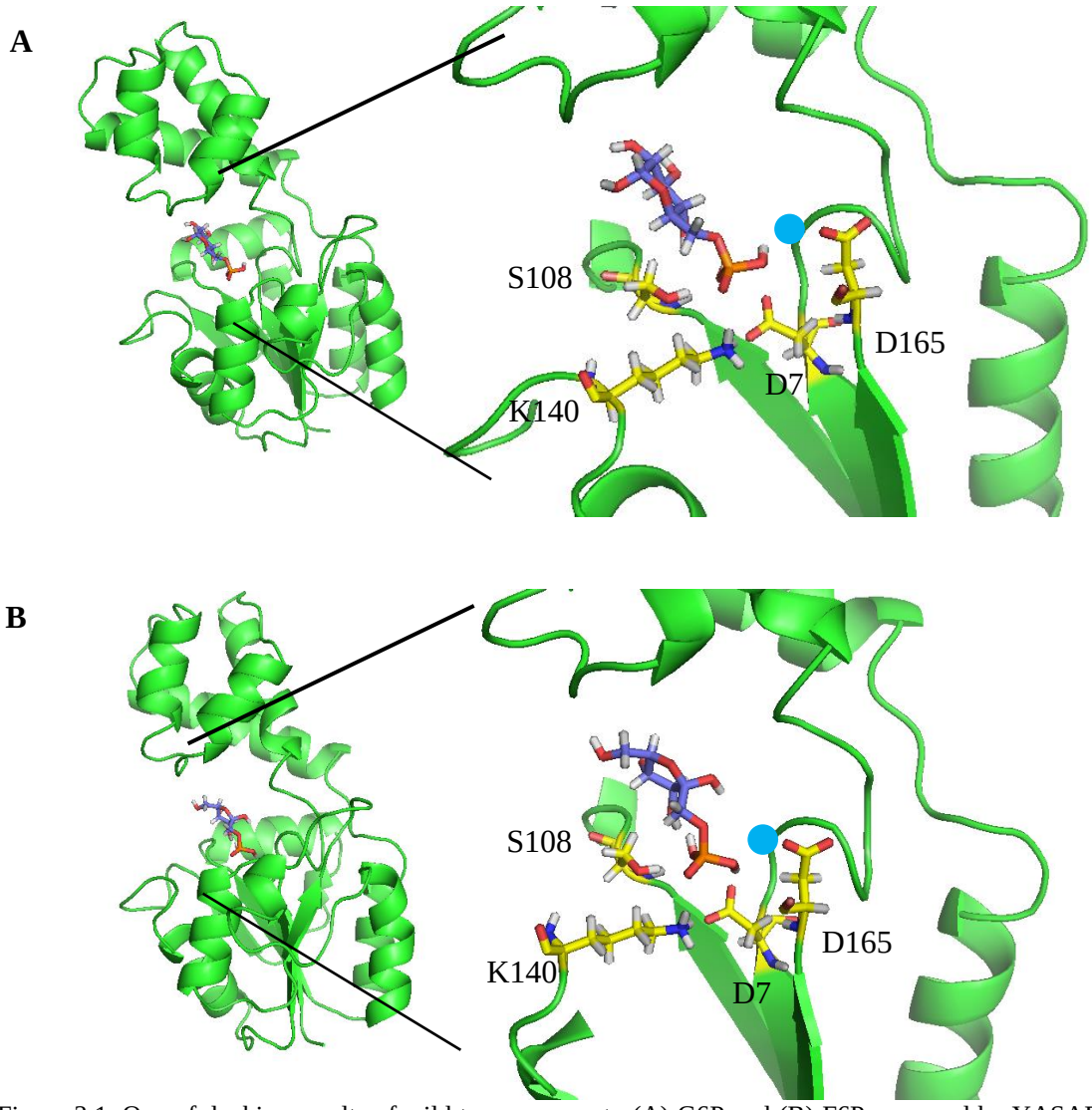

Figure 3.1. One of docking results of wild type enzyme to (A) G6P and (B) F6P proposed by YASARA. Right side is the zoom in of active site consisting of some amino acids that may play role in catalytic reaction based on sequence alignment. Cyan-filled circle was manually drawn to represent possible position of Mg (II) (the size of the circle does not represent the actual size of magnesium ion). Carbon atoms of ligands are given in blue and of amino acids are in yellow. Picture was generated by PyMol.

In addition to amino acids that may play a role in the catalytic reaction, YASARA dockings also suggested several other amino acids that showed interaction with each ligand such as- D14, E16, E47, R117, S166. Furthermore, several single or double mutations based on these amino acids were generated with YASARA. These dockings were performed for every mutant and ligand (G6P and F6P) in order to calculate the affinity of the enzyme toward its ligands. Affinity was represented by binding energy and dissociation constant (K_d) that were calculated for every docking. The binding energy is defined as the energy needed to dissociate an enzyme from its ligand (G6P or F6P) (European Nuclear Society, 2016). The higher the energy, the stronger the interaction between enzyme and its ligand. The dissociation constant is defined as the constant calculating inclination of enzyme-ligand complex dissociates into enzyme and ligand in equilibrium. The higher this value, the more inclined an enzyme-ligand complex dissociates. A higher affinity is characterised by a high binding energy and low K_d. Each docking was performed at least 25 times by YASARA.

Only binding energy and K_d from enzyme-ligand complexes that had the highest probability considering HAD conserved active site and catalytic mechanism are summarised in Table 3.2

Table 3.2. Summary of YASARA docking calculations

No	Mutation	Ligand	Binding energy [kcal/mol][1]	K_d [mM][2]	Ratio of binding energy[3]	Ratio of K_d[4]
1	WT[1]	Glu6P	5.96	42.57	0.97	1.31
		Fru6P	5.81	55.57		
2	D14P	Glu6P	6.06	36.44	0.98	1.22
		Fru6P	5.94	44.33		
3	E47D	Glu6P	5.75	60.78	0.92	2.18
		Fru6P	5.29	132.33		
4	D14E	Glu6P	5.47	97.66	1.00	1.00
		Fru6P	5.47	97.33		
5	D14G	Glu6P	5.80	56.52	0.98	1.26
		Fru6P	5.66	71.47		
6	D14H	Glu6P	5.85	51.25	0.94	1.81
		Fru6P	5.50	92.52		
7	**D14P E47D**	**Glu6P**	**6.12**	**32.71**	**1.06**	**0.53**
		Fru6P	**6.50**	**17.25**		
8	D14P E47G	Glu6P	5.06	197.08	1.05	0.63
		Fru6P	5.33	124.95		
9	D14P E47R	Glu6P	5.93	45.00	0.88	3.42
		Fru6P	5.20	153.77		
10	D14P E16D	Glu6P	5.90	47.18	0.93	1.93
		Fru6P	5.51	91.28		
11	D14P E16H	Glu6P	6.09	34.24	0.91	2.52
		Fru6P	5.54	86.34		
12	D14P R117N	Glu6P	5.51	91.75	0.90	2.47
		Fru6P	4.97	226.33		
13	D14P E113R	Glu6P	5.53	88.10	0.91	2.41
		Fru6P	5.01	212.63		
14	D14P K75R	Glu6P	5.63	74.80	0.95	1.56
		Fru6P	5.36	116.99		

[1]Binding energy is defined as the energy needed to dissemble ligand from enzyme

[2]K_d is a constant that measuring the extent of ligand and enzyme dissociate

[3]Ratio of binding energy is the ratio of binding energy of F6P to G6P, the higher the value the higher affinity of the enzyme toward F6P is

[4]Ratio of K_d is the ratio of K_d of F6P to G6P, the lower the value the higher the affinity of the enzyme toward F6P

The highest ratio of binding energy and the lowest ratio of K_d is marked bold in Table 3.2. Based on YASARA docking calculation, D14P gave slightly higher ratio of binding energy and lower ratio of K_d. Other single mutations at this position did not give desired effect thus D14P was used as a template to create double mutations. A combination of D14P

and E47D showed a higher ratio of binding energy and a lower ratio of K_d than D14P mutation alone. The double mutation D14P and E47G gave a similar result, but the K_d towards F6P was significantly higher compared to the wild type and was therefore neglected. Several other mutations based on D14P were also generated, but none of them gave a comparable result like the double mutation D14P, E47D.

An additional mutation at position 168 was carried out although this amino acid was not detected by YASARA docking. This was done to see if a mutation near the active site (D165), with a big amino acid such as tyrosine, lysine, etc would reorient the ligands such that the interaction of the sugar backbone with the cap domain would create a different specificity. Saturation mutagenesis with NDT motif to mutate S168 was carried out. The mutation S168V was also performed to check if serine at this position had a role in helping D165 position dock the Mg (II). Due to the close proximity of these two positions, a double mutation was done using a single set of primers (Appendix 2).

3.2 Initial wild type characterisation

A standard buffer as suggested by Kuznetsova, et al. (2005) was used for V_{max} and K_m determination. V_{max} is defined as the maximum rate of substrate transformation while K_m is defined as the amount of substrate required (mM) to achieve half of the V_{max}. Specific activity was used to represent V_{max} and is defined as the amount of substrate converted (µmol) per minute per mg of enzyme used. The result of enzyme assay is presented in Figure 3.2

.

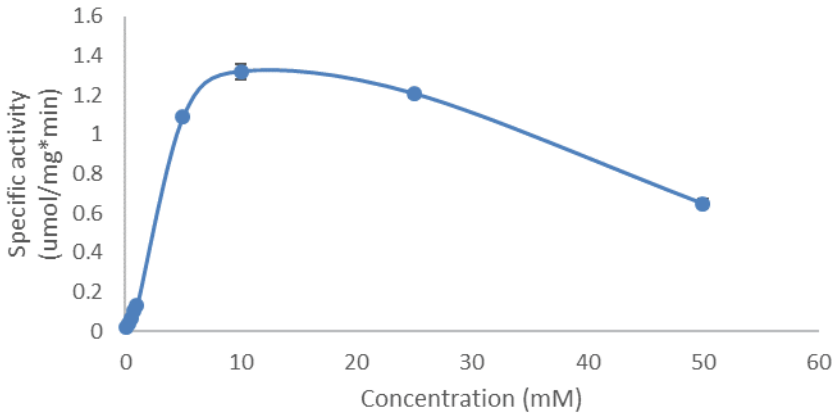

Figure 3.2. Enzyme kinetics toward G6P. The assay was performed in buffer HEPES-K 50 mM pH 8, Mg (II) 5 mM, wild type HADTn 0.05 mg/ml at 70°C, 300 rpm.

Based on non-linear regression calculation, V_{max} and K_m are 1.61 µmol/min*mg and 4.1 mM respectively. For further initial characterisations, 5 mM of G6P was used because it is desirable to run an enzymatic assay in substrate concentrations higher than the K_m. For initial characterisation, a higher concentration, e.g. 10 mM was not necessary because the aim was only to the see the effect of different parameters (pH, buffer composition, cofactor concentration).

Different buffers at a pH range were tested to see the effect of pH on the enzyme activity (Figure 3.3). Several enzymes have their unique pH optimum and it is an intrinsic

characteristic of that particular enzyme. Reaction of the enzymes in higher or lower pH will affect their activity. Optimum pH was determined with different buffer.

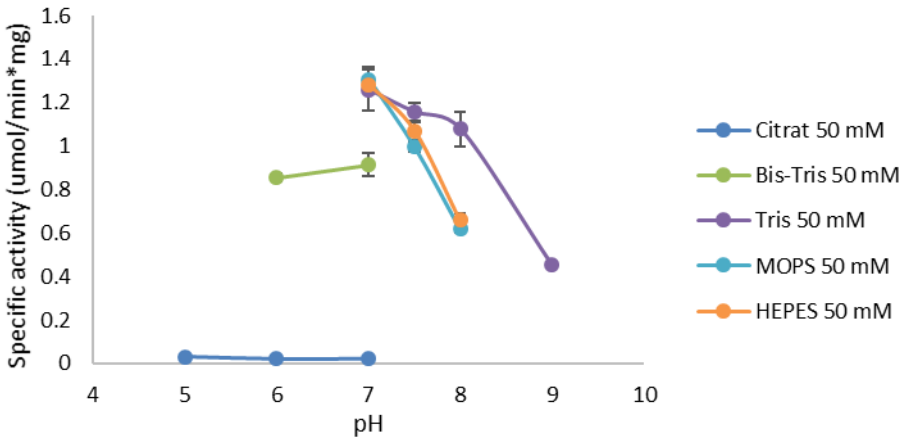

Figure 3.3. Effect of different buffers and pH on enzyme activity. The assay was performed in buffer 50 mM, Mg (II) 5 mM, G6P 5 mM, and wild type HADTn 0.05 mg/ml at 70°C, 300 rpm, and 60 minutes. Line is drawn to ease reading.

Results of the buffer tests (Figure 3.3) showed that pH 7 was the optimum pH for maximum enzyme activity and no difference in activity was observed for Tris, MOPS, and HEPES-K at pH 7. It is to be noted that no activity was observed when citrate buffer was used, irrespective of the pH, hence, this buffer was not used for further tests.

Mn (II) 0.5 mM was suggested to be used along with Mg (II) in a general phosphate assay (Kuznetsova, et al., 2005). The effect of Mn (II) addition was tested by incubating the enzyme in a buffer solution containing different concentration of Mg (II) and Mn (II), which showed that the addition of Mn (II) decreased the enzyme activity (Figure 3.4).

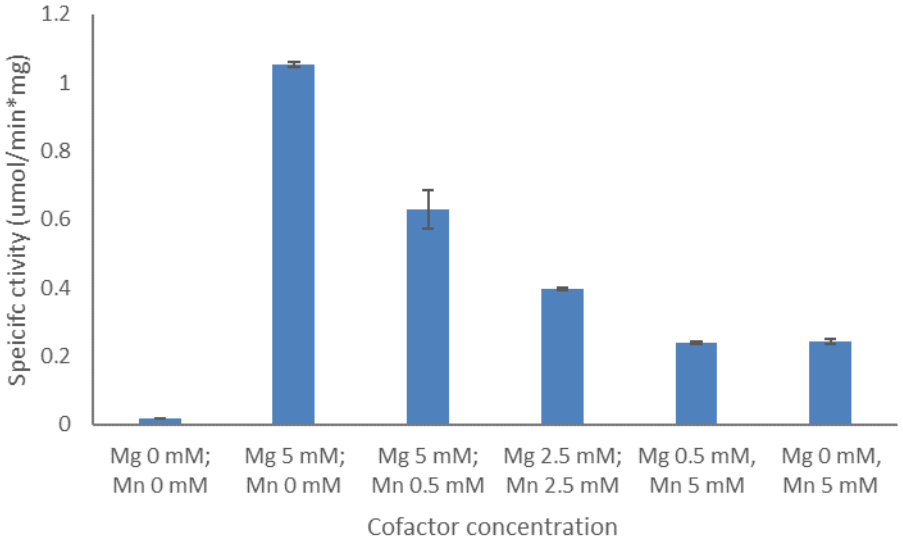

Figure 3.4. Effect of cofactor concentration on enzyme activity. The assay was performed in buffer HEPES-K 50 mM, pH 7, G6P 5 mM, and wild type HADTn 0.05 mg/ml at 70°C, 300 rpm, and 60 minutes.

Mg (II) at different concentrations and its effect on enzyme activity was also studied. It showed that there was no increased enzyme activity observed when the concentration of Mg (II) was higher than 2.5 mM (Figure 3.5). This study also confirmed that Mg (II) is

necessary for enzymatic activity; the activity decreased on decreasing the concentration to <2.5 mM.

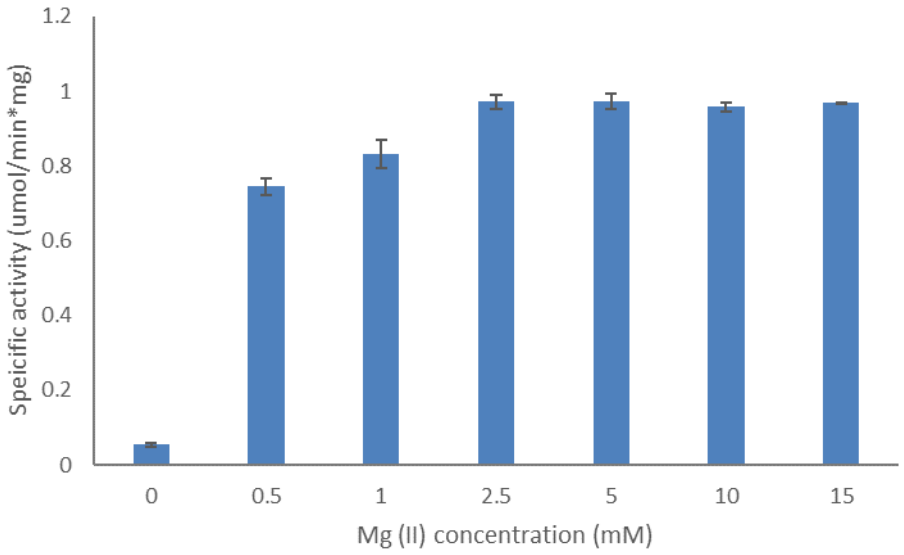

Figure 3.5. Effect of Mg (II) concentration on enzyme activity. The assay was performed in buffer HEPES-K 50 mM, pH 7, G6P 5 mM, and wild type HADTn 0.05 mg/ml at 70°C, 300 rpm, and 1 hour.

Based on the test for pH, buffer compatibility, and cofactor requirement (Figure 3.3 – Figure *3.5*); standard condition (HEPES-K 50 mM, pH 7, Mg (II) 5 mM and incubation at 70°C) were used for all subsequent tests if not stated otherwise.

Several mutants developed by QC were characterised further to determine their kinetic parameters. Six to eight different concentrations (1, 2.5, 5, 7,5, 10, 15, 25 mM) of ligands (G6P and F6P) were used to calculate the V_{max} and K_m. Sampling time was 0, 15, 30, 45 minutes. SigmaPlot was employed to calculate the Michaelis-Menten parameters. In the wild type enzyme as well as mutants, the concentration of ligands up to 25 mM showed an inhibition effect. This could be due to the substrate or the product and was to be investigated further. Since the Michaelis-Menten model does not consider inhibition effects, the initial rates (v_0) were used for calculation up to 15 mM (unless otherwise stated) as at this concentration the inhibition effect was not severely observed (Appendix 3). The turnover number (k_{cat}) and catalytic efficiency (k_{cat}/K_m) were calculated from V_{max} and K_m generated from SigmaPlot. These two parameters were used to compare the WT and mutant enzymes. The turnover number is directly proportional to V_{max} (Equation 2). However, catalytic efficiency is a better parameter to measure specificity than Km (Plesner, 1986), but it has to be used with caution. It was proposed to compare specificity of an enzyme toward its substrates. It should not be used to compare different enzymes acting on the same substrate (Eisenthal, et al., 2007). Thus, to make this powerful parameter become useful in comparing a decrease or an increase in the characteristic of the mutant enzymes, a ratio was calculated. The ratio of k_{cat}/K_m of F6P over G6P of the same enzyme can measure the specificity of the enzyme towards F6P over G6P. The higher value of this ratio, the greater the specificity of the enzyme towards F6P than G6P.

A point mutation at position 14 seemed to lower the k_{cat} by almost 40% toward F6P and G6P (Table 3.3. *Turnover number (kcat) and catalytic efficiency of mutants*). A similar result was observed for a mutation at position 47 and a double mutation at position 14 and 47 gave almost an 80% decrease in F6P and G6P. Mutation at 166, in general, very much

decreased the activity (Table 3.3. *Turnover number (kcat) and catalytic efficiency of mutants*). By combining the mutation at S166 with S168, a different k_{cat} was obtained. Substituting the serine (S) at position 168 to arginine (R), aspartic acid (D), leucine (L), proline (P) also seemed to decrease the ratio of k_{cat}.

Different results were observed for the catalytic efficiency k_{cat}/K_m for mutation at position 14 (Table 3.3. *Turnover number (kcat) and catalytic efficiency of mutants*). There was an increase up to 40% for ratio of k_{cat}/K_m indicating that the specificity was increased towards G6P for this mutant. Substitution of a serine at position 168 (in conjunction with S166V) to arginine (R), lysine (K), and leucine (L) appeared to give comparable specificity to WT, while substitution of the same amino acid with threonine (T) and cysteine (C) demonstrated an increase of specificity toward G6P.

Table 3.3. Turnover number (kcat) and catalytic efficiency of mutants

Mutation	G6P		F6P		Ratio of k_{cat}[1]	Ratio of k_{cat}/K_m[2]
	k_{cat} (s^{-1})	k_{cat}/K_m ($M^{-1}s^{-1}$)	k_{cat} (s^{-1})	k_{cat}/K_m ($M^{-1}s^{-1}$)		
WT	0.80 ± 0.04	275 ± 14	3.40 ± 0.07	1463 ± 28	4.26	5.33
D14P	0.49 ± 0.04	111 ± 9	1.93 ± 0.11	323 ± 18	3.97	2.90
E47D	0.54 ± 0.05	89 ± 9	1.73 ± 0.04	400 ± 10	3.19	4.52
D14P, E47D	0.18 ± 0.00	42 ± 1	0.65 ± 0.03	146 ± 6	3.72	3.47
S166V, S168R	0.11 ± 0.01	30 ± 2	0.14 ± 0.01	121 ± 5	1.25	4.10
S166V, S168K	0.07 ± 0.01	11 ± 1	0.21 ± 0.01	48 ± 3	2.86	4.53
S166V, S168D	0.63 ± 0.11	20 ± 3	0.54 ± 0.08	66 ± 10	0.85	3.35
S166V, S168T	0.08 ± 0.00	28 ± 1	0.33 ± 0.02	30 ± 3	3.93	1.05
S166V, S168L	0.30 ± 0.01	53 ± 2	0.38 ± 0.01	227 ± 12	1.26	4.28
S166V, S168V	0.18 ± 0.01	62 ± 3	0.29 ± 0.00	107 ± 5	1.65	1.71
S166V, S168C	0.06 ± 0.00	25 ± 1	0.10 ± 0.01	15 ± 1	1.69	0.60
S166V, S168P	0.17 ± 0.02	16 ± 2	0.21 ± 0.05	53 ± 3	1.24	3.27

[1]Ratio is calculated as ratio of turnover number (kcat) toward F6P over G6P

[2]Ratio is calculated as ratio of catalytic efficiency (k_{cat}/K_m) toward F6P over G6P

Screening of potential amino acids positioned around the active site was also studied. Alanine scanning was used to identify residues responsible for substrate recognition. Three amino acids were chosen based on YASARA docking. The substitution of methionine at position 8 (M8), proline at position 110 (P110) and glutamic acid at position 113 (E113) to alanine showed an increase in the ratio of the binding energy and a decrease in K_d. Three mutants based on this result were developed and further characterised to determine their kinetic parameters (Table 3.4. *Turnover number (kcat) and catalytic efficiency of mutants from alanine scanning*). The same substrate concentration, incubation time, and SigmaPlot calculation also apply from previous experiments (Table 3.4. *Turnover number (kcat) and catalytic efficiency of mutants from alanine scanning*) for these mutants.

Mutation of M8 and E113 to alanine seemed to decrease the k_{cat} ratio slightly, while substitution of P110 to alanine showed a significant decrease in the k_{cat} ratio. An additional mutation at position 47 to P110A (E47D, P110A) further decreased the k_{cat} ratio. The ratio of k_{cat}/K_m for M8A showed a slight decrease than the WT, while the ratio for P110A exhibited more than 50% decrease. An addition of E47D to P11A (double mutation) seemed to increase the specificity towards F6P since the k_{cat}/K_m ratio of this mutant increased. Mutation at position 113 to alanine (E114A) decreases the ratio

Table 3.4. Turnover number (kcat) and catalytic efficiency of mutants from alanine scanning

Mutation	G6P		F6P		Ratio of k_{cat}[1]	Ratio of k_{cat}/K_m[2]
	k_{cat} (s^{-1})	k_{cat}/K_m ($M^{-1}s^{-1}$)	k_{cat} (s^{-1})	k_{cat}/K_m ($M^{-1}s^{-1}$)		
WT	0.80 ± 0.04	275 ± 14	3.40 ± 0.07	1463 ± 28	4.26	5.33
M8A	0.43 ± 0.01	71 ± 2	1.35 ± 0.05	285 ± 10	3.14	4.00
P110A	0.99 ± 0.01	334 ± 2	2.02 ± 0.06	638 ± 19	2.03	1.91
P110A, E47D	1.33 ± 0.17	145 ± 18	1.77 ± 0.13	433 ± 31	1.33	2.99
E113A	0.40 ± 0.00	153 ± 2	1.07 ± 0.01	441 ± 8	2.65	2.89

[1]Ratio is calculated as ratio of turnover number (kcat) toward F6P over G6P

[2]Ratio is calculated as ratio of catalytic efficiency (k_{cat}/K_m) toward F6P over G6P

3.3 High-Throughput Screening

Before any experiments to develop the screening method were performed, two important problems needed to be addressed. First being the media used and second is the method used to quantify phosphate produced. In a standard auto-induction media, a considerable amount of phosphate is present (Table 2.2). This was a problem because the product measured was also phosphate. On modifying the media with no or negligible amount of phosphate, *E. coli* BL21 (DE3) strain could not grow. Kanamycin concentration was lowered to compromise the lack of phosphate components. With the new modified auto-induction media (Table 2.2), *E. coli* BL21 (DE3) was able to grow and produce the protein.

The second problem that needed to be addressed was the method of detection. It was preferable to use low substrates' concentration because the number of libraries would be used. A sensitive method needed to be devised. P I assay is sensitive but a quick incubation (2 minutes) was not preferable. Higher concentrations of cations in P II assay was tested and the sensitivity of the method was greatly improved (Appendix 5.1-D). It could reach the same sensitivity as in P I assay (100 µM or 3 nmol). However, at high Mo (IV) concentrations, precipitation occurred in the storage condition (4^{o}C). In the modified method, the pH of ascorbic acid was not adjusted to 5 as in P II assay, rather it was kept unadjusted. At a low pH, the sensitivity of this modified method (P III assay) was greatly increased. With this method, it was possible to detect phosphate concentrations below 3 nmol (100 µM) (Appendix 5.1-C). These two modifications allowed the HTS to be performed even at low substrates concentrations.

3.3.1 High-Throughput Screening development

Reliability and quality are the main criteria for the evaluation of a screening method. Several parameters were tested such as concentration of substrates, incubation time, and whether or not to include OD in the calculation for their effect. In a high throughput screening, one important consideration is the distribution of variation. Using the standard deviation is one possibility to interpret the distribution of variation. One statistical test that is widely used for high throughput screening is based on the Z-factor (Z') (Zhang, et al., 1999). The Z-factor formula is described in Equation 3

$$Z' = 1 - \frac{3(\sigma_p - \sigma_n)}{|\mu_p - \mu_n|} \qquad \text{Equation 3}$$

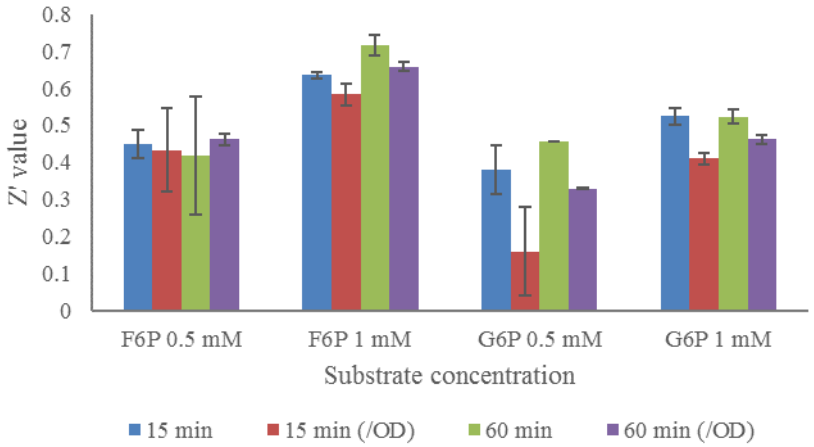

Figure 3.6. Result of Z' value of wild type landscape tested on 96 well plate format. The Z' values were obtained from the average of two independent plates. The incubations were performed in PCR plates at standard condition with different substrates concentrations.

Three times standard deviation (σ) was used because 99.73% of the data distribution will lie within this range ($\mu \pm 3\sigma$). This parameter calculates the difference between the data from positive control (p) to negative control (n). Higher Z' corresponds to higher separation between data from positive control to negative control.

Table 3.5. Correlation of Z-factor value to screening performance

Z-factor value (Z')	Relation to screening
1	An ideal assay
$1 > Z \geq 0.5$	An excellent assay
$0.5 > Z \geq 0$	A double assay
0	A "yes/no" assay
< 0	Screening is not possible

Adapted from (Zhang, et al., 1999)

In general, a higher concentration of the substrate and a longer incubation time, improved the Z'. The effect was different in relation to the substrates used, for 1 mM F6P the effect was more pronounced than for 1 mM G6P. Incorporation of OD slightly decreased the Z' value (Figure 3.6). Based on this result, concentration of 1 mM substrate and 15 minutes of incubation were chosen as the standard parameters for library screening.

Although Z' is a popular statistical parameter to evaluate the quality of a screening method, it does not actually give enough information on how each value in each well differ from the average value (Zhang, et al., 2008). Thus, the activity landscape of wild type for both substrates as well as the landscape of the activity ratio (F/G) were also presented. This analysis would further tell the percentage of outliers.

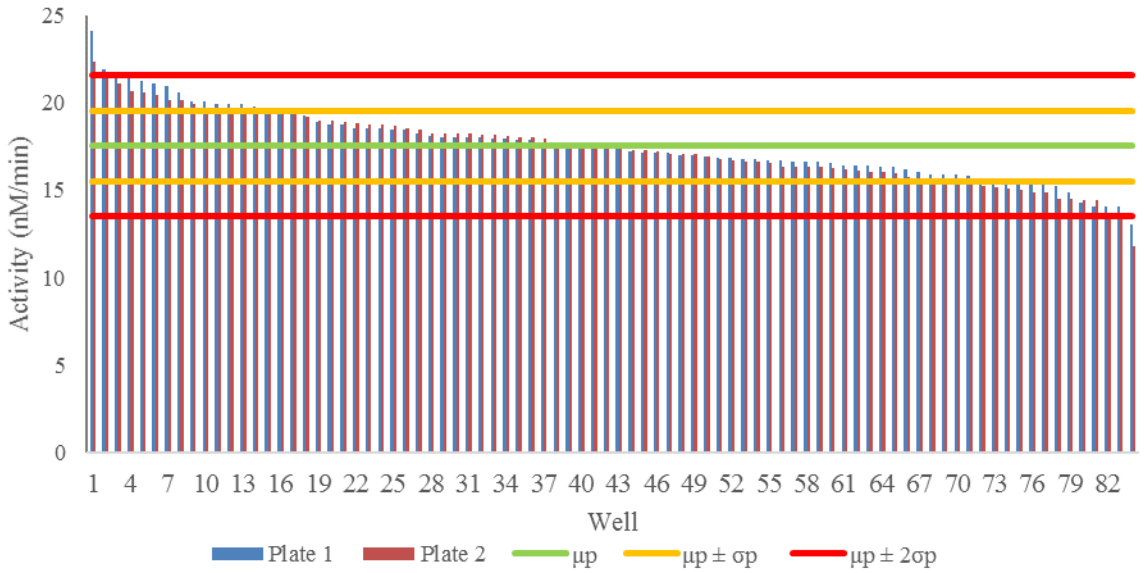

Figure 3.7. Activity landscape of wild type toward F6P tested on 96 well plate format. The values were obtained from the average of two independent plates. The incubations were performed for 15 minutes at 70°C in PCR tubes at standard condition with F6P 1 mM.

The analysis of the activity landscape for F6P shows that there are 28 variants of the wild type (17.5%) showed a higher activity than the average plus one standard deviation ($\mu_p + \sigma_p$) while 26 variants (16.3%) showed a lower activity than $\mu_p - \sigma_p$. There are 5 variants (3%) that showed a higher activity than $\mu_p + 2\sigma_p$ and 3 variants (1.9%) that showed lower activity than $\mu_p - 2\sigma_p$ (Figure 3.7).

A similar result was observed when G6P was used as the substrate. From the analysis of the result (Figure 3.8). 23 of wild type variants (14%) showed a higher activity than $\mu_p + \sigma_p$ and 56 variants (35%) showed lower activity than $\mu_p - \sigma_p$. These make it a total of up to 50% of the variants outside the range of $\mu_p \pm \sigma_p$. It is because the activity between each plate differed noticeably (18% difference calculated from the plate with smallest activity). The result of the activity landscape towards G6P also shows that there are 4 variants (2.5%) that had a higher activity than $\mu_p + 2\sigma_p$ and 2 variants (1.3%) lower than $\mu_p - 2\sigma_p$. This finding confirms that a reliable comparison can only be performed within one plate and not between plates.

The result of the activity landscape towards F6P (Figure 3.7) and G6P (Figure 3.8) were used to calculate the ratio of the activity (Figure 3.9). This value is important for consideration in determining the improved variants so the evaluation of data variation homogenous to WT was needed. Results presented in Figure 3.9 show that there were 58 variants (36%) that lie outside the range of $\mu_p \pm \sigma_p$ (20% higher and 16% lower). There are 5 variants (3%) that showed an activity outside the range of $\mu_p \pm 2\sigma_p$ (2% higher and 1% lower).

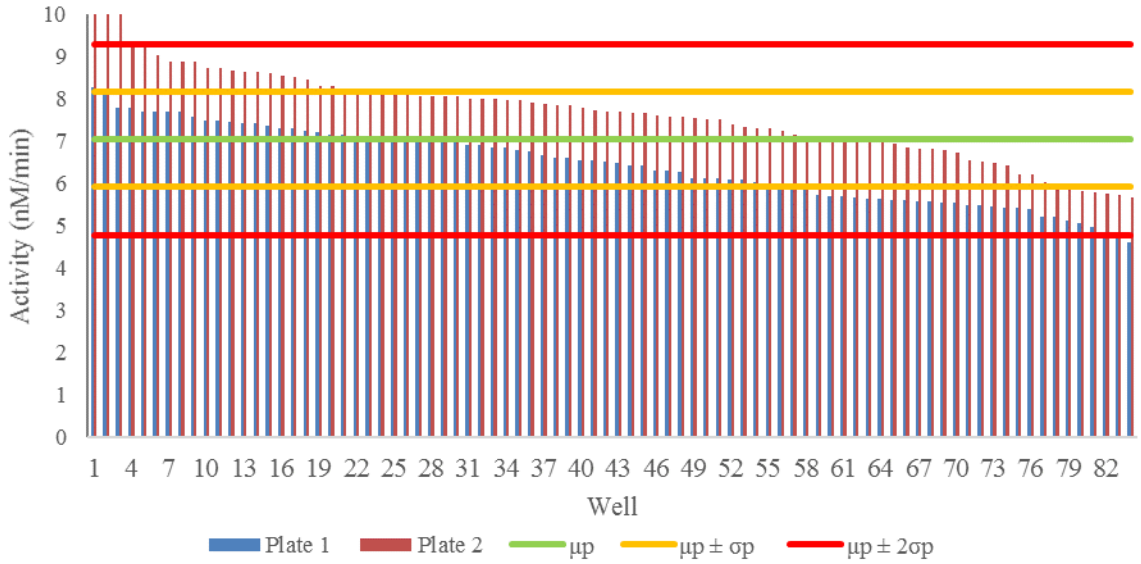

Figure 3.8. Activity landscape of wild type toward G6P tested on 96 well plate format. The values were obtained from the average of two independent plates. The incubations were performed for 15 minutes at 70°C in PCR tubes at standard condition with G6P 1 mM.

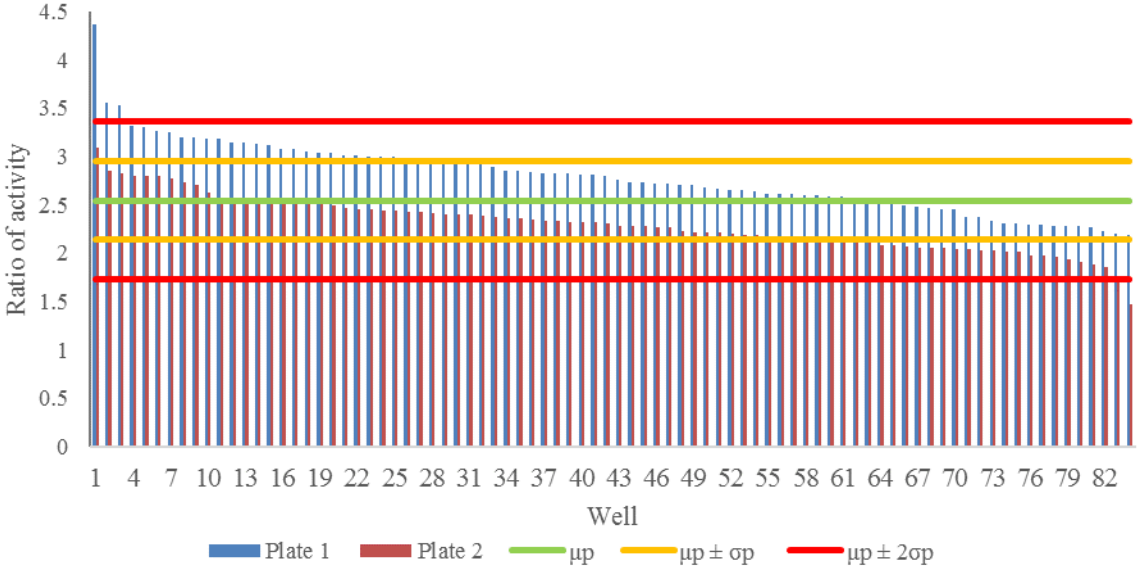

Figure 3.9. Ratio of activity landscape of wild type tested on 96 well plate format. The values were obtained from the ratio of activity from two independent plates (value of each well from Figure 3.7 divided by value from respective well in Figure 3.8)

3.3.2 High-Throughput Screening for Library

HTS for the library evaluation was aimed to screen variants from several libraries developed through QuikChange™ Site-Directed Mutagenesis (Table 3.6). The HTS consisted of three screening rounds to ensure the detection of improved variants.

3.3.2.1 First screening

This step was to detect possible improved variants. There were certain criteria set to decide whether one variant (from one well) is a hit or not. Variants were considered for the next screening if and only if it showed one of these behaviours (the cut-off),

- Increased activity toward F6P (at least by 20% over $\mu_{WT} + \sigma_{WT}$) and decreased or the same activity toward G6P (group A). The 20% was added to compensate the fact that there were WT variant that showed a higher activity than $\mu_{WT} + 2\sigma_{WT}$ (*Figure 3.7*). The same phenomenon could also be found for the mutants. An additional 20% would eliminate false positives because σ_{WT} for F6P is around 10% (*Figure 3.7*)
- Decreased activity towards both but the effect is severe for G6P (at least by 30%) (group B). This cut-off was set because variants that might belong to this group could be used as a starting point to combine with other mutations as they had shown some mutations with decreased activity towards G6P (Table 3.3)
- Showed increased activity toward both but the effect is higher for F6P (at least by 20% over average of ratio F/G + 1SD) (group C). This cut-off was set due to similar consideration as for variants that might belong to group B
- A different categorisation was also made to see the effect of the mutation in general. The fourth categorisation (group D) included variants that showed an increased activity towards both substrates but with higher effect for G6P. However, variants of group D were neglected for the following screening steps because the aim of this work was to find variants with improved activity and specificity toward F6P.

For P46NNK library, 4 negative controls were used and those were media alone. This was because from previous experiments, the negative control with *E. coli* transformed with empty pET28 plasmid did not show any significant activity (Appendix 3.1). 8 positive controls consisting of wild type enzyme were used as an internal control compensating the difference in activity towards G6P among plates (Figure 3.11). Due to the poor quality of the developed library (75% WT background), four plates were used.

Table 3.6 List of libraries screened

No	Mutation*
1	Y19NNK
2	E47NNK
3	E47 NNK, D14P
4	P46NNK
5	46_47insNNK[1]
6	R117NNK
7	M8NNK
8	P110NNK

*Explanations of abbreviations are presented in Figure 1.5

[1]Insertion of an amino acid (NNK motif) to the position between 46 and 47 in HADTn

The results of the first screening of other libraries are presented in Appendix 3.1 and will not be discussed in this section. An insertion between amino acid at position 46 and 47 with NNK (Figure 1.5) only resulted in a single variant (46_47insMet). Activity assay of this variants gave no activity (Appendix 3.1).

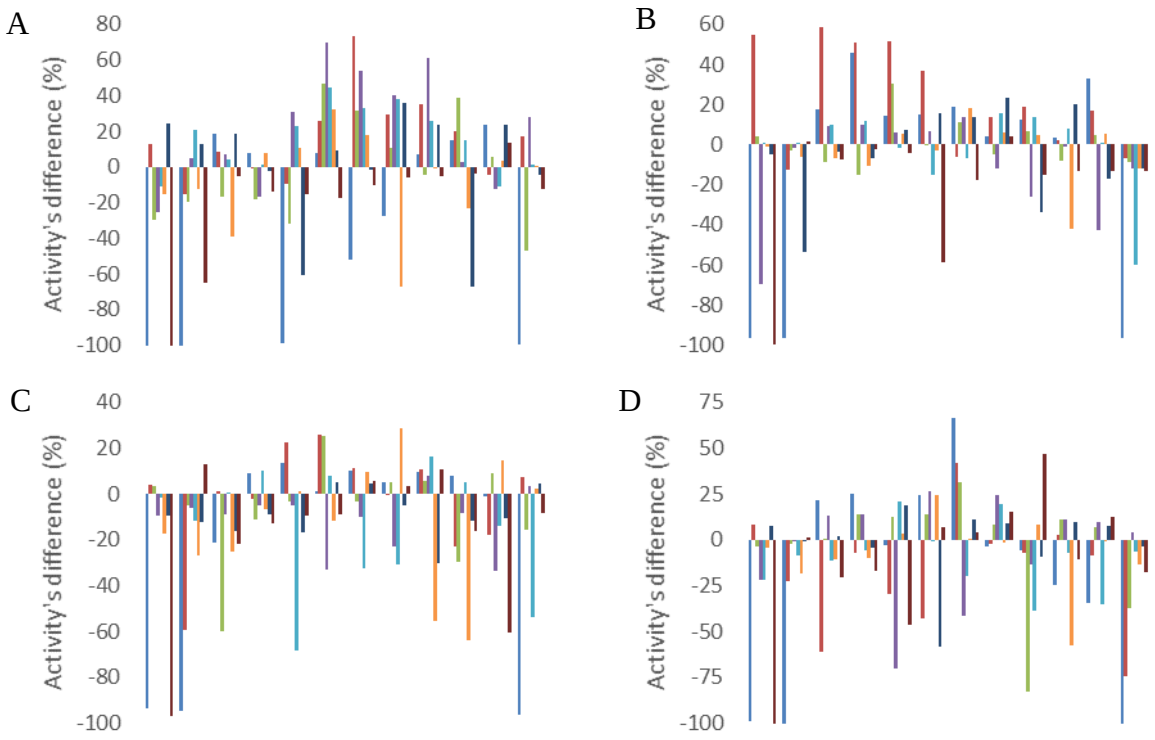

Figure 3.10. Activity assay of P46NNK library from 4 plates toward F6P. Zero value represents no difference with WT. Total variants in one plate are 84. Average of activity of WT in plate 1 was 13.5±10.8%, in plate 2 was 14.4±11%, in plate 3 was 17±7.1%, and in plate 4 was 15.5±8.1% ng/min.

A mutation at this position (P46NNL) gave 80 variants (26.8%) that appeared to have an increased activity (activity > $\mu_{WT} + \sigma_{WT}$ for each plate), while 111 variants (33%) seemed to show decreased activity (activity < $\mu_{WT} - \sigma_{WT}$ for each plate) towards F6P (Figure 3.10). A similar result was observed towards G6P; there were 109 variants (32.4%) that appeared to have an increased activity and 110 variants (32.7%) that appeared to have a decreased activity (Figure 3.11). The F/G ratio is an important parameter to confirm further if an increase in activity toward F6P also observed for G6P. 110 variants (27.1%) appeared to have a higher F/G ratio and 131 variants (39%) appeared to have lower F/G ratio (Figure 3.12)

Based on the cut-off set previously, there were 33 variants picked for the second screening. Fifteen variants (4.5%) appeared to belong to the group A, 9 variants (2.7%) seemed to belong to group B, and 9 variants (2.7%) appeared to belong to group C. There were 4 variants (1.2%) that belonged to group D, but these variants were not of interest for further screening

.

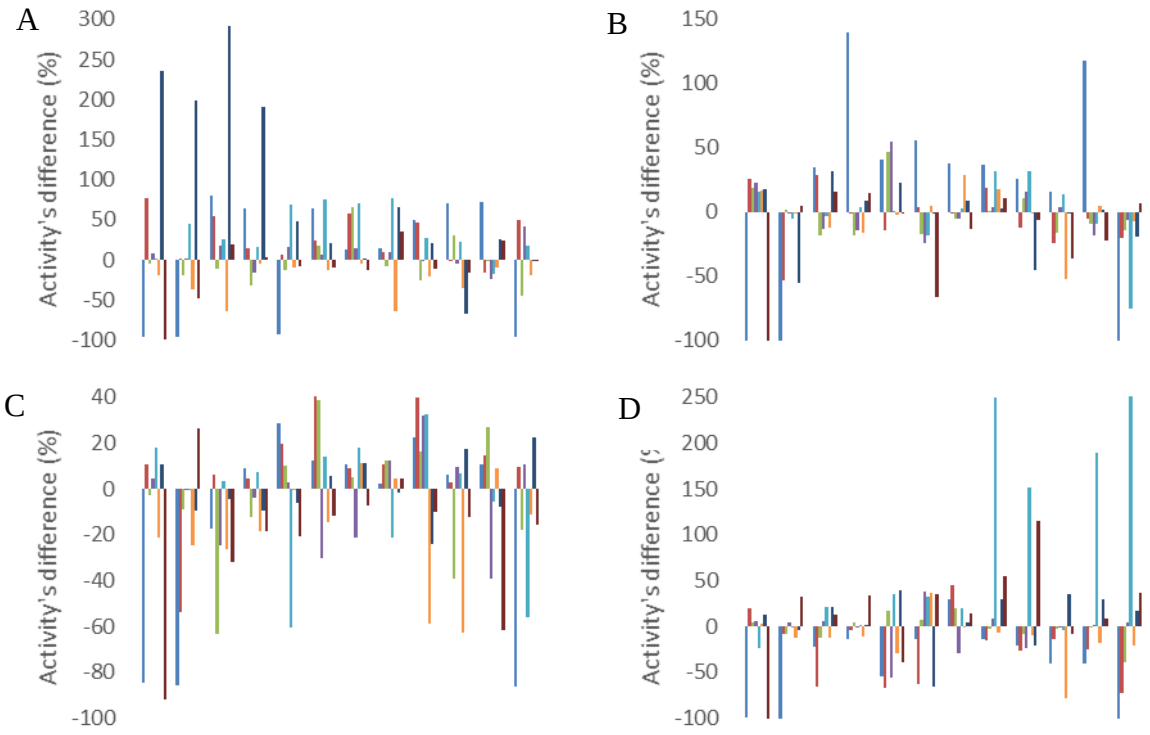

Figure 3.11. Activity assay of P46NNK library from 4 plates toward G6P. Zero value represents no difference with WT. Total variants in one plate are 84. Average of activity of WT in plate 1 was 5.1±13.8%, in plate 2 was 4±10.3%, in plate 3 was 6.4±10.9%, and in plate 4 was 4.9±8% ng/min.

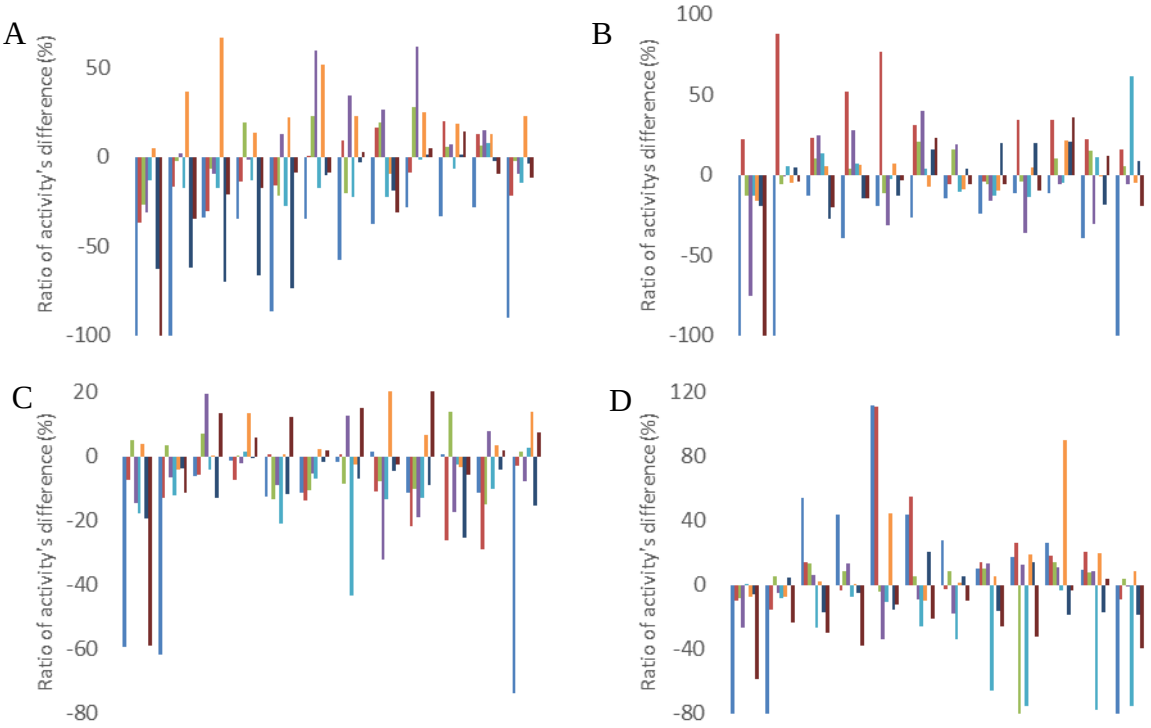

Figure 3.12. Ratio of activity assay (F6P/G6P) of P46NNK library from 4 plates. Zero value represents no difference with WT. Total variants in one plate are 84. Average of F/G ratio of WT in plate 1 was 2.7±8.3%, plate 2 was 3.6±5.7%, in plate 3 was 2.6±10.9%, and in plate 4 was 3.2±7.8%.

3.3.2.2 Second screening

This step was performed to make further confirmations from hits detected from the first screening. Similar criteria were also used to confirm the hits in the second screening. In every figure (Figure 3.13 and Figure 3.14) that follows, a coloured arrow was used to point the hit and to categorise them into the groups that have been previously defined. A blue arrow represents variants that appears to belong to group A, orange is for group B while purple is for group C. Similar to the first screening rounds, only the results from P46NNK library will be discussed while results from other libraries are presented in Appendix 3.2.

From the 33 variants picked, there were only P46X.23 and P46X. 29 variant that showed a slightly higher F/G ratio (Figure 3.13). These variants also showed higher activities towards F6P than the wild type. In the first screening, both variants appeared to belong to group C. Other variants did not show any significant difference in F/G ratio. There might be a possibility that one colony picked from the first screening consisted of cells bearing more than one type of plasmid. Thus this colony would develop to more than one type of cells producing different kinds of mutant enzymes which might explain variants that showed a high standard deviation. Each replicate of these variants were then considered independently and replicates that showed activity that appeared to belong to group A-C were picked for further screening. In the first screening, P46X.5, P46X.8, P46X.10, P46X.13, and P46X.31 appeared to belong to group C, A, B, A, and C respectively. In the end, only P46X.8 and P46X.13 retained their behaviour.

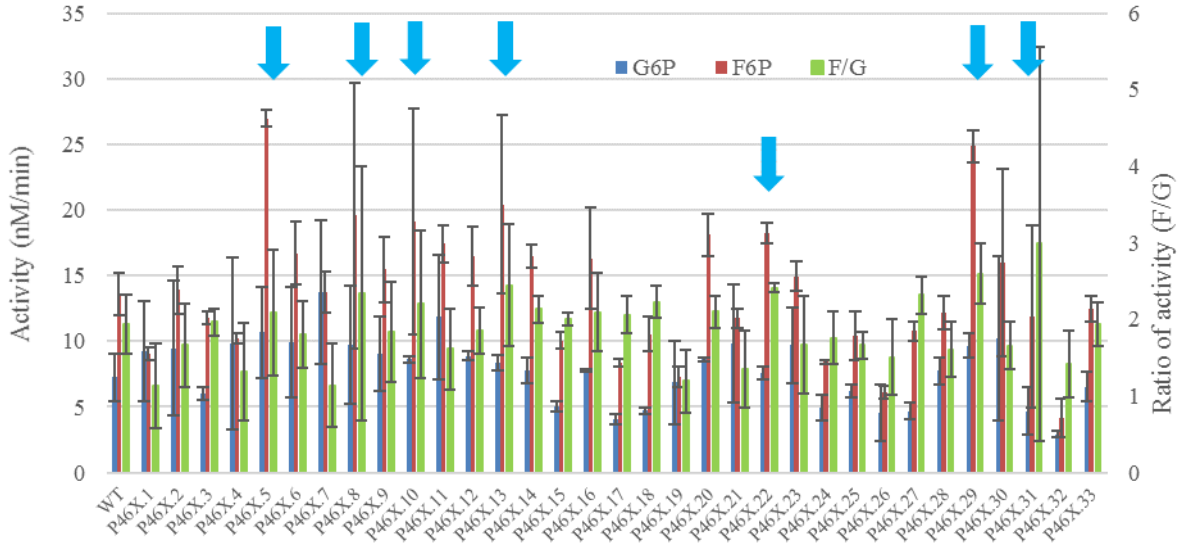

Figure 3.13. Result of second screening from variants picked from first screening of P46NNK library. Arrows represents variants that were picked for third screening.

3.3.2.3 Third screening

This step was to further purify the variants by isolating plasmids of each variant chosen from the second screening. Plasmids isolated were then transformed to *E. coli* BL21 (DE) for enzyme production. As a continuation from the first and second screening, only the P46NNK library will be discussed hereafter.

Results shows that F/G ratio showed no significant difference in all variants (Figure 3.14) However, P46X.5 and P46X.30 variants demonstrated a significant increase of activity toward F6P. Both were sent for sequencing and the results of sequencing showed that both of them have a mutation at position 46 to threonine (P46T).

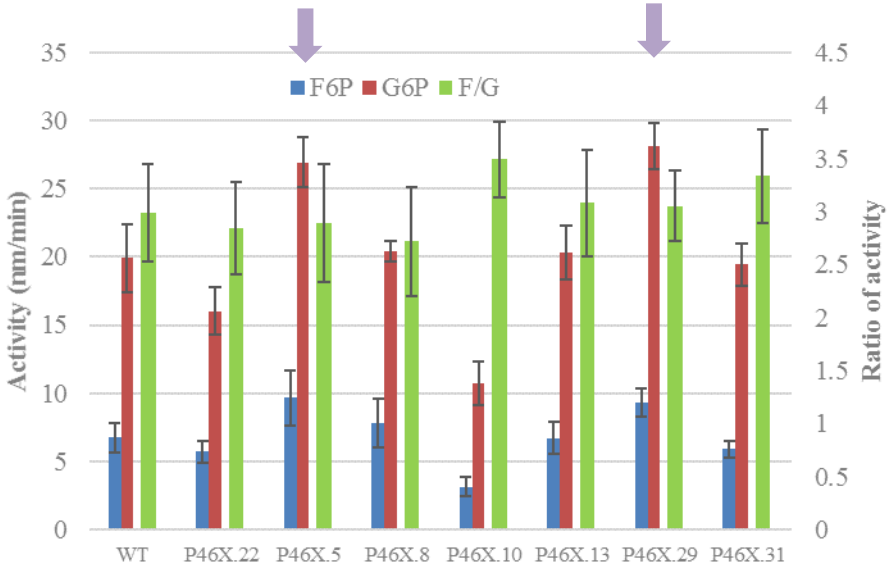

Figure 3.14. Result of third screening from second screening of P46NNK libraries. Arrow represents variants picked for sequencing.

3.3.2.4 Summary of high-throughput screening for library

In each screening round considerable amounts of what identified hits decreased (Figure 3.15). In the first screening rounds, 120 variants were picked (8.1% relative to samples). They consisted of 52 variants that appeared to belong to group A, 54 to group B, and 14 to group C. in the next screening rounds, 4 variants were identified to appear activity of group A, 11 variants of group B, and 7 variants of group C making in total, 22 variants (1.5% relative to samples or 18.3% to variants tested in second screening) were picked for last screening. There were 5 variants picked for sequencing, 3 appeared to belong to group A and 2 appeared to belong to group C. Variants picked for sequencing represented only 0.33% relative to variants generated or 22% relative to variants tested in third screening. Three variants were sequenced as wild type while the other two were the same P46T.

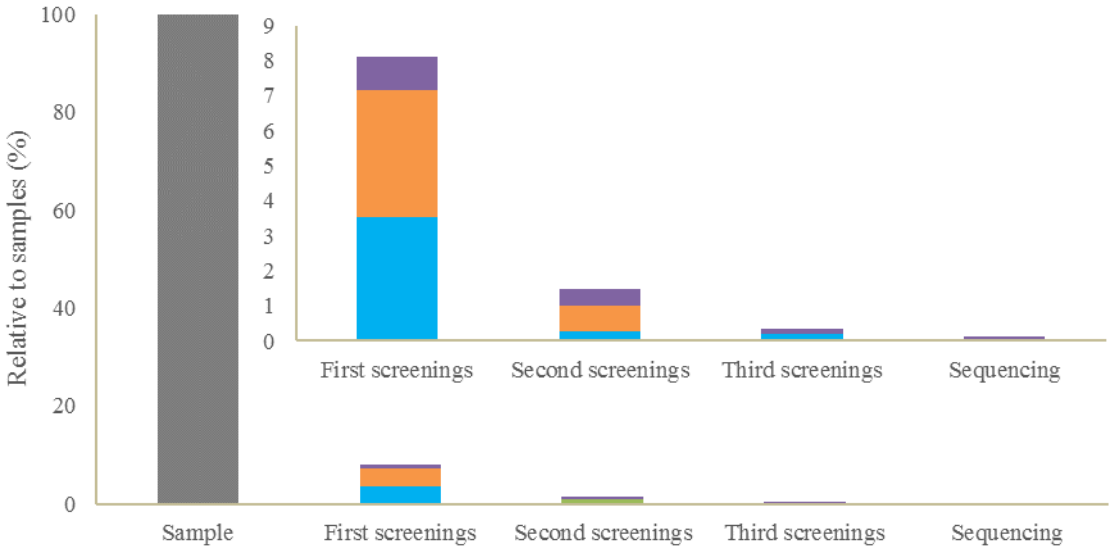

Figure 3.15. Summary of HTS for library. One hundred percent samples consisted of 1480 colonies picked that could be different variants from 7 libraries. Second diagram is the zoom out of data from the main diagram to give better visualisation of small data. Blue colour represents colonies that appeared to belong to group A, orange was for group B, and purple was for group C (similar colour explanation as in Figure 3.13 and 3.14).

3.4 Final Characterisation

The wild type enzyme as well as HADTnP46T were purified for final characterisations. Kinetic characterisation was performed as previously described. The mutant enzyme showed an increased k_{cat} compared to wild type toward both substrates. K_m of HADTnP46T appeared to decrease for F6P and increase for G6P in relation to WT. Catalytic efficiency ($k_{cat}//K_m$) of the wild type enzyme was higher towards F6P than G6P. The mutant also exhibited a higher $k_{cat}//K_m$ towards F6P than G6P. Ratio of catalytic activity (F6P/G6P) of WT is 5.5 while for HADTnP46T is 8.8 (Figure 3.16). A possible interaction of the amino acid at position 46 is depicted in Figure 3.17.

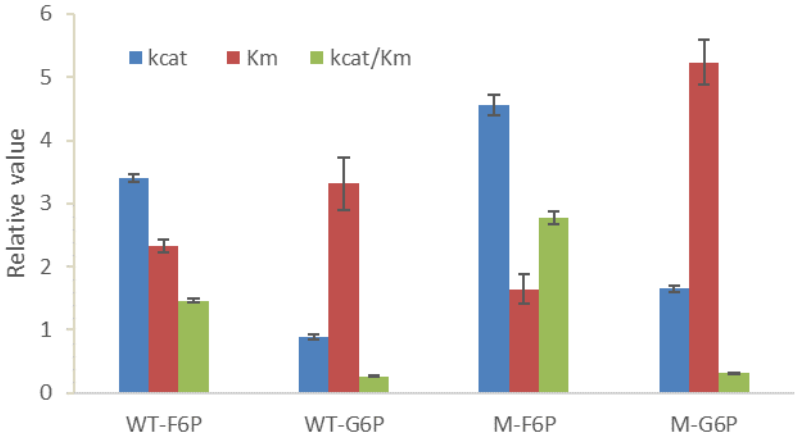

Figure 3.16. Kinetic parameters for final characterisation. Mutant enzyme was P46T. Unit for Vmax, Km and Vmax/Km is µmol/min*mg, mM, x 1000 $M^{-1}s^{-1}$) respectively. The incubations were performed in PCR tubes with standard condition using different G6P and F6P concentration

A probable fifth loop that may play a role in the substrate recognition proposed by (Lahiri, et al., 2004) is depicted in Figure 3.18. The fifth loop is a helix-loop-helix and started with conserved glycine (in HADTn is G44). Mutations of amino acids in this loop performed in this work (P46T, E47D) are also depicted to give a view of the relative mutations to the substrate (F6P).

The temperature stability was also investigated. In this final characterisation, concentration of Mg (II) in the incubation buffer was increased to 100 mM because it was observed in previous experiments that adding Mg (II) up to 5 mM did not give any effect on temperature stability. Incubation time in Tris buffer (desalting solution) was also prolonged from 240 minutes to 1440 minutes. Two substrates (G6P and F6P) were used. Results showed that prolonged incubation at high temperatures decreased the enzyme activity towards G6P (Figure 3.19) and F6P (Figure 3.20). There was no apparent difference for wild type and mutant enzyme in term of activities. Both showed lower enzyme activity after 1440 minutes of incubation at high temperatures. Addition of 100 mM magnesium ions seemed to stabilise the enzyme, for both the wild type and mutant (P46T).

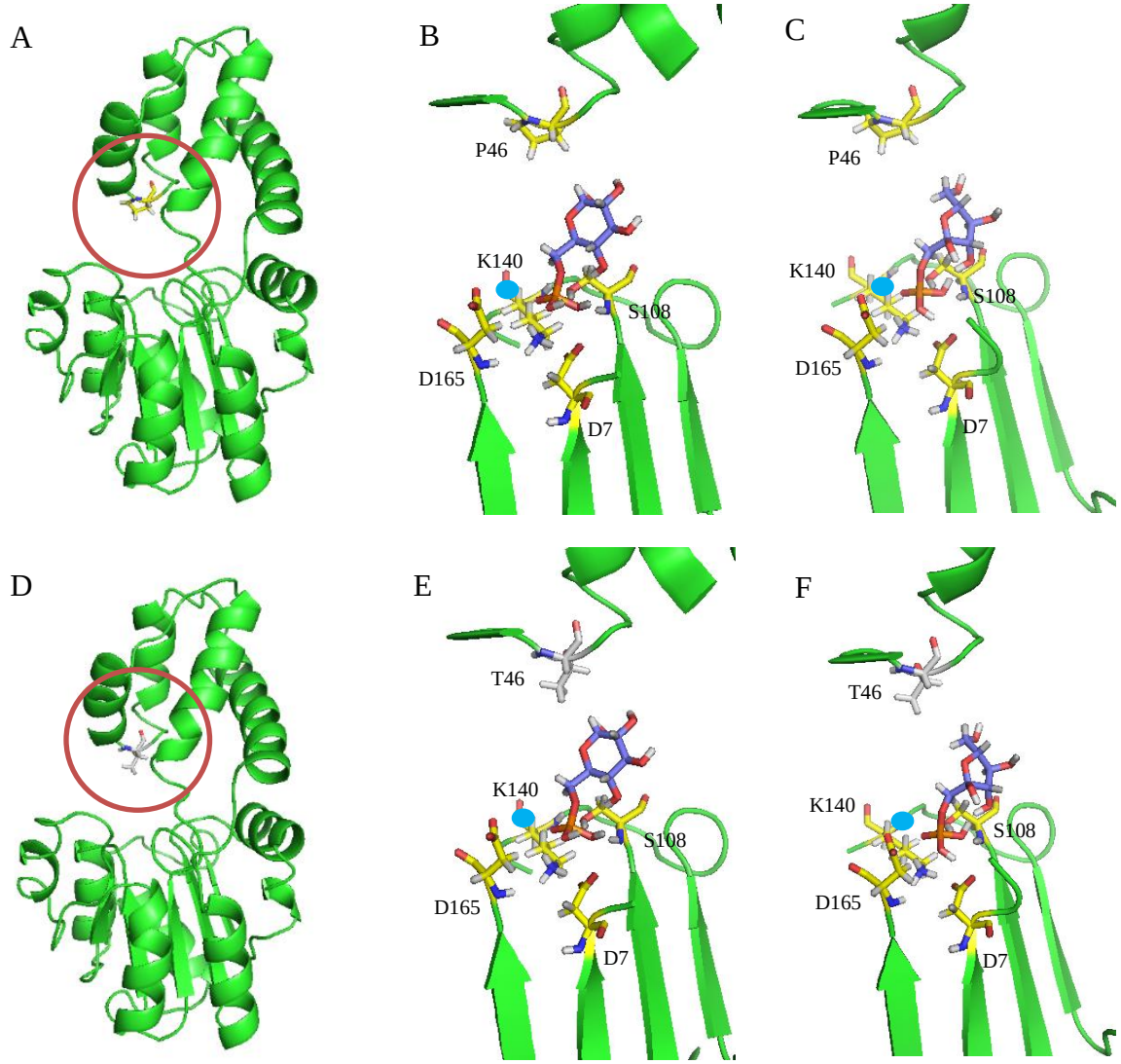

Figure 3.17. Visualisation of possible interaction of amino acid at position 46 from wild type (A, B, C) and mutant enzyme (D, E, F) toward G6P (B, E) and F6P (C, F). Mutation of proline at position 46 to threonine (T) was done in PyMol using the result of docking by YASARA (Figure 3.1). Carbon atoms of mutant (Threonine) are given in white.

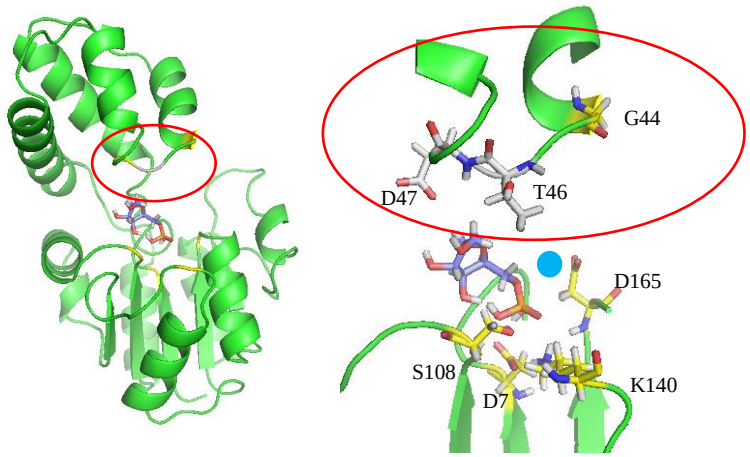

Figure 3.18. Visualisation of the possible fifth loop (red circles) of HADTnP46T according to the proposal by (Lahiri, et al., 2004) docked with F6P.

Further analyses were performed to see the effect of Mg (II) and mutation in relation to the enzyme stability at higher temperatures. Two useful parameters were used, thermal inactivation constant (k) and half-life ($t_{1/2}$). Thermal inactivation constant (k) describes the rate of loss of enzyme activity in relation to the temperature. A higher value of k corresponds to a more pronounced effect of temperature to an enzyme. Half-life ($t_{1/2}$) is defined as the time at which the enzyme retains 50% of its activity. A shorter half-life corresponds to a higher k value. A simple first order kinetic reaction was used to calculate the values as per the work by Sadana (1988). For this purpose, the enzyme stability data at 94°C with F6P as substrate (Figure 3.20) were used to calculate k and $t_{1/2}$.

The result clearly shows that the addition of Mg (II) helps to stabilise the enzyme at a high temperature (Table 3.7). The half-time of WT and mutant enzymes were doubled in the presence of magnesium (100 mM). Mutation at position 47 appeared to decrease the enzyme stability slightly with a shorter half-life for the mutant rather than the wild type in the absence of magnesium. The assumption that the reaction was of first order was also investigated to be correct, as seen from high R^2 values (>0.96).

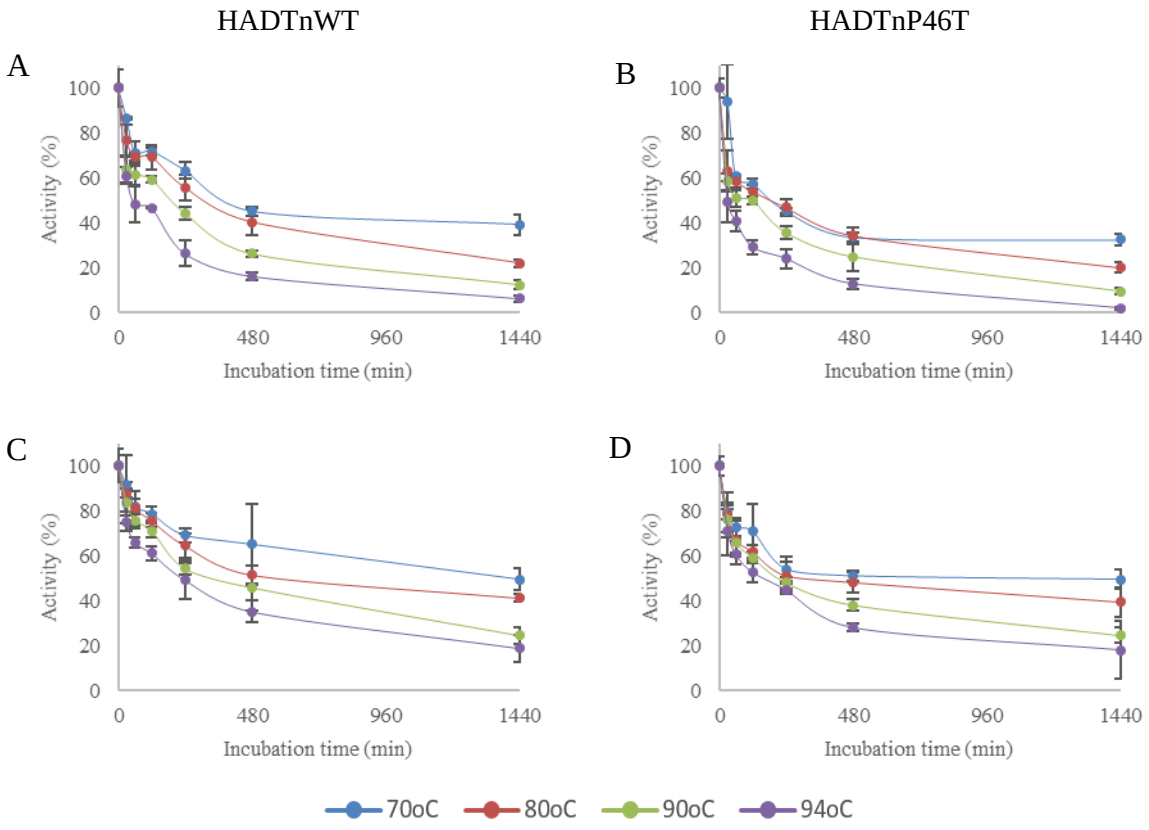

Figure 3.19. Effect of Mg (II) addition on wild type (A, C) and mutant enzyme (P46T) (B, D) stability at different temperatures over time measured as activity toward G6P. The incubations were performed in PCR tubes containing enzyme 1.7 mg/ml for both in buffer Tris-HCl 50 mM pH 7.5 with Mg (II) 100 mM (C, D) and without (A, B). After rapid cooling, the remaining activity was measured in standard condition with G6P 5 mM, and enzyme concentration 0.01 mg/ml at 70°C for 15 minutes. One hundred percent activity is 1.2 (A, C), 2.2 (B, D) µmol/min*mg.

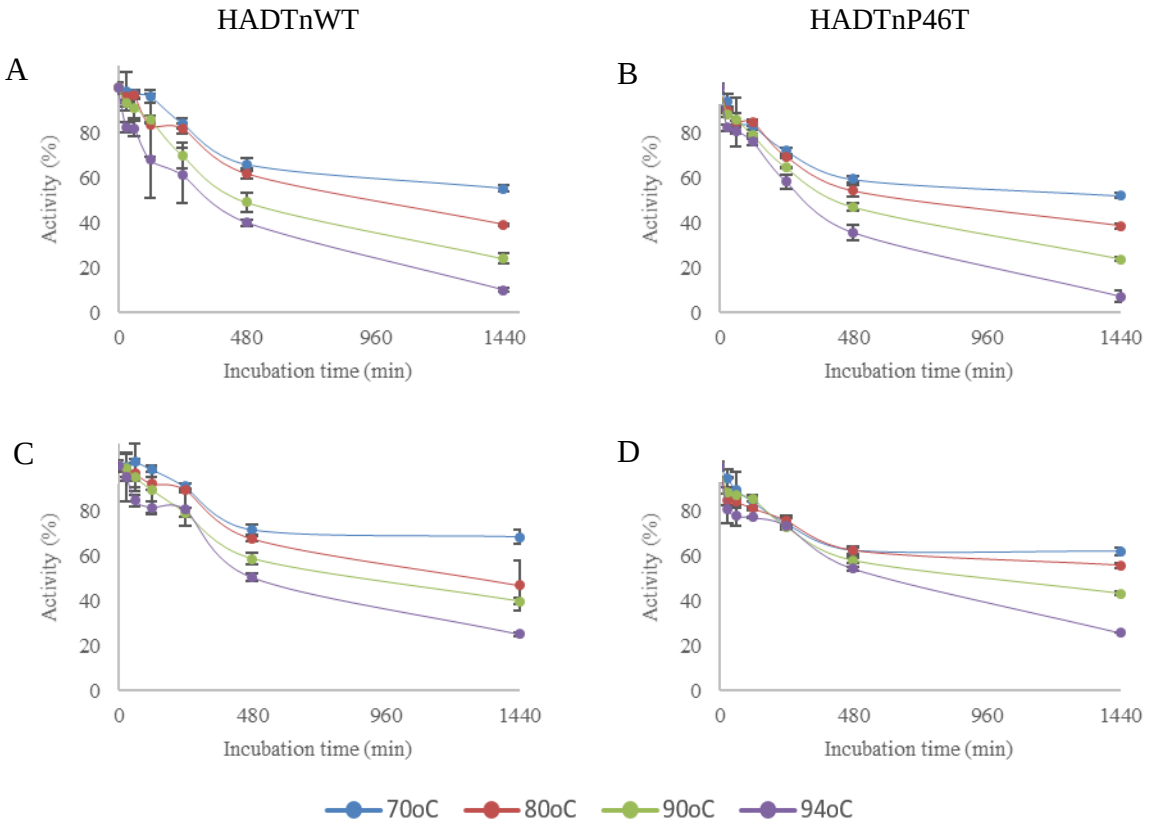

Figure 3.20. Effect of Mg (II) addition on wild type (A, C) and mutant enzyme (P46T) (B, D) stability at different temperatures over time measured as activity toward F6P. All condition was performed the same as in Figure 3.19. One hundred percent activity is 1.1 (A), 4.8 (C), 7.5 (B, D) µmol/min*mg.

Table 3.7. Thermal stability parameters for wild type and D46T HADTn.

Parameters*	Enzyme			
	Wild type		Mutant P47T	
	Without Mg (II)	With Mg (II)	Without Mg (II)	With Mg (II)
k (x 10^{-3} min^{-1})	1.52 ± 0.09	0.94 ± 0.04	1.77 ± 0.04	0.86 ± 0.02
$t_{1/2}$ (min)	454 ± 26	736 ± 30	392 ± 9	809 ± 17
R^2	0.9929	0.9694	0.9957	0.9742

*All values were calculated at temperature 94ºC from Figure 3.20.

The effect of product inhibition was tested in two different setting. Fructose was used for reaction with F6P as substrate and glucose was used for reaction with G6P as substrate. Different concentration of fructose and glucose as well as F6P and G6P were used to determine the type of product inhibition. A lineweaver-Burk plot was derived to determine the type of inhibition. However, the plots could not show clear-cut distinction making the determination of inhibition type became difficult. Further analysis was carried out to make unbiased judgement. There parameters (V_{max}, K_m, and slope) were calculated from the plots (Figure 3.21 and Figure 3.22). Further analysis of those values shows K_m from all combination of inhibitors and enzymes had the lowest standard deviation compared to standard deviation of V_{max} and slope (Table 3.8. *Effect of product inhibition.*). Based on these results, the observed inhibition was classified as a noncompetitive inhibition (Figure 1.1).

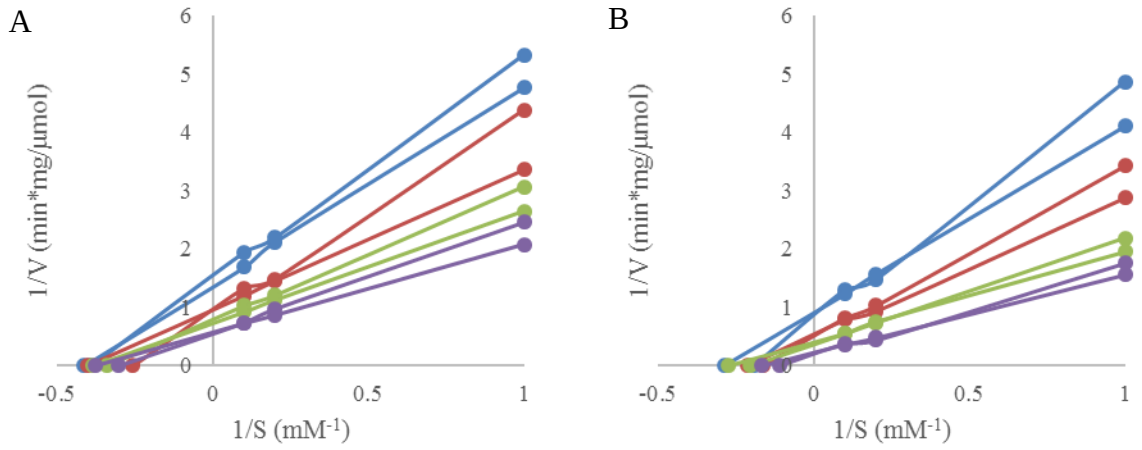

Figure 3.21. Lineweaver-Burk plot of wild type enzyme (A) and P46T (B) toward G6P in the presence of glucose. Blue line represents 1500 mM glucose, red is 1000 mM glucose, green is 500 mM glucose, and purple is no glucose presents. Reactions were performed at standard condition.

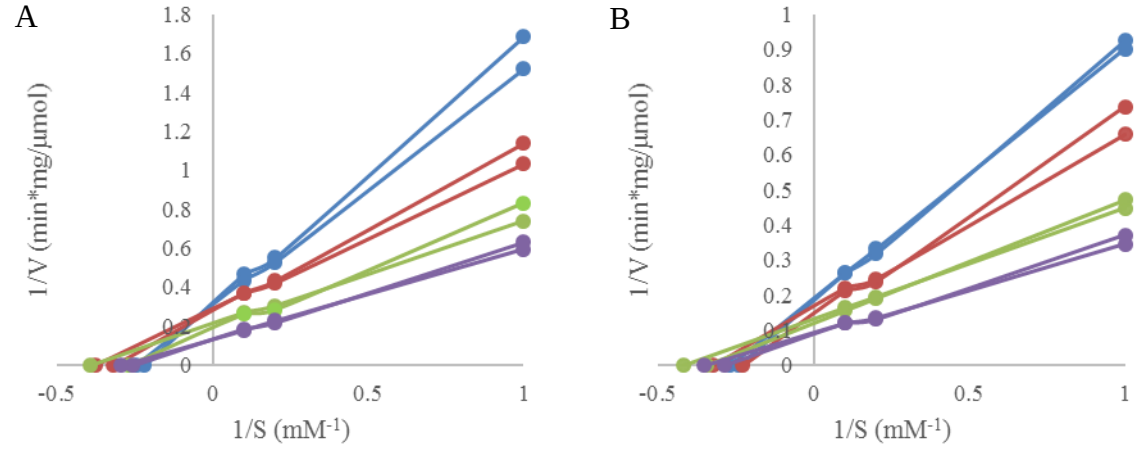

Figure 3.22. Lineweaver-Burk plot of wild type enzyme (A) and P46T (B) toward F6P in the presence of fructose. Blue line represents 300 mM, red is 200 mM fructose, green is 100 mM fructose, and purple is no fructose. Reactions were performed at standard condition.

Table 3.8. Effect of product inhibition.

Parameters*	Enzyme			
	Wild type		Mutant P47T	
	G6P/Glucose	F6P/Fructose	G6P/Glucose	F6P/Fructose
V_{max} (µmol/min*mg)	1.21 ± 34%	4.92 ± 37%	2.72 ± 59%	7.95 ± 32%
K_M (mM)	2.86 ± 18%	3.49 ± 19%	5.39 ± 33%	3.37 ± 20%
Slope (K_M/V_{max})	2.58 ± 33%	0.79 ± 43%	2.35 ± 41%	0.46 ± 42%

*All values were calculated from and Figure 3.21 and Figure 3.22

4 Discussion

4.1 Identification of catalytic centre and substrate docking

HADTn has a very close similarity with the sequence of putative β-phosphoglucomutase from *Thermotoga maritima* (Strange, et al., 2009). The crystal structure of that enzyme has been devised (1.74 Å resolution) and registered in the Protein Data Bank (RCSB PDB) as 3KBB. Sequence alignment using NCBI Blast show a 99% similarity between HADTn and 3KBB with a difference of a single amino acid. In HADTn, the amino acid at position 125 was arginine (R), while in 3KBB it was lysine (K). Amino acid 125 is located at a considerable distance from the active site (Figure 3.1 and Table 3.1) making this amino acid to be of negligible importance. 3KBB has two domains- a core domain and a flexible cap domain and consists of 53% helical (15 helices) and 12% beta sheets (9 strands). Homology modelling was carried out to get a model of HADTn for *in silico* analysis. For the homology modelling, two conditions are important. First is the availability of the crystal structure of the other enzyme that will be used as template and the second is the template should have a reasonable degree of similarity (Martí-Renom, et al., 2000). It was suggested that for two proteins bigger than 100 amino acids, they should have 30% of similarity in the sequence alignment in order to build a useful model (Sander & Schneider, 1991). Based on this suggestion, a reliable 3D structure was built with 3KBB as the template employing modelling of YASARA (Krieger & Vriend, 2014).

Although 3KBB model has a high resolution, the model devised is in the apo form. It does not have a cofactor or a substrate with the enzyme in the crystal structure. Sequence alignment was performed to identify amino acids that may participate in the catalytic reaction. Several conserved amino acids have been identified based on the sequence alignment with enzymes from the same family or enzymes that have similar activities (Table 3.1). Results of the sequence alignment shows that the amino acid residues are conserved among the same HAD family but not at the relative position of the respective amino acids. It further justifies the theory that the 3D structures of proteins are more conserved than the sequences within the family (Lesk & Chothia, 1980). Sequence alignment (Table 3.1) also recognises four consensus motifs of the HAD family. Loop 1 is the aspartic acid at position 7 (D7), loop 2 is the serine at position 108 (S108), loop 3 is the lysine at position 140 (K140), and loop 4 is the aspartic acid at position 165 (D165). Loop 4 of HAD family usually consist of more than one aspartic acid to hold magnesium (II) or other cations (Lu, et al., 2005). Based on several studies the second aspartic acid required for Mg (II) orientation is located at position 3 or 4 after the first conserved aspartic acid (D165 in HADTn) (Aravind, et al., 1998; Ridder & Dijkstra, 1999; Shin, et al., 2003; Wang, et al., 2001). In HADTn, amino acids located 3 or 4 amino acids further from D165 are neither aspartic acid nor glutamic acid (amino acid that has the closest structure to aspartic acid). A closer look at the structure suggests that E164 may help D165 in the positioning of Mg (II). This configuration resembles β-phosphoglucomutase from *L. lactis* (Lahiri, et al., 2004). This was also the reason that 3KBB was identified putatively as β-phosphoglucomutase (Strange, et al., 2009).

After a successful HADTn model based on 3KBB had been built, docking was performed between HADTn and ligands (G6P and F6P) with YASARA. Docking in YASARA employs AutoDock Vina (default setting in YASARA), a new and improved program developed by (Trott & Olson, 2010). Prior to docking, energy minimisation of ligands was always performed to relax the ligands. The docking with YASARA resulted in

several possible conformations (Figure 3.1 and Appendix 1D). A plausible conformation was decided by considering the conformation at which a phosphate was situated in the active site (Figure 3.1) because crystal structure of 3KBB is in apoenzyme form without substrates and cofactor. It was the case for both ligands that the conformations were calculated to have the highest binding energy and the lowest K_d (Appendix 1D-A and -B) had a lesser likelihood to be the correct conformation than the conformation with lower binding energy and higher K_d (Figure 3.1). Phosphates in those conformations (Appendix 1D.A and B) are facing to the cap domain while the active site is situated in the core domain (Lu, et al., 2005). This approach was also used to analyse the result of the docking towards mutants (Table 3.2).

4.2 Initial characterisation

The standard buffer suggested by Kuznetsova, et al. (2005) was used for initial characterisation. For phosphate quantification, two spectrophotometric methods were used. P I assay was able to detect phosphate released in amounts up to 100 µM (2 nmol) making this method very sensitive. In general, a sensitive method is desirable, but for the kinetic characterisation Phosphate I was not suitable. It was used to measure phosphate only when the G6P was used below a concentration of 1 mM. Higher concentrations of G6P, produced phosphate that were higher than the range of Phosphate I. Dilution could have been done but during quantitative measurement, fewer steps are preferable to minimise errors. Thus, P II assay was used. This method has a detection range between 0.1 to 5 mM (3 – 150 nmol). This method bases its detection on the reduction of the molybdate-phosphatase complex with ascorbic acid. P II assay was also more suitable than PI assay because of a very short incubation time in P I assay (2 minutes) compared to 10 minutes of incubation in P II assay. Very short incubation time was a problem for this experiment because all the measurements were based on microtiter (96 well plate). Thus, the short difference in incubation between wells in row A and row H was unavoidable and also cannot be neglected. There was also always a small difference in the reading of the results from the wells in row A than row H. As a result, Phosphate I was no longer used after the initial kinetic characterisation of HADTn with G6P (Figure 3.2). Initial kinetic characterisation showed an inhibition effect of G6P to HADTn in higher concentration than 10 mM. Substrate inhibition could be regarded as a deviation from the Michaelis Menten model. Thus, the calculation of kinetic parameters only considers reaction rates when inhibition effects had not been observed (G6P = 10 mM). Substrate inhibition may play an important role in the metabolic regulation in several organisms. One example is inhibition of phosphofructokinase, a glycolysis enzyme by ATP. This could be explained because the aim of glycolysis is to produce ATP and higher ATP concentration tells that glycolysis may not be needed (Reed, et al., 2010). For HADTn, its role has yet to be explored, but this result may suggest that it may play an important role in bacterial metabolism.

HADTn showed the highest activity at pH = 7 (Figure 3.3) for Tris, MOPS, and HEPES. A decreased activity at higher pH may be associated with partial deprotonation of the lysine (pKa=10.67). Lysine has a pivotal role in intermediate stabilisation (Burroughs, et al., 2006). Lower activity of HADTn in Bis-Tris than in Tris at the same pH suggest that the additional two hydroxylethyl groups in Bis-Tris had a negative effect on the enzyme activity. No enzyme activity in citrate buffer confirmed that Mg (II) is essential for enzyme activity. Citrate can form complex with magnesium at relatively low concentration (Walser, 1961) hence, Mg (II) would not be available for the enzyme. HADTn can also interact with other

divalent cations, such as Mn (II). A decreased activity when small amount of Mn (II) was used in the presence of Mg (II) (1:10) may suggest that HADTn has a higher affinity toward Mn (II) than Mg (II) (Figure 3.4). It was suggested that Mn (II) has very similar properties to Mg (II) (Zea, et al., 2008). However, manganese as cofactor is more likely to be found with enzyme that has amino acids with a nitrogen side chain (e.g. histidine and lysine) (Bock, et al., 1999). HADTn contains only a few of histidine (H) and several lysine (K) residues, but none of them are situated near the active site (except for K140). In some enzymes, replacing Mg (II) by Mn (II) will increase the enzyme's activity as a part of the enzyme regulation (Brown & Cook, 1981). One report suggests that Mn (II) would have an activating effect if it were used at a higher concentration than Mg (II). In low concentration, Mn (II) could have a reversal effect (Sakharov & Makarova, 1988). In a standard buffer suggested by (Kuznetsova, et al., 2005), zinc (II) was added for the enzymatic activity of HAD. However, it has also been known that zinc (II) is one of the most potent inhibitors of bacterial phosphatase (Muginova & Zhavoronkova, 2005). Thus, the effect of this cation was not tested further. An optimum concentration of Mg (II) was also tested and concentrations higher than 2.5 mM did not show any increased activity suggesting that 2.5 mM Mg (II) had saturated the active site of 0.05 mg/ml HADTn. For further experiments, 5 mM Mg (II) was used.

The results suggested that the dissociation constant calculated by YASARA (Table 3.2) did not correspond to the K_m obtained from experiments (Table 3.3 and Appendix 2). In general, docking is a relatively cheap method for ligand prediction. However, the accuracy of docking depends on many factors. In one case, the docking prediction could result in a 50 to 70% deviation (Totrov & Abagyan, 2008). The docking calculations can have as low as 0% accuracy to as high as 93% accuracy compared to experimental results (Chen, 2015). A decreased k_{cat} in variants with S166V mutation (Table 3.3) revealed that this amino acid is important for catalytic activity. One possible role is in the positioning of Mg (II) due to its close proximity to D165, conserved aspartic acid for holding Mg (II). In general, the decrease in the ratio of k_{cat} was followed by a decrease in the ratio of k_{cat}/K_m. However, a double mutation (D14P, E47D) had a lower ratio of k_{cat}/K_m than D14P alone, while the ratio of k_{cat} for both were comparable. The ratio of the double mutation showed an increase in the ratio of k_{cat} but a decrease in the ratio of k_{cat}/K_m in comparison to the single mutation at position 47 (E47D). This suggests that either one of those amino acids may have a role in substrate recognition. Another double mutation was generated (P110A, E47D) to see if amino acid at 47 play the role of substrate recognition. Both ratios of k_{cat} and k_{cat}/K_m for P110A, E47D decreased in comparison to E47D, thus following the general rule discussed before. A different result was observed if both ratios (k_{cat} and k_{cat}/K_m) from P110A, E47D were compared to the ones from the single mutation at 110 alone (P110A). The ratio of k_{cat} of P110A, E47D decreased but the ratio of k_{cat}/K_m increased in comparison to P110A. This deviation from the general rule suggests that the amino acid at position 47 has a role in substrate recognition and in the direction of favouring F6P. If the addition of a mutation results in a decreased in the ratio of k_{cat}, it will also decrease the ratio of k_{cat}/K_m by default. A deviation from this behaviour could only be caused if the ratio of K_m (F6P over G6P) for the mutation is very much lower than the ratio of K_m of the variant without that particular mutation such that it could compensate the decrease of ratio of k_{cat}. The ratio of K_m (F6P over G6P) could be considered as a parameter to an extent as it describes the affinity of the enzymes. A higher value of this ratio implies a lower affinity towards F6P and vice versa.

4.3 High-throughput screening analysis

At high substrate concentration, the enzymatic reaction is faster than at lower substrates concentration. It explained a higher Z' with increasing substrate concentration. Z' value is calculated as the difference of the lowest value of the positive control's activity ($\mu_p - 3\sigma_p$) and the highest value of the negative control's activity ($\mu_n + 3\sigma_n$). Due to fast reaction at higher substrate concentrations, the difference between the positive and negative controls will be greater at any given time compared to low substrate' concentration. This was also shown by the Z' of HADTn's activity toward F6P and G6P. In the same concentration, Z' is greater toward F6P than G6P. Enzymatic reaction is faster towards F6P (almost 2.5 times faster) and activity towards F6P was also much more constant between two independent plates than the activity towards G6P. Reliable comparison could only be performed within one plate. Incorporation of OD_{600} in the Z' calculation did not lead to huge improvements.

In order to compensate the difference in activity of the WT toward G6P that would also happen for mutant enzymes, a cut-off was set and has been explained previously (3.4.2). 1n total, 1480 variants were generated and two variants that had the same mutation (D46T) were confirmed by sequencing. The ratio of mutants obtained to the samples size is only 0.13%. The efficiency of screening depends on many factors. In these experiments, the factors were the choice of amino acids, QC performance, and HTS method. Choice of amino acid is the first and very critical step. Numbers of amino acids could be chosen, but if by nature those amino acids did not play any role in the substrate specificity then it would be a futile attempt. A rational design was employed by considering the docking calculations of YASARA but as presented earlier, YASARA prediction quite deviated from results generated by the in vitro experiments. Interaction of two mutations (double mutation) also gave unexpected results making the rational design even more challenging. The other factor is the limitation of QC for generating libraries. It is reported that QC for site saturation mutagenesis is 10 to 54% (Zheng, et al., 2004). Ideally from 7 independent saturation mutagenesis with NNK degenerated primer, 672 variants (96 variants for each position) are enough to cover 90% probability that all variants are present (Nov, 2012). However, with a library generated by QC having a mutation rate lower than 100%, more plates needed to be screened to achieve the same level of 90% coverage. Thus, initial variants screened were doubled. Using the primers designed in this work (Appendix 2), a mutant library could be generated with a higher mutation rate (25 to 75%) than the one reported by (Zheng, et al., 2004). One hundred percent efficiency was reported by (Liu & Naismith, 2008), but they used a single point mutation and not site saturation mutagenesis. One method has been devised to increase the mutation efficiency in site saturation mutagenesis up to 100%but the primers need to be phosphorylated (Hogrefe, et al., 2002). Several other approaches have been tested in the experiment, e.g. addition of DMSO to the QC, increasing primers' concentration, and running the reaction in a single pot. However, none of them gave any improvement in a predicted way rather, improvement happened in several cases randomly.

There were 3 variants sequenced as wild type after third screening from R117NNK library. This might show that the cut-off set for HTS for the library was not enough to eliminate wild type variants. Stricter cut-offs could have been set, i.e. $\mu p + 3\sigma p$, but with stricter cut-off no variant would be picked for further screening. The other problem observed during the screening was some variants showed a different behaviour in different screenings. For example, P46X.5 and P46X.29 appeared to belong to group A in the second screening (Figure 3.13) but they showed activity that may belong to group C in the third screening

(Figure 3.14). These phenomena could also happen for other variants with other mutation contributing to a lower number of success rates. The reason for these phenomena is unknown since that happened in some libraries randomly. One of the improvement that could be done to eliminate this problem is by increasing concentration of substrates used, in particular G6P. It was shown earlier that higher substrate concentration contributed to higher Z' (Figure 3.6). The presence of wild type variants after sequencing also rule out the assumption used that during second and third screenings, a variant that showed high standard deviation might consist of cells bearing different mutant plasmids. P46T mutant showed higher activity than wild type in every screening round (P46X.5 and P6X.29 in Figure 3.13 and 3.14). They also showed acceptable standard deviations (<10%).

4.4 Final characterisation

In addition to four conserved loops, an additional loop located in the cap domain was be hypothesised to play a role in substrate recognition (Lahiri, et al., 2004). They propose a conserved glycine at position 46 in β-phosphoglucomutase (G44 in HADTn) to identify the fifth loop. They show mutation of G46 and adjacent amino acid (R49) severely decreased catalytic efficiency. The possibility of fifth loop playing a role in substrate recognition is also supported by findings in this work. The mutant enzyme (HADTnP46T) showed an improvement in the catalytic efficiency than the wild type enzyme (Figure 3.16). The ratio of catalytic efficiency of F6P/G6P is a good index to compare specificity between two enzymes because direct comparison of the catalytic efficiency for the wild type and mutant enzyme for each substrate would be misleading (Eisenthal, et al., 2007). It was shown that the ratio of catalytic efficiency is higher for the mutant than for the wild type enzyme (8.8 to 5.5). Amino acid at position 46 is located in the fifth loop (Figure 3.18) and is located quite distant from the active site (Figure 3.17). This importance of the fifth loop is further supported by the fact that an insertion mutation between position 46 and 47 (46_57insMet) showed no activity,

Stability of the mutant enzyme was slightly lower than the wild type enzyme while incubated at 94^{o}C (Table 3.7). Proline is a rigid amino acid and this amino acid is suggested to have a role in enzymtica thermostability (Matthews, et al., 1987). The effect of proline mutation depends on the position of the respective amino acid. It was shown by (Li, et al., 1997) that the mutation of partially buried serine to proline show an increase in the thermostability by presumably decreasing the entropy of the unfolded state. The number of prolines introduced or replaced also play a significant role in enzyme thermostability (Suzuki, et al., 1991). Addition of 100 mM Mg (II) was shown to increase significantly the wild type and mutant enzymes' thermostability (Table 3.4). Higher concentration of Mg (II) was used because in the previous experiment, addition of 5 mM Mg (II) did not give any positive effect. Half-life of each enzyme was two times longer than without Mg (II). This finding suggests that Mg (II) helps to stabilise the active form of enzymes at higher temperature. Effect of stabilisation may be dependent on the cation used (Heinen & Lauwers, 1976) thus it might be interesting to see if other divalent ions would have a similar effect.

Both enzymes appeared to be inhibited by either glucose or fructose via a non-competitive mechanism since there was no apparent change in the K_m (Table 3.8). There is no report describing the effect of product inhibition for this class of enzyme. One small molecule is reported to inhibit HAD enzyme via noncompetitive mechanisms (Seifried, et al., 2013). A Nnoncompetitive inhibitor, also known as allosteric inhibitor is commonly found in

metabolisms (Kent, 2000). Further experiments with different ligands' concentration and their respective sugar is needed to reliably determine inhibition constants.

5 Conclusion and Future Outlook

5.1 Conclusion

Haloacid dehalogenase (HAD) superfamily is a family of hydrolases that is able to catalyse a broad set of reactions (CO-P, C-halogen, C-P) and can be found in all super kingdoms (Burroughs, et al., 2006). Phosphatase-like activity of this superfamily is known to exceed other phosphatases (Koonin & Tatusov, 1994) marking the significance of these enzymes in the control of metabolic fluxes as metabolomes with phosphate functional groups account up to 40% (Nobeli, et al., 2003). One enzyme that belongs to HAD super family from *Thermatoga neapolitana* (HADTn) was studied due to its distinctive characteristic of a higher activity towards fructose-6-phosphate (F6P) than glucose-6-phosphate (G6P). This work was presented as the preliminary study of this enzyme to probably increase its specificity toward F6P even further. Sequence alignment and three dimensional comparisons together with docking calculations toward both substrates by YASARA were performed in order to identify potential amino acids for substrate recognition. Characterisation of the wild type showed that HADTn can use Mg (II) and Mn (II) as cofactor, but Mg (II) gave a higher activity. Optimum pH of HADTn was 7, with the same compatibility among HEPES, MOPS, and Tris buffers. Single and double mutations predicted by YASARA and further tested by in vitro experiments suggested that S166 is important for the enzyme activity and E47 appeared to have a role in substrate recognitions. Mutants were developed by employing QuikChange™ site-directed mutagenesis. Several libraries based on site-saturation mutagenesis with NNK motifs were developed to investigate the role of six different amino acids (8M, Y19, P46, E47, P110, R117) independently in the enzyme activity and specificity. High-throughput screening method has been developed to screen those libraries for an improved variant. The variant has mutation at position 46 to threonine (P46T). Kinetic characterisations showed that HADTnP46T had almost doubled specificity toward F6P than the wild type, calculated by the ratio of k_{cat}/K_m of F6P over G6P. Temperature stability studies revealed that the addition of 100 mM Mg (II) could prolong the half-life of HADTnP46T and the wild type enzyme by a factor of two. The studies also showed that HADTnP46T had a slight decrease in temperature stability at 94^oC than the wild type enzyme. Inhibition studies with its respective sugar exhibited inhibition followed noncompetitive mechanisms. Findings from this work were similar to the proposal by (Lahiri, et al., 2004) that there is an additional fifth loop in the HAD superfamily located in the cap domain that play a role in substrate recognition. HADTnP46T discovered from this work could be also used as a good starting template for future research aiming to improve the specificity towards F6P.

5.2 Future outlook

The results of this work have indicated the presence of a loop located in the cap domain of HADTn that could play a pivotal role in substrate recognition. In the future, experiments should be directed to generate mutations of amino acids in this loop to further justify if this loop really has a significant role in the substrate recognition as suggested by (Lahiri, et al., 2004) and this work. Due to a huge cleft between the main domain and the cap domain, it would be interesting to test the activity of HADTn toward different sugar phosphates. The findings from that investigation may further imply the importance of the proposed loop.

Besides engineering of the enzyme, other parameters from this work can still be improved. Reaction rates at different temperatures with different incubation time could be performed to find the best combinations yielding the highest activity. Specificity of the enzyme may be changed at different temperatures, thus it is also interesting to investigate if that is true. Although high-throughput screening developed from this work was robust enough to screen the libraries generated, higher concentration of substrates, in particular G6P could be tested if that would be possible to achieve an ideal assay performance (Z' = 1). With higher Z', screening can be done with different concentrations of substrates, e.g. 1, 5, 10 mM like the one reported by (Pick, et al., 2014) such that catalytic efficiency (k_{cat}/K_m) can be compared during the screening resulted in a much improved screening approach.

References

Agilent, 2005. *QuikChange® Site-Directed Mutagenesis Kit.* [Online]
Available at: https://www.agilent.com/cs/library/usermanuals/Public/200523.pdf
[Accessed 25 November 2015].

Akhtar, M., Ahmad, A. & Bhakuni, V., 2002. Divalent cation induced changes in structural properties of the dimeric enzyme glucose oxidase: dual effect of dimer stabilization and dissociation with loss of cooperative interactions in enzyme monomer. *Biochemistry,* 41(22), pp. 142-149.

Allen, K. & Dunaway-Mariano, D., 2004. Phosphoryl group transfer: evolution of a catalytic scaffold. *Trends Biochem Sci,* Volume 29, pp. 495-503.

Anastas, P. & Warner, J., 1998. *Green chemistry: theory and practice.* New York: Oxford University Press.

Andrade, C., Pereira, N. J. & Antranikian, G., 1999. Extremely thermophilic microorganisms and their polymer-hidrolytic enzymes. *Rev. Microbiol.* , 30(4), pp. 287-298.

Antonov, A. et al., 1978. Mechanisms of Pepsin Catalysis: General Base Catalysis By The Active Site Carboxylate Ion. *FEBS Letter,* 88(1), pp. 87-90.

Aravind, L., Galperin, M. & Koonin, E., 1998. The catalytic domain of the P-type ATPase has the haloacid dehalogenase fold. *TIBS,* Volume 23, pp. 127-129.

Axe, D., 2004. Estimating the prevalence of protein sequences adopting functional enzyme folds. *J Mol Bio,* Volume 341, pp. 1295-1315.

Baykov, A. A., Evtushenko, O. A. & Avaeva, S. M., 1988. A Malachite Green Procedure for Orthophosphate Determination and Its Use in Alkaline Phosphatase-Based Enzyme Immunoassay. *Analytical Biochemistry,* Volume 171, pp. 266-270.

Benkovic, S. & Hammes-Schiffer, S., 2003. A Perspective on Enzyme Catalysis. *Science,* Volume 301, pp. 1196-1202.

Bock, C. W. et al., 1999. Manganese as a Replacement for Magnesium and Zinc: Functional Comparison of DIvalent Ions. *J. Am. Chem. Soc.*, Volume 121, pp. 7360-7372.

Brown, D. & Cook, R., 1981. Role of metal cofactors in enzyme regulation. Differences in the regulatory properties of the Escherichia coli nicotinamide adenine dinucleotide phosphate specific malic enzyme, depending on whether magnesium ion or manganese ion serves as divalent cation. *Biochemistry,* 20(9), pp. 2503-2512.

Bunchanan, C. et al., 1999. An extremely thermostable aldolase from Sulfolobus solfataricus with specificity for non-phosphorylated substrates. *Biochem J.*, Volume 343, pp. 563-570.

Burroughs, A., Allen, K., Dunaway-Mariano, D. & Aravind, L., 2006. Evolutionary Genomics of the HAD Superfamily: Understanding the Structural Adaptations and Catalytic Diversity in a Superfamily of Phosphoesterases and Allied Enzymes. *J. Mol. Biol.*, Volume 361, p. 1003–1034.

Cadwell, R. & Joyce, G., 1992. Randomization of genes by PCR mutagenesis. *PCR Methods Appl,* Volume 2, pp. 28-33.

Caparros-Martin, J., McCarthy-Suarez, I. & Culianez-Macia, F., 2013. HAD hydrolase function unveiled by substrate screening: enzymatic characterization of Arabidopsis thaliana subclass I phosphosugar phosphatase AtSgpp. *Planta,* Volume 237, p. 943–954.

Caravaca, J. & Grisolia, S., 1959. Decrease in thermal stability of frog liver carbamyl phosphate synthetase by substrates and cofactors. *Biochemical and Biophysical Research Communications,* 1(2), pp. 94-97.

Castle, L. et al., 2004. Discovery and directed evolution of a glyphosate tolerance gene. *Science,* Volume 304, pp. 1151-1154.

Centi, G. & Perathoner, S., 2009. From Green to Sustainable Industrial Chemistry. In: F. Cavani, G. Centi & S. T. F. Perathoner, eds. *Sustainable Industrial Processes.* Weinheim: WILEY-VCH Verlag GmbH & Co., pp. 1-72.

Chen, K. & Arnold, F., 1993. Tuning the activity of an enzyme for unusual environments: sequential random mutagenesis of Subtilisin E for catalysis in dimethylformamide. *Proc Natl Acad Sci USA,* Volume 90, pp. 5618-5622.

Chen, Y.-C., 2015. Beware of Docking!. *Trends in Pharmacological Sciences* , 36(2), pp. 78-95.

Cohen, J., 2001. How DNA Shuffling Works. *Science,* Volume 293, p. 237.

Currin, A., Swainston, N., Day, P. & Kell, D., 2015. Synthetic biology for the directed evolution of protein biocatalysts: navigating sequence space intelligently. *Chem. Soc. Rev.*, Volume 44, pp. 1172-1239.

Drueckes, P., Schinzel, R. & Palm, D., 1995. Photometric Microtiter Assay of Inorganic Phosphate in the Presence of Acid-Labile Organic Phosphates. *Analyticial Biochemistry,* Volume 230, pp. 173-177.

Eisenthal, R., Danson, M. J. & Hough, D. W., 2007. Catalytic efficiency and kcat/KM: a useful comparator?. *Trends in Biotechnology,* 25(6), pp. 247-249.

EMBL-EBI, 2016. *Clustal Omega.* [Online]
Available at: http://www.ebi.ac.uk/Tools/msa/clustalo/
[Accessed 22 May 2016].

European Nuclear Society, 2016. *Binding Energy.* [Online]
Available at: http://www.euronuclear.org/info/encyclopedia/bindingenergy.htm
[Accessed 11 05 2016].

Greener, A. L. & Jerpseth, B. D., 2004. *Highly transformable bacterial cells and methods for producing the same.* United States of America, Patent No. US 6706525 B1.

Greimel, K. et al., 2013. Banning toxic heavy-metal catalysts from paint: enzymatic cross-linking of alkyd resins. *Green Chemistry,* 381-388(2), p. 15.

Heinen, W. & Lauwers, A., 1976. Amylase activity and stability at high and low temperature depending on calcium and other divalent cations. *Experientia Suppl.* , Volume 26, pp. 77-89.

Hoenig, M., Lee, R. J. & C, F. D., 1989. A microtiter late assay for inorganic phosphate. *Journal of Biochemical and Biophysical Methods,* Volume 19, pp. 249-252.

Hogrefe, H., Cline, J., Youngblood, G. & Allen, R., 2002. Creating randomized amino acid libraries with the QuickChange Multi Site-Directed Mutagenesis kit. *BioTechniques,* Volume 33, pp. 1151-1165.

Illanes, A., 2008. *Enzyme Biocatalysis.* 9 ed. Dordrecht: Springer Science + Business Media B.V..

Integrated DNA Technologies, Inc, 2015. *OlygoAnalyzer 3.1.* [Online]
Available at: https://eu.idtdna.com/calc/analyzer
[Accessed 25 November 2015].

Kent, M., 2000. *Advanced Biology.* 10 ed. Oxford: Oxford University Press.

Kim, D., 2015. *Baker Laboratory.* [Online]
Available at: http://depts.washington.edu/bakerpg/primertemp/
[Accessed 25 November 2015].

Koonin, E. & Tatusov, R., 1994. Computer Analysis of Bacterial Haloacid Dehalogenases Defines a Large Superfamily of Hydrolases with Diverse Specificity: Application of an Iterative Approach to Database Search. *Journal of Molecular Biology,* 244(1), pp. 125-132.

Kriege, E. et al., 2009. Improving physical realism, stereochemistry, and side-chain accuracy in homology modelling:: Four approaches that performed well in CASP8. *Proteins,* 77(9), pp. 114-122.

Krieger, E., n.d. *Docking a ligand to a receptor.* [Online]
Available at: http://www.yasara.org/dock_run.mcr
[Accessed 11 05 2016].

Krieger, E. & Vriend, G., 2014. YASARA View - molecular graphics for all devices - from smartphones to workstations. *Bioinformatics* , Volume 30, pp. 2981-2982.

Kuznetsova, E. et al., 2006. Genome-wide Analysis of Substrate Specificities of the Escherichia coli Haloacid Dehalogenase-like Phosphatase Family. *The Journal of Biological Chemistry,* 281(47), p. 36149 –36161.

Kuznetsova, E. et al., 2005. Enzyme genomics: Application of general enzymatic screens to discover new enzymes. *FEMS Microbiology Reviews,* Volume 29, pp. 263-279.

Lahiri, S. D. et al., 2004. Analysis of the Substrate Specificity Loop of the HAD Superfamily Cap Domain. *Biochemistry,* Volume 43, pp. 2812-2820.

Lahiri, S., Zhang, G., Dunaway-Mariano, D. & Allen, K., 2002. Caught in the act: the structure of phosphorylated beta-phosphoglucomutase from Lactococcus lactis. *Biochemistry,* Volume 41, p. 8351–8359.

Leisola, M. & Turunen, O., 2007. Protein engineering: opportunities and challenges. *Appl Microbiol Biotechnol* , Volume 75, pp. 1225-1232.

Lesk, A. & Chothia, C., 1980. How different amino acids sequences determine similar protein structures: The structure and evolutionary dynamics of globins. *J. Mol Biol.,* Volume 136, pp. 225-270.

Leung, D., Chen, E. & Goeddel, D., 1989. A method for random mutagenesis of a defined DNA segment using a modified polymerase chain reaction. *Technique,* Volume 1, pp. 11-15.

Liu, H. & Naismith, J., 2008. An efficient one-step site-directed deletion, insertion, single and multiple-site plasmid mutagenesis protocol. *BMC Biotechnology,* 8(91).

Li, Y., Reilly, P. & Ford, C., 1997. Effect of introducing proline residues on the stability of Aspergillus awamori. *Protein Eng.,* 10(10), pp. 1199-1204.

Lutz, S., 2010. Beyond directed evolution - semi-rational protein engineering and design. *Curr Opin Biotechnol,* 21(6), p. 734–743.

Lu, Z., Dunaway-Mariano, D. & Allen, K. N., 2005. HAD Superfamily Phosphotransferase Substrate Diversification: Structure and Function Analysis of HAD Subclass IIB Sugar Phosphatase BT4131. *Biochemistry,* Volume 44, pp. 8684-8696.

Martí-Renom, M. A. et al., 2000. Comparative Protein Structure Modeling of Genes and Genomes. *Annu. Rev. Biophys. Biomol. Struct.* , Volume 29, p. 291–325.

Matthews, B., Nicholson, H. & WJ, B., 1987. Enhanced protein thermostability from site-directed mutations that decrease the entropy of unfolding. *Proc Natl Acad Sci U S A*, 84(19), pp. 6663-6637.

McCullum, E., Williams, B., Zhang, J. & Chaput, J., 2010. Random mutagenesis by error-prone PCR. *Methods Mol Biol*, Volume 634, pp. 103-109.

Morais, M. et al., 2000. The crystal structure of Bacillus cereus phosphonoacetaldehyde hydrolase: insight into catalysis of phosphorus bond cleavage and catalytic diversification within the HAD enzyme superfamily. *Biochemistry*, Volume 39, p. 10385–10396.

Muginova, S. & Zhavoronkova, A. S. T., 2005. Potentialities and Prospects for the Use of Alkaline Phosphatases for Determining Metal Ions. *Journal of Analytical Chemistry*, 60(3), p. 247–263.

NEB, 2016. *BL21(DE3) Competent E. coli.* [Online]
Available at: https://www.neb.com/products/c2527-bl21de3-competent-e-coli
[Accessed 9 May 2016].

Nelson, D. & Cox, M., 2008. *Lehninger Principles of Biochemistry.* 5 ed. s.l.:W. H. Freeman and Company.

Nissen, J. A., 1982. Limited enzymic degradation of proteins: A new approach in the industrial application of hydrolases. *Journal of Chemical Technology and Biotechnology*, 32(1), p. 138–156.

Nobeli, I., Ponstingl, H., Krissinel, E. & Thornton, J., 2003. A Structure-based Anatomy of the *E. coli* Metabolome. *Journal of Molecular Biology*, 334(4), p. 697–719.

Nov, Y., 2012. When Second Best Is Good Enough: Another Probabilistic Look at Saturation Mutagenesis. *Appl Environ Microbiol.*, 78(1), p. 258–262.

Pick, A. et al., 2014. Improving the NADH-cofactor specificity of the highly active AdhZ3and AdhZ2 from Escherichia coli K-12. *Journal of Biotechnology 189* , Volume 189, p. 157–165.

Plesner, I., 1986. The apparent Km is a misleading kinetic indicator. *BIochem J.*, Volume 239, pp. 175-178.

Porter, J., Rusli, R. & Ollis, D. L., 2016. Directed Evolution of Enzymes for Industrial Biocatalysis. *ChemBioChem*, Volume 17, pp. 197-203.

Premier Biosoft, 2016. *PCR Primer Design Guidelines.* [Online]
Available at: http://www.premierbiosoft.com/tech_notes/PCR_Primer_Design.html
[Accessed 11 May 2016].

Ranaldi, F., Vanni, P. & Giachetti, E., 1999. What students must know about the determination of enzyme kinetic parameters. *Biochemical Education*, Volume 27, pp. 87-81.

Reed, M. C., Lieb, A. & Nijhout, H. F., 2010. The biological significance of substrate inhibition: A mechanism with diverse functions. *Bioessays*, Volume 32, p. 422–429.

Ridder, I. & Dijkstra, B., 1999. Identification of the Mg2+-binding site in the P-type ATPase and phosphatase members of the HAD (haloacid dehalogenase) superfamily by structural similarity to the response regulator protein CheY. *Biochem J.*, Volume 339, pp. 223-226.

Sadana, A., 1988. Enzyme deactivation. *Biotechnol Adv*, 6(3), pp. 349-446.

Sakharov, I. Y. & Makarova, I. E. G., 1988. *Biokhimiya*, 53(6), p. 974.

Sander, C. & Schneider, R., 1991. Database of homology-derived protein structures and the structural meaning of sequence alignment. *Protein*, 9(1), pp. 56-68.

Seifried, A., Schultz, J. & Gohla, A., 2013. Human HAD phosphatases: structure, mechanism, and roles in health and disease. *FEBS Journal*, Volume 280, pp. 549-571.

Shin, D. H. et al., 2003. Crystal structure of a phosphatase with a unique substrate binding domain from Thermotoga maritima. *Protein Science*, Volume 12, p. 1464–1472.

Sigma Aldrich, 2015. *Buffer Refence Center.* [Online]
Available at: http://www.sigmaaldrich.com/life-science/core-bioreagents/biological-buffers/learning-center/buffer-reference-center.html
[Accessed 26 December 2015].

Strange, R. et al., 2009. Structure of a putative beta-phosphoglucomutase (TM1254) from Thermotoga maritima. *Acta Crystallogr Sect F Struct Biol Cryst Commun*, Volume 65, pp. 1218-1221.

Suzuki, Y., Hatagaki, K. & Oda, H., 1991. A hyperthermostable pullulanase produced by an extreme thermophile, Bacillus flavocaldarius KP 1228, and evidence for the proline theory of increasing protein thermostability. *Appl Microbiol Biotechnol*, 34(6), pp. 707-714.

Tenenbaum, D. J., 2008. Food vs. Fuel: Diversion of Crops Could Cause More Hunger. *Environmental Health Perspectives*, 116(6), pp. A254-A257.

ThermoFisher, 2015. *One Shot® TOP10 Electrocomp™ E. coli.* [Online]
Available at: https://www.thermofisher.com/order/catalog/product/C404052
[Accessed 30 04 2016].

Thomas, T. & Scopes, R., 1998. The effects of temperature on the kinetics and stability of mesophilic and thermophilic 3-phosphoglycerate kinases. *Biochem. J.*, Volume 330, pp. 1087-1095.

Thompson, J. & Raines, R., 1994. Value of General Acid–Base Catalysis to Ribonuclease A. *J Am Chem Soc.*, 116(12), p. 5467–5468.

Totrov, M. & Abagyan, R., 2008. Flexible ligand docking to multiple receptor conformations: a practical alternative. *Curr Opin Struct Biol.,* 18(2), pp. 178-184.

Trott, O. & Olson, A., 2010. AutoDock VINA: improving the speed and accuracy of docking with a new scoring function, efficient optimization and multithreading. *J.Comput.Chem.,* Volume 31, pp. 455-461.

Trott, O. & Olson, J., 2010. AutoDock VINA: improving the speed and accuracy of docking with a new scoring function, efficient optimization and multithreading. *J.Comput.Chem.,* Volume 31, pp. 455-461.

van Loo, B. et al., 2004. Directed evolution of epoxide hydrolase from A. radiobacter toward higher enantioselectivity by error-prone PCR and DNA shuffling. *Chem Bio,* Volume 11, pp. 981-990.

Vinogradov, V. & Avnir, D., 2015. Enzyme renaturation to higher activity driven by the sol-gel transition: Carbonic anhydrase. *Scientific Report,* Volume 5, pp. 1-7.

Walser, M., 1961. Ion Association. V. DIssociation Constans for Complexesof Citrate with Sodium, Potassium, Calcium, and Magnesium Ions. *J. Phys. Chem.,* Volume 65, p. 159–161.

Wang, W. et al., 2001. Crystal Structure of Phosphoserine Phosphatase from Methanococcus jannaschii, a Hyperthermophile, at 1.8 A°. *Structure,* Volume 9, p. 65–71.

Wang, W. & Malcom, B., 1999. Two-stage PCR protocol allowing introduction of multiple mutations, deletions and insertions using Quik-Change site-diredetd mutagenesis. *BioTechniques,* Volume 26, pp. 680-682.

Xia, Y., Chu, W., Qi, Q. & Xun, L., 2014. New insights into the QuikChangeTM process guide the use of Phusion DNA polymerase for site-directed mutagenesis. *Nucleic Acids Research,* Volume 1, pp. 1-9.

Yoshikuni, Y., Ferrin, T. & Keasling, J., 2006. Designed divergent evolution of enzyme function. *Nature,* Volume 440, pp. 1078-1082.

Zea, C. J., Camci-Unal, G. & Pohl, N. L., 2008. Thermodynamics of binding of divalent magnesium and manganese to uridine phosphates: implications for diabetes-related hypomagnesaemia and carbohydrate biocatalysis. *Chem Cent J.,* 2(15).

Zhang, J.-H., Chung, T. D. Y. & Oldenburg, K. R., 1999. A Simple Statistical Parameter for Use in Evaluation and Validation of High Throughput Screening Assays. *Journal of Biomolecular Screening,* 4(2), pp. 67-73.

Zhang, X. D. et al., 2008. Integrating Experimental and Analytic Approaches to Improve Data Quality in Genome-wide RNAi Screens. *Journal of Biomolecular Screening,* 13(5), pp. 378-389.

Zheng, L., Baumann, U. & Reymond, J.-L., 2004. An efficient one-step site-directed and site-saturation mutagenesis protocol. *Nucleic Acids Research,* 32(14), p. 115.

Appendices

Appendix 1. Supporting Data for *In Silico* Analysis

Appendix 1A. DNA sequence of wild type enzyme (haloacid dehalogenase from *Thermatoga neaopolitana*)

ATGGAAGCGGTGATTTTCGACATGGATGGAGTGCTCATGGACACAGAGCCTCTCTACTTCGAAGCT
TACAGAAGAGTCGCGGAAAGCTATGGAAAACCTTACACGGAGGATCTCCACAGGAGAATAATGG
GAGTTCCTGAAAGAGAAGGTCTTCCCATCCTCATGGAAGCTCTGGAGATAAAAGATTCTCTGGAG
AACTTCAAAAAGAGGGTCCACGAAGAAAAAAAGCGCGTTTTCTCTGAGCTTCTCAAGGAAAATCC
GGGTGTAAGAGAGGCGCTCGAGTTCGTAAAGAGCAAAAGAATAAAACTCGCGCTCGCAACCTCCA
CACCACAGCGAGAAGCGCTGGAGAGATTGAGAAGACTCGATCTCGAAAGGTACTTCGATGTCATG
GTGTTCGGTGATCAGGTGAAGAACGGAAAGCCTGATCCAGAGATATACCTTCTCGTTCTGGAAAG
GTTGAATGTGGTCCCAGAGAAGGTTGTGGTCTTCGAAGACTCAAAGAGCGGTGTTGAAGCCGCAA
AAAGCGCCGGCATAGAAAGAATCTATGGAGTCGTTCACTCTTTGAACGACGGTAAAGCGCTTCTTG
AAGCGGGTGCGGTTGCTCTGGTGAAACCCGAGGAAATCCTGAACGTTCTCAAAGAGGTTCTTTAA

Appendix 1B. Amino acid sequence of wild type enzyme.

MEAVIFDMDGVLMDTEPLYFEAYRRVAESYGKPYTEDLHRRIMGVPEREGLPILMEALEIKDSLENFK
KRVHEEKKRVFSELLKENPGVREALEFVKSKRIKLALATSTPQREALERLRRLDLERYFDVMVFGDQV
KNGKPDPEIYLLVLERLNVVPEKVVVFEDSKSGVEAAKSAGIERIYGVVHSLNDGKALLEAGAVALVK
PEEILNVLKEVL

Appendix 1C. Plasmid construct of wild type enzyme. This picture was obtained from Clone Manager 9 Professional

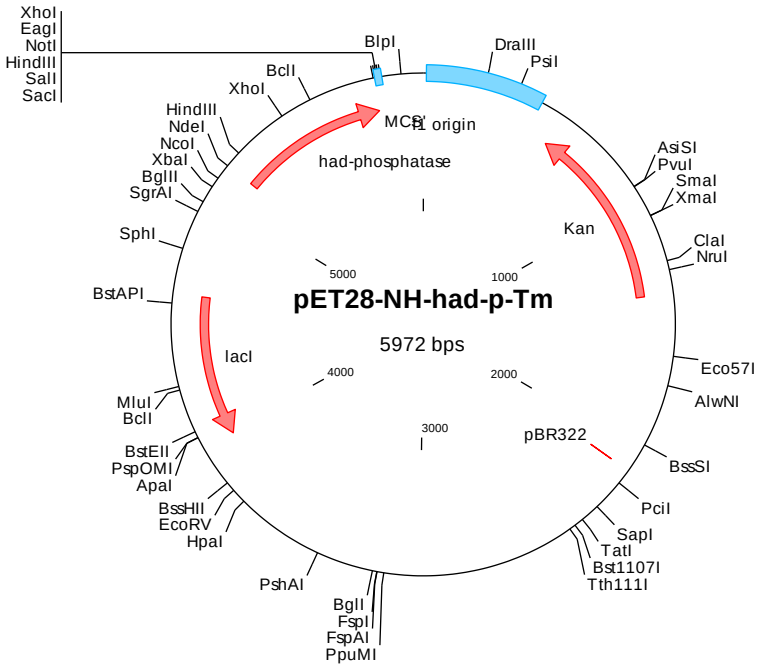

Appendix 1D. Sequence alignment of wild type enzyme (HADTn) to several homolog proteins (protein are presented under PDB entry). Alignment was performed using Clustal

Omega (EMBL-EBI, 2016). Psp is Pseudomonas, Xa is xanto, Tm is Thermatoga maritima, and Mj is Methanococcus jannaschii. Red marks represent conserved amino acids in the four motifs situated in the active site of HAD family. Motif I contains D and G, motif II contains S, motif III contains K, and motif IV contains D. Note the distant position of S (motif II) in 1NF2_Tm relative to other proteins.

CLUSTAL O (1.2.1) multiple sequence alignment

```
HADTn       ----MEAVIFDMDGVLMDTEPLYFEA---YR----RVAESYGKP-YTEDLHRRIMGV---
1JUD_Psp                                                                -
MDYIKGIAFDLYGTLFDVHSVVGRCDEAFPGRGREISALWRQKQLEYTWLRSLMNRYVN
1QQ5_Xa                                                                 ---
MIKAVVFDAYGTLFDVQSVADATERAYPGRGEYITQVWRQKQLEYSWLRALMGRYAD
1NF2_Tm      ---MYRVFVFDLDGTLLNDNLEISEKDRRNI------EKLSRKCYVVFASGRMLVST-LN
1F5S_Mj      MEKKKKLILFDFDSTLVNNETIDEIAREAGV------EEEVKKITK-----EAMEGK-LN
                . . ** ..*.: .               :      . :

HADTn       ---P----EREGLPILMEALEIKDSLENFKKRVHEEKKRVFSELLKEN------------
1JUD_Psp     FQQA----TEDALRFTCRHLGLDLD-ARTRSTLC----DAYL-RLAPF------------
1QQ5_Xa      FWSV----TREALAYTLGTLGLEPD-ESFLADMA----QAYN-RLTPY------------
1NF2_Tm      VEKKYFKRTFPTIAYNGAIVYLPEEGVILNEKIPPEVAKDIIEYIKPLNVHWQAYIDDVL
1F5S_Mj      FEQSLRK------------------RVSLLKDLPIEKVEKAIKRITPT------------
                                      :        :

HADTn       --PG-----------------VREALEFVKSKRIKLALATSTPQREALERLRRLDLERYF
1JUD_Psp     --SE-----------------VPDSLRELKRRGLKLAILSNGSPQSIDAVVSHAGLRDGF
1QQ5_Xa      --PD-----------------AAQCLAELA--PLKRAILSNGAPDMLQALVANAGLTDSF
1NF2_Tm      YSEKDNEEIKSYARHSNVDYRVEPNLSELVSKMGTTKLLLIDTPERLDELKEILSERF--
1F5S_Mj      --EGAEETIKELKN---RGYVVAVV-------SGGFDI-------AVNKIKEKLGLDYAF
                          .          :

HADTn       DVMVFGDQVKNGKPDPE-------------IYLLVLERLNVVPEKVVVFEDSKSGVEAAK
1JUD_Psp     DHLLSVDPVQVYKPDNR-------------VYELAEQALGLDRSAILFVSSNAWDATGAR
1QQ5_Xa      DAVISVDAKRVFKPHPD-------------SYALVEEVLGVTPAEVLFVSSNGFDVGGAK
1NF2_Tm      KDVV-----KVFKSFPTYLEIVPKNVDKGKALRFLRERMNWKKEEIVVFGDNENDLFMFE
1F5S_Mj      ANRLI---VKDGKLTGDVEGEVLKENAKGEILEKIAKIEGINLEDTVAVGDGANDISMFK
             :    : *               :      : . .      .

HADTn       SAGIERIYGVVHSLNDGKALLEAGAVALV-----------------KPEEILNVLKEVL-
1JUD_Psp     YFGFPTCWINRTGNVFE------------------------EMGQTPDWEVTSLRAVVE
1QQ5_Xa      NFGFSVARVARLSQEALARELVSGTIAPLTMFKA--LRMREETYAEAPDFVVPALGDLPR
1NF2_Tm      EAGLRVAMENAIEKVKEASDIVTLTNN-DSGVSYVLERISTDCLDE--------------
1F5S_Mj      KAGLKIAFCAKPI-LKEKADICIEKRDLREILKYIK-----------------------
                *:

HADTn       --------------
1JUD_Psp     LFETAAGKAEKG--
1QQ5_Xa      LVRGMAGAHLAPAV
1NF2_Tm      --------------
1F5S_Mj      --------------
```

Appendix 1E. Other possible docking conformations of wild type enzyme to glucose-6-phosphate (G6P) or to fructose-6-phosphate (F6P). Docking was performed using YASARA and pictures were generated by PyMol. The ligand for picture A, C, E, G is G6P wile for B, D, F, H is F6P. The pictures are arranged such that from top to bottom (A to G or B to H) the likelihood of the respective conformation decreases. Decreased likelihood is represented by decreased binding energy and increased dissociation constant (K_d).

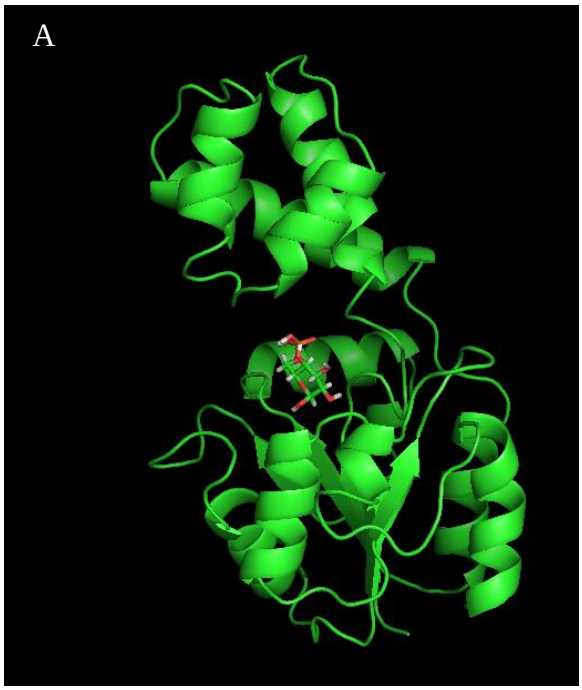

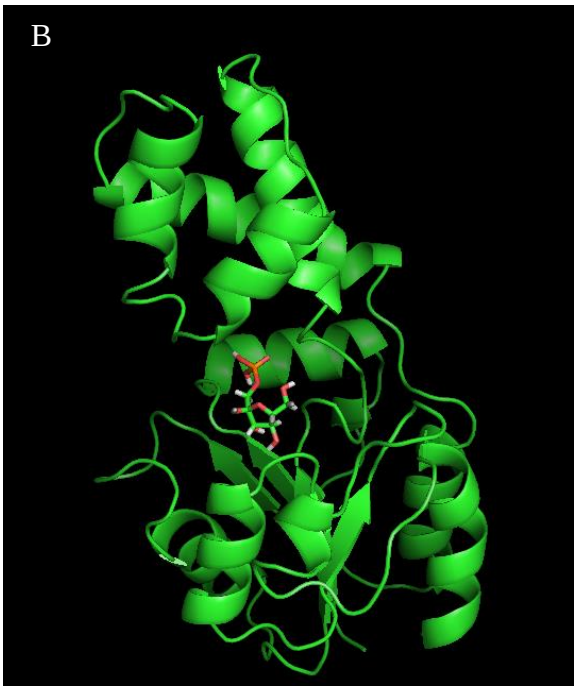

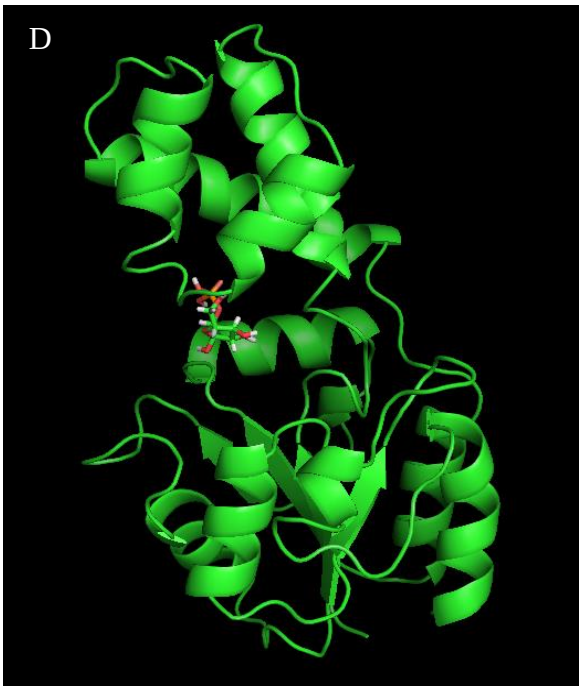


E


F

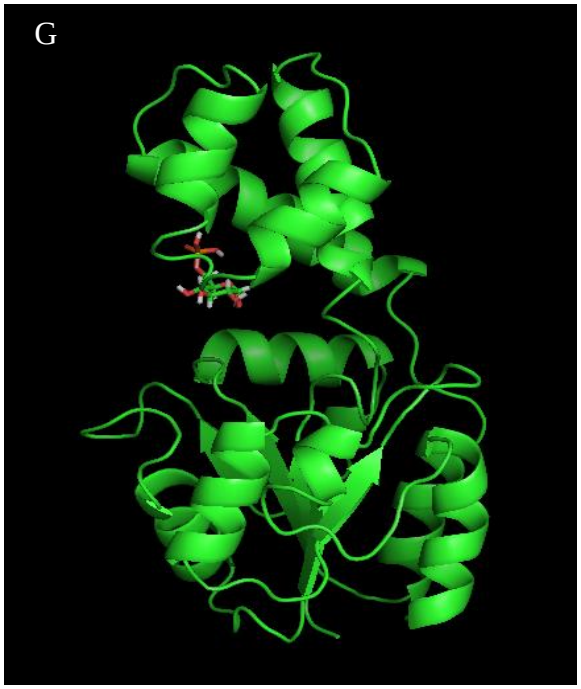
G


H

Appendix 2 Molecular Biology Data

Appendix 2A. Summary of primer design

No	Mutation	Primer (5' – 3')*	ΔG_P (kcal/mole)	ΔG_{CD} (kcal/mole)	BPs	Tm (°C)
1	D14P	GTGCTCATGCCGACAGAGCCTCTCTACTTCGAAGC	-67.9	-40.66	20	85.6
		GGCTCTGTCGGCATGAGCACTCCATCCATGTCG	-66.89			85.9
2	D47E	GAGTTCCTGATAGAGAAGGTCTTCCCATCCTCATGG	-65.5	-31.63	19	83.2
		CCTTCTCTATCAGGAACTCCCATTATTCTCCTGTGG	-65.25			82.1
3	S166V S166NDT	GAAGACGTGAAGNDTGGTGTTGAAGCCGCAAAAAGCG	-75.56	-34.17	19	83.3
		CACCNDTCTTCACGTCTTCGAAGACCACAACCTTC	-65.5			82.2
4	M8A	GATTTTCGACGCGGATGGAGTGCTCATGGACACAG	-69.43	-41.66	20	84.5
		CTCCATCCGCGTCGAAAATCACCGCTTCCATATG	-70.78			83.4
5	P110A	CCTCCACAGCGCAGCGAGAAGCGCTGGAGAGATTG	-74.45	-39.53	18	88.0
		CTCGCTGCGCTGTGGAGGTTGCGAGCGCGAG	-71.37			88.8
6	E113A	CACAGCGAGCGGCGCTGGAGAGATTGAGAAGACTCG	-74.39	-43.1	18	87.8
		CCAGCGCCGCTCGCTGTGGTGTGGAGGTTGCGAGC	-80.38			91.5
7	Y19NNK	GAGCCTCTCNNKTTCGAAGCTTACAGAAGAGTCGC	-66.76	-36.26	20	82.2
		CTTCGAAMNNGAGAGGCTCTGTGTCCATGAGCAC	-64.09			82.2
8	E47NNK	GAGTTCCTNNKAGAGAAGGTCTTCCCATCCTCATGG	-66.49	-32.62	19	82.2
		CCTTCTCTMNNAGGAACTCCCATTATTCTCCTGTGG	-66.25			80.9
9	P46NNK	GGGAGTTNNKGAAAGAGAAGGTCTTCCCATCCTCATGG	-65.5	-31.63	19	83.3
		CTCTATCMNNAACTCCCATTATTCTCCTGTGGAGATCC	-65.25			81.0
10	46_47insNNK	GGGAGTTCCTNNKGAAAGAGAAGGTCTTCCCATCC	-67.71	-24.53	13	82.2
		MNNAGGAACTCCCATTATTCTCCTGTGGAGATCCTC	-66.06			80.9
11	R117NNK	GCTGGAGNNKTTGAGAAGACTCGATCTCGAAAGG	-64.37	-33.13	18	80.8
		CTTCTCAAMNNCTCCAGCGCTTCTCGCTGTGGTG	-68.14			83.5
12	M8NNK	GATTTTCGACNNKGATGGAGTGCTCATGGACACAG	-65.21	-37.38	19	80.9
		CTCCATCMNNGTCGAAAATCACCGCTTCCATATG	-70.78			79.6
13	P110NNK	CCTCCACANNKCAGCGAGAAGCGCTGGAGAGATTG	-74.45	-36.07	18	84.8
		CTCGCTGMNNTGTGGAGGTTGCGAGCGCGAG	-71.37			85.2
14	E113NNK	CACAGCGANNKGCGCTGGAGAGATTGAGAAGACTCG	-71.16	-39.87	18	84.7
		CCAGCGCMNNTCGCTGTGGTGTGGAGGTTGCGAGC	-80.38			88.6

*Mutated nucleotide is highlighted yellow

Primer properties are represented by Gibbs free energy of individual primer (ΔG_P), of cross dimer between forward and reverse (ΔG_{CD}), and amount of matched base pairs between forward and reverse primers (BPs). ΔG_P is defined as the amount of energy to break down perfect hybridisation of the primer with its complement. Large negative value of ΔG_P represents more specific primer binding (Premier Biosoft, 2016). Similar definition applies for ΔG_{CD} but between forward and reverse primers. Large negative value gives more probability two primers anneal to each other than to DNA template (plasmid). Melting temperature (Tm) is defined as the temperature at which 50% of primer forms stable double helix with its complement (Premier Biosoft, 2016). Calculation of primer's Tm for QuikChange is not the same as regular primer. It follows the formula suggested by (Agilent, 2005). Higher Tm value corresponds to higher primer specificity.

Appendix 3. Kinetic Characterisation Data

Appendix 3.1 Kinetic parameters of all mutants toward G6P generated calculated by SigmaPlot 13. R^2 is fitness factor to Michaelis Menten model. Unit for V_{max} is μmol/min*mg and for K_m is mM. Stdev is standard deviation

Variant	G6P				
	V_{max}	stdev	K_m	stdev	R^2
WT	1.989	0.081	3.316	0.410	0.964
D14P	1.089	0.085	4.371	0.946	0.872
E47D	1.212	0.118	6.113	1.418	0.885
D14P, E47D	0.392	0.007	4.158	0.208	0.995
S166V, S168R	0.243	0.019	3.686	0.792	0.940
S166V, S168K	0.165	0.020	6.967	1.930	0.914
S166V, S168D	1.420	0.247	32.243	7.495	0.988
S166V, S168T	0.190	0.005	3.007	0.294	0.976
S166V, S168L	0.665	0.030	5.617	0.629	0.980
S166V, S168V	0.392	0.018	2.814	0.451	0.937
S166V, S168C	0.128	0.007	2.325	0.461	0.893
S166V, S168P	0.377	0.045	10.354	2.335	0.961
M8A	0.960	0.025	6.012	0.369	0.994
P110A	2.223	0.016	2.970	0.063	0.930
P110A, E47D	2.972	0.369	9.185	2.273	0.948
E113A	0.810	0.010	2.633	0.083	0.956
P46T	3.689	0.100	5.233	0.353	0.992

Appendix 3.1 Kinetic parameters of all mutants toward F6P generated calculated by SigmaPlot 13. R^2 is fitness factor to Michaelis Menten model. Unit for V_{max} is μmol/min*mg and for K_m is mM. Stdev is standard deviation

Variant	G6P				
	V_{max}	stdev	K_m	stdev	R^2
WT	7.611	0.148	2.325	0.106	0.985
D14P	4.324	0.237	5.990	0.788	0.975
E47D	3.870	0.097	4.320	0.303	0.990
D14P, E47D	1.458	0.057	4.456	0.479	0.979
S166V, S168R	0.305	0.013	1.128	0.287	0.774
S166V, S168K	0.473	0.026	4.398	0.671	0.960
S166V, S168D	1.203	0.174	8.151	2.471	0.913
S166V, S168T	0.747	0.067	11.289	1.868	0.980
S166V, S168L	0.841	0.045	1.658	0.376	0.882
S166V, S168V	0.648	0.029	2.715	0.433	0.927
S166V, S168C	0.217	0.009	6.591	0.644	0.987
S166V, S168P	0.467	0.026	3.919	0.647	0.947
M8A	3.018	0.110	4.726	0.460	0.984
P110A	4.513	0.136	3.162	0.314	0.977
P110A, E47D	3.959	0.280	4.087	0.833	0.928
E113A	2.387	0.045	2.417	0.158	0.992
P46T	10.205	0.357	1.647	0.241	0.928

Appendix 4 HTS data

Appendix 4.1 First screening

Y19NNK

Library generated from QC for this mutation gives only 25% of mutants (the remaining was wild type). Two plates were used for library screening albeit four plates should have been used. It was because there were not enough colonies to perform four plates screening. The results from plate 1 (A, C, E) and plate 2 (B, D, F) are presented below. Zero value represents no difference with WT. Total variants in each plate was 80.

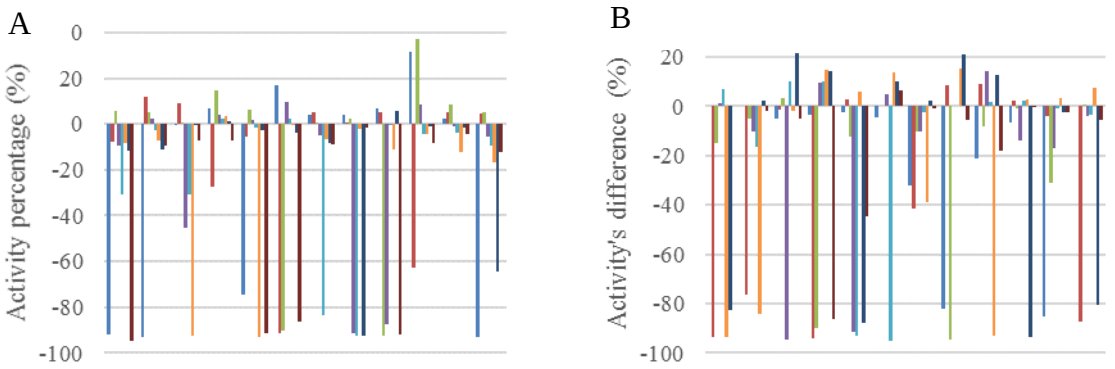

Activity assay of Y19NNK library from plate 1 (A) (SD=6.4%) and 2 (B) (SD=9.6%) toward F6P. Average of activity of WT in plate 1 was 22.6 and in plate 2 was 18.1 ng/min. First screening of Y19NNK library showed that 18 variants appeared to have increased activity toward F6P while there were 58 variants (36.3%) seemed to have decreased activity. The remaining variants (52.5%) were in the range of one standard deviation.

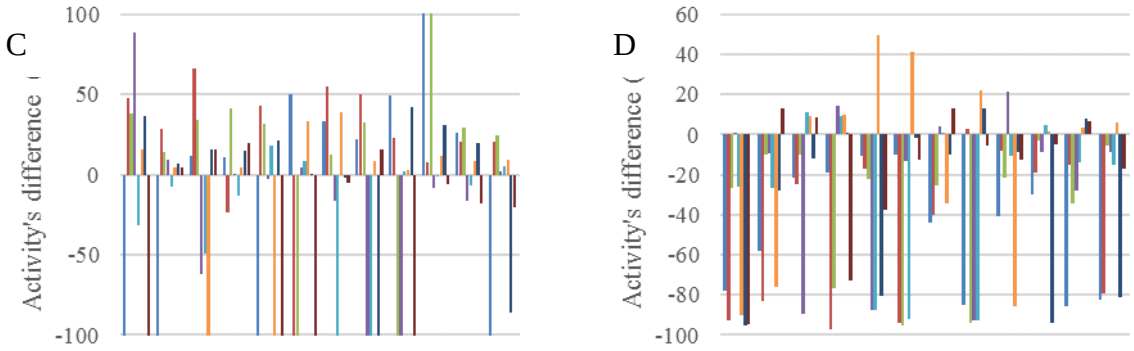

Activity assay of Y19NNK library from plate 1 (C) (SD=9.1%) and 2 (D) (SD=10.4) toward G6P. Average of activity of WT in plate 1 was 5.1 and in plate 2 was 8.8 ng/min. Mutation of this position appeared to give 50 variants (31.3%) increased activity toward G6P while 63 variants (39.4%) seemed to have decreased activity

E

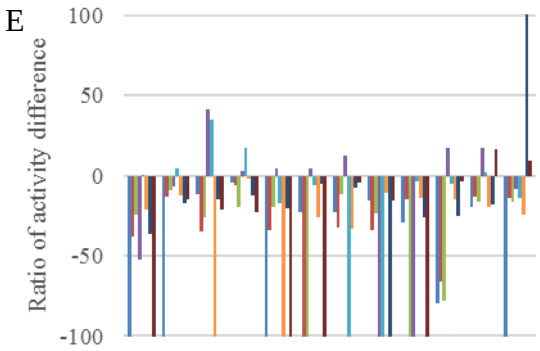

F

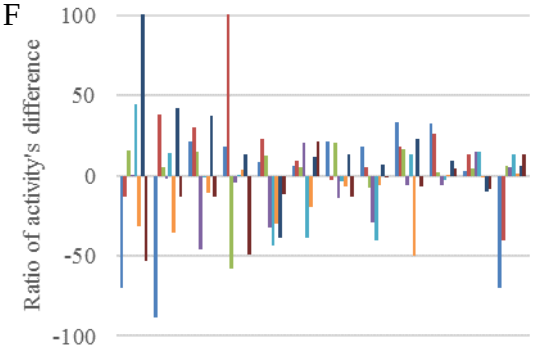

Ratio of activity assay (F6P/G6P) of Y19NNK library from plate 1 (E) (SD=10.8%) and 2 (F) (SD=7.9%). Average of F/G ratio of WT in plate 1 was 4.5 and plate 2 was 2.1. F/G ratio is important parameter to further confirm if increase in activity toward F6P also observed for G6P. It shows that mutation at position 19 (E and F) appeared to give 41 variants (25.6%) higher F/G ratio while 83 variants (51.9%) seemed to have lower F/G ratio.

Results from A-F were used to choose the hits and categorise them to group A, B, or C (explanation is in Result of Second Screening). There were 22 variants picked from 2 plates (160 variants) for second screening. In detail, 6 variants (4%) appeared to belong to group A and 16 variants (10%) appeared belong to group B. There were 2 variants seemed to belong to group D.

E47NNK

Library generated from QC for this mutation gives only 50% of mutants (the remaining was wild type). Two plates were used for library screening. The results from plate 1 (A, C, E) and plate 2 (B, D, F) are presented below. Zero value represents no difference with WT. Total variants in one plate were 80.

A

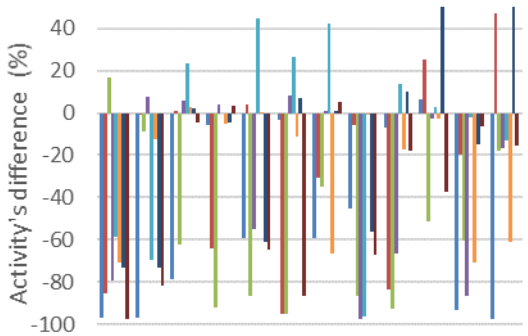

B

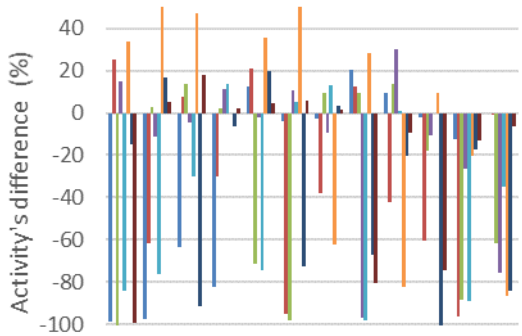

Activity assay of E47NNK library from plate 1 (A) (SD=6.2%) and 2 (B) (SD=10.3%) toward F6P. Average of activity of WT in plate 1 (A) was 14.3 and in plate 2 (B) was 13.4 ng/min. Mutation of this position appeared to give 30 variants (18.8%) increased activity toward F6P while other 95 variants (53.1%) seemed to have decreased activity.

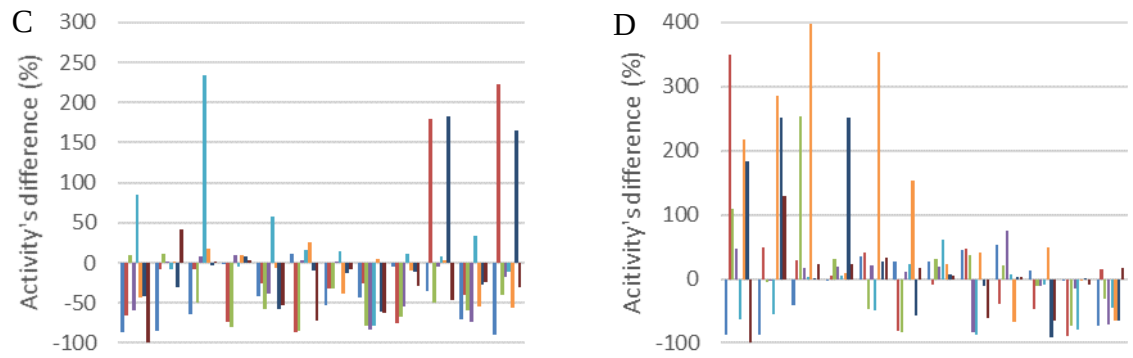

Activity assay of E47NNK library from plate 1 and 2 toward G6P. Average of activity of WT in plate 1 (C) was 2.7 and in plate 2 (D) was 1.9 ng/min. Result for activity toward G6P was slightly difference. Sixty variants (37.5%) appeared to have increased activity while the other 69 variants (43%) seemed to have decreased activity

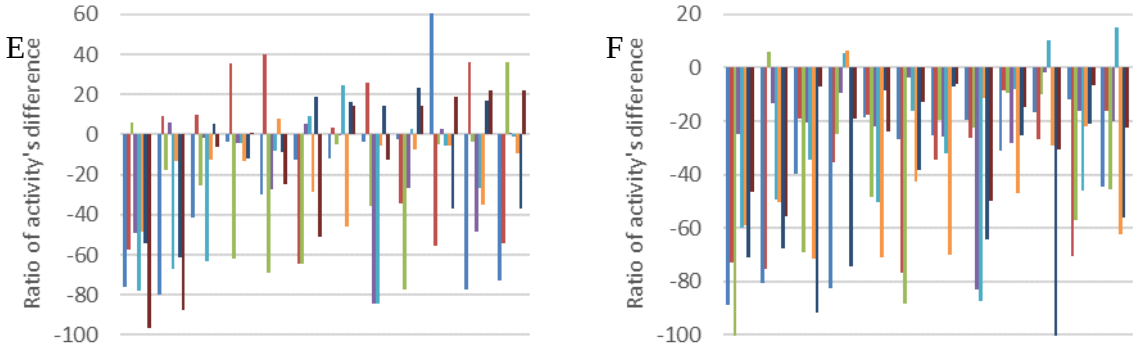

Ratio of activity assay (F6P/G6P) of E47NNK library from plate 1 (SD=12.4%) and 2 (SD=8.2%). Average of F/G ratio of WT in plate 1 (E) was 5.4 and plate 2 (F) was 7.1. Due to higher number of variants that seemed to have increased activity toward G6P than F6P, there were more variants that appeared to have lower F/G ratio. Result of this library indicates 106 variants (66.3%) appeared to have lower F/G ratio compared to only 16 variants (10%) that appeared to have higher F/G ratio. From this library 18 variants were chosen for second screening. In details, 7 variants (4%) appeared to belong to group A while the other 11 (7%) appeared to belong to group B.

E47NNK, D14P

QuikChange™ site directed mutagenesis of these positions was performed using sequence of mutant enzyme (D14P) as template DNA. Library for this mutation had 50% confirmed mutant thus two plates (A, C, E for plate 1 and B, D, F for plate 2) were used. Results of first screening for this library are presented below. Zero value represents no difference with WT. Total variants in one plate were 80.

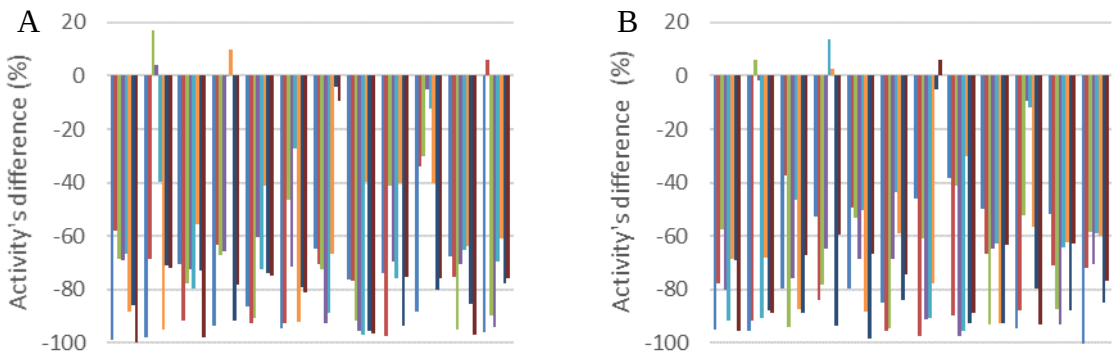

Activity assay of E47NNK, D14P library from plate 1 (SD=9.8%) and 2 (SD=8.7%) toward F6P. Average of activity of WT in plate 1 (A) was 15.5 and in plate 2 (B) was 15.1 ng/min. Additional mutation at position 14 (D14P) to 47's library apparently decreased the activity of enzyme. There were no variants that appeared to have higher activity than wild type, rather all variants from this library showed decreased activity toward F6P

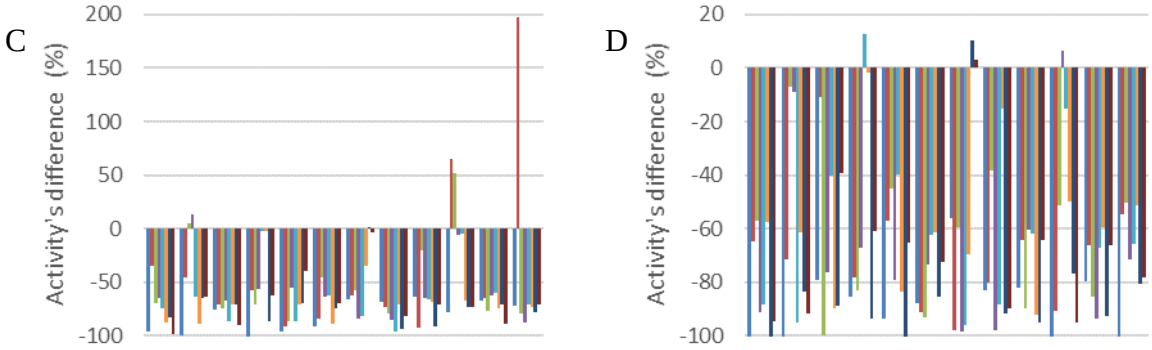

Activity assay of E47NNK, D14P library from plate 1 (SD=6.5%) and 2 (SD=9.9%) toward G6P. Average of activity of WT in plate 1 (C) was 3.6 and in plate 2 (D) was 3.3 ng/min. Similar result was found for G6P. There were only 3 variants (1.9%) that seemed to increase activity toward G6P while others show apparent decreased activity.

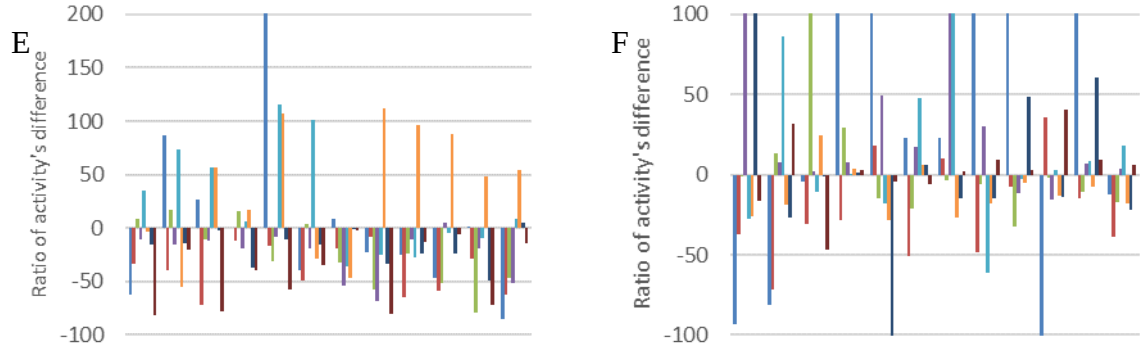

Ratio of activity assay (F6P/G6P) of E47NNK, D14P library from plate 1 (SD=12%) and 2 (SD=10.1%). Average of F/G ratio of WT in plate 1 (E) was 4.2 and plate 2 (F) was 4.6. Although variants from this library almost all showed decreased activity toward both substrates. The effect is not the same for every variant. Results (E and F) show 53 variants (33.1%) appeared to have higher F/G ratio while 72 variants (45%) appeared to have lower F/G ratio. Higher F/G ratio for variants that have decreased activity toward F6P and G6P means that the decrease of activity is much higher for G6P than F6P. Due to no positive

effect of mutation in this library, there were only 3 variants were picked for second screening. All variants seemed to belong to group B.

R117NNK

Library for this mutation only had 75% wild type background so two plates were used for first screening. The first screening results of this library are presented in A, C, E for plate 1 and B, D, F for plate 2. Zero value represents no difference with WT. Total variants in one plate are 80.

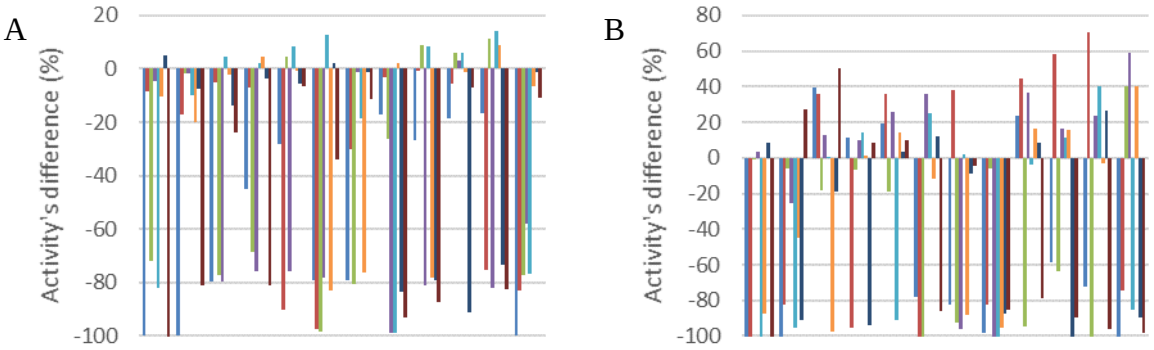

Activity assay of R117NNK library from plate 1 (SD=5.5%) and 2 (SD=14%) toward F6P. Average of activity of WT in plate 1 (A) was 22.2 and in plate 2 (B) was 11.2 ng/min. There were 32 variants (19.4%) from this library appeared to have increased activity toward F6P while 93 variants (58.1%) appeared to have decreased activity.

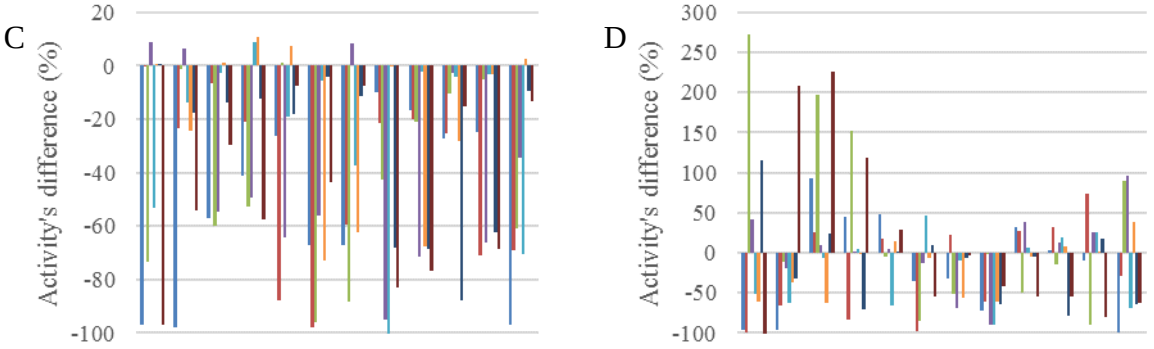

Activity assay of R117NNK library from plate 1 (SD=8%) and 2 (SD=12.7%) toward F6P. Average of activity of WT in plate 1 (C) was 10.3 and in plate 2 (D) was 4.6 ng/min. Similar to F6P, there were 29 variants (18.1%) that appeared to have increased activity, mainly from plate 2 (D) while 94 variants (58.9%) seemed to have increased activity.

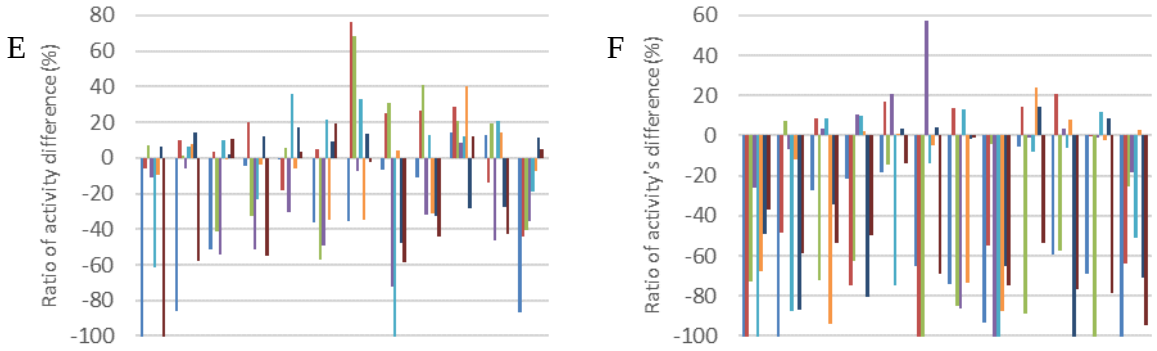

Ratio of activity assay (F6P/G6P) of R117NNK library from plate 1 (SD=7.8%) and 2 (SD=5.8%). Average of F/G ratio of WT in plate 1 (E) was 4.3 and plate 2 (F) was 2.4. Result of F/G ratio shows there were 39 variants (24.4%) and 87 (54.4%) that appeared to have increased and decreased F/G ratio, respectively. From the analysis of A to F, there were 21 variants were picked for second screening. In detail, 13 variants (8%) appeared to belong to group A, 6 variants (4%) appeared to belong to group B, and 2 variants (1.3%) appeared to belong to group C. There were 2 variants (1.3%) that appeared to belong to group D, but these variant were not of interest for further screening.

46_47insMet

At first, 46_47insNNK was aimed to be one of the libraries developed. However, two times QC (one was ordinary QC, the other one with higher primer concentration and 46_47insMet template) were not successful to develop the library, first QC was only successful to insert methionine to position between 46 and 47.

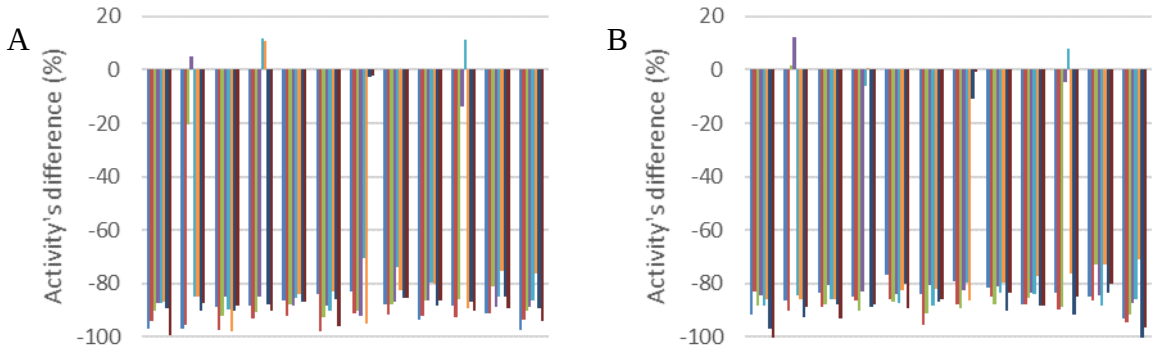

Activity assay of 46_47insMet from 1 plate toward F6P (A) and G6P (B). Zero value represents no difference with WT. Total variants in one plate are 84. Average of activity of WT toward F6P was 14.8±12.1% and toward G6P was 4.5±6.5% ng/min. Methionine insertion gave no activity for F6P and G6P. A and B show negative values for all variants of this mutation.

M8NNK

Similar to P46NNK library, quality of M8NNK library was also low (25%) thus 4 plates: plate 1 (A, E, I, M), plate 2 (B, F, J, N), plate 3 (C, G, K, O), plate 4 (D, H, L, P) were used. Four negative controls containing only media were used for each plate. Zero value represents no difference with WT. Total variants in one plate are 84

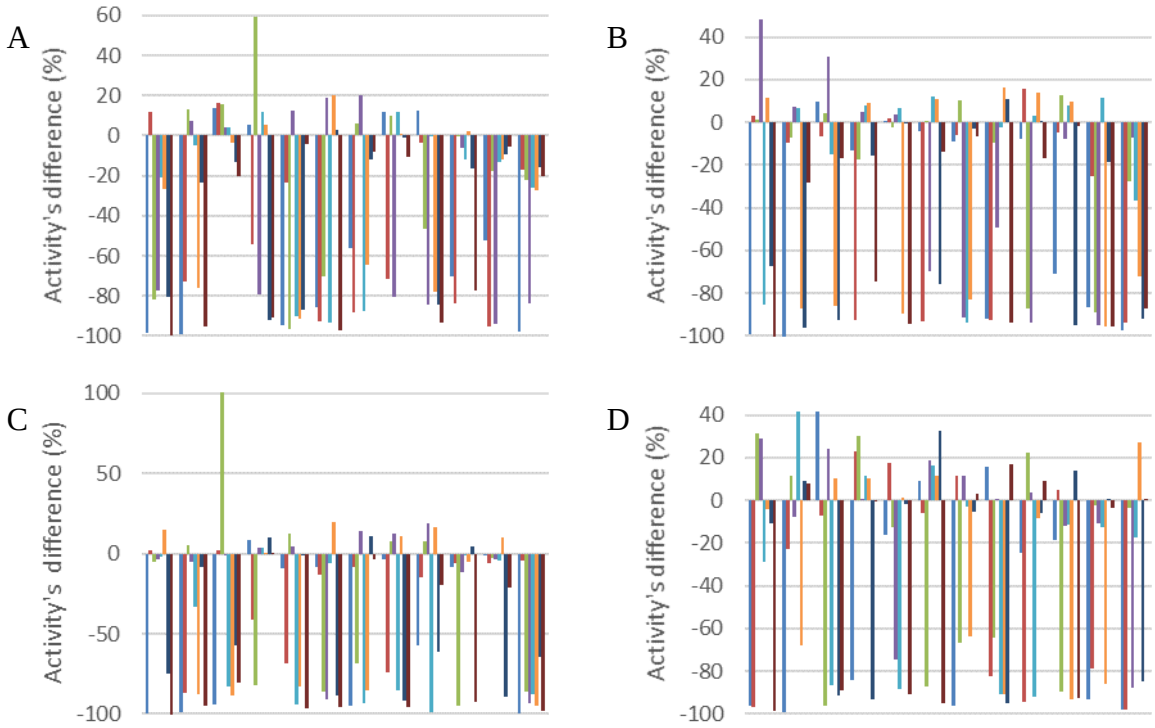

Activity assay of M8NNK library from 4 plates toward F6P. Average of activity of WT in plate 1 (A) was 15.6±10.6%, in plate 2 (B) was 16.7±7.7%, in plate 3 (C) was 14.4±6.7%, and in plate 4 (D) was 9.6±10.2% ng/min. Mutation at position 8 gave 45 variants (13.4%) apparent increased activity while 185 variants (55.1%) appeared to have decreased activity toward F6P.

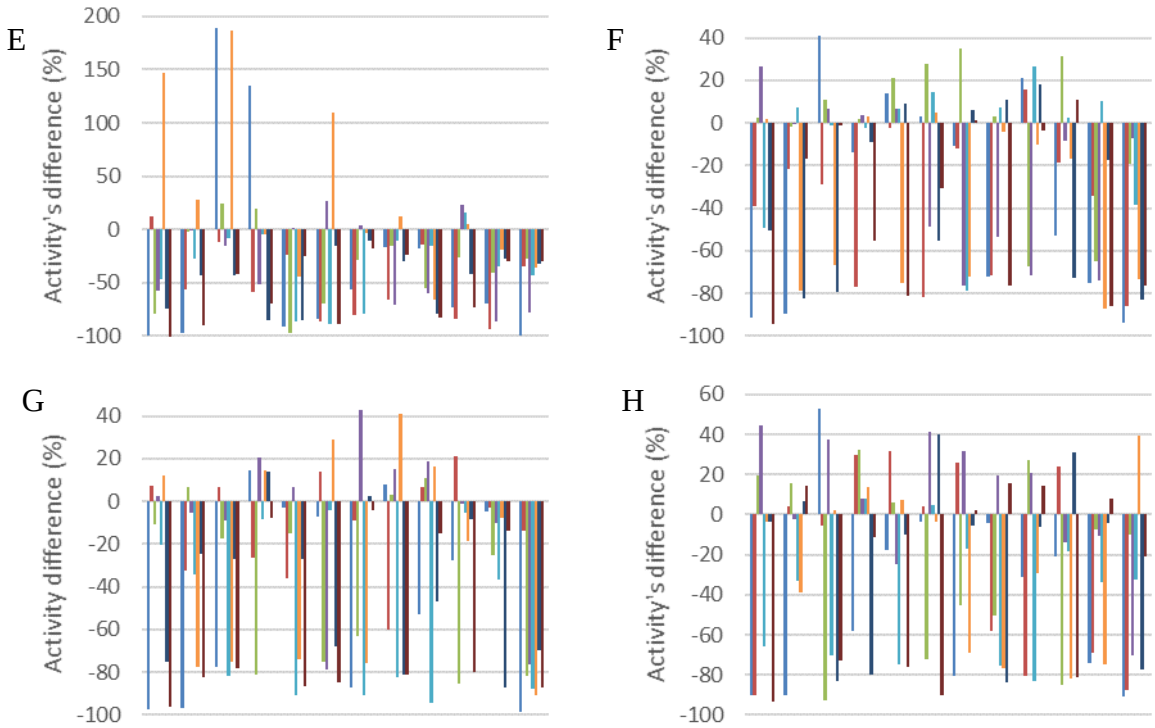

Activity assay of M8NNK library from 4 plates toward G6P. Average of activity of WT in plate 1 (E) was 13.5±10.8%, in plate 2 (F) was 14.4±11%, in plate 3 (G) was 17±7.1%, and in plate 4 (H) was 15.5±8.1% ng/min. Activity of these mutants shows similar pattern. Sixty-

four variants (19.0%) appeared to have increased activity while 192 variants (57.1%) appeared to have decreased activity.

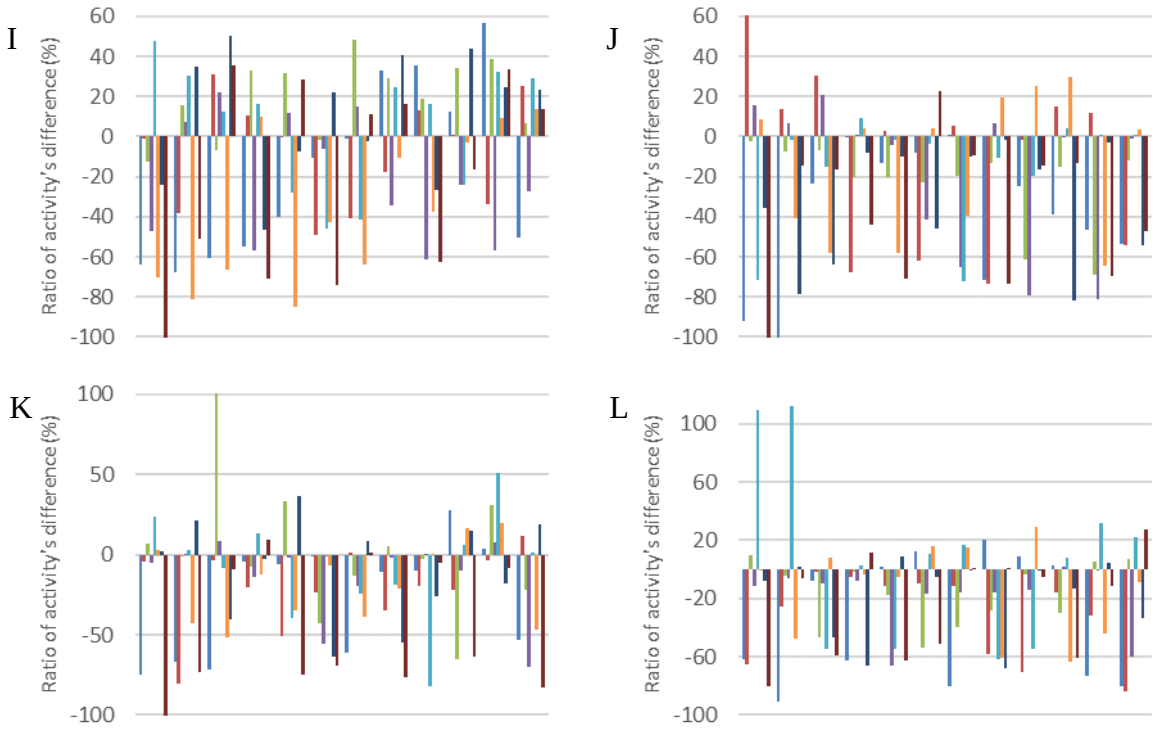

Ratio of activity assay (F6P/G6P) of M8NNK library from 4 plates. Average of F/G ratio of WT in plate 1 (I) was 2.7±8.3%, plate 2 (J) was 3.6±5.7%, in plate 3 (K) was 2.6±10.9%, and in plate 4 (L) was 3.2±7.8% ng/min. Although percentages of increase and decrease activity are similar between F6P and G6P, there are still many variants show deviating F/G ratio. There were 69 variants (20.5%) appeared to have higher F/G ratio and 154 variants (45.8%) appeared to have lower F/G ratio. This result shows that most variants that showed apparent increase activity toward F6P were not the same to variants that showed apparent increase activity toward G6P. Analysis of A to L resulted in in 11 variants were picked for second screening from 336 variants. In detail, 5 variants (1.5%) appeared to belong to group A, 4 variants (2%) appeared to belong to group B, and 2 variants (0.6%) appeared to belong to group C. One variant appeared to show activity that falls in group D, but this variant was not picked for further screening.

P110NNK

QC of this mutation gave 75% mutants thus there were two plates used for screening. Similar to three previous libraries, 4 negative controls containing media only were used. First plate is A, C, E and second is B, D, F. Zero value represents no difference with WT. Total variants in one plate are 84.

A

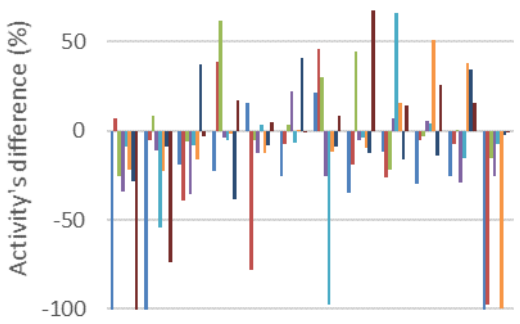

B

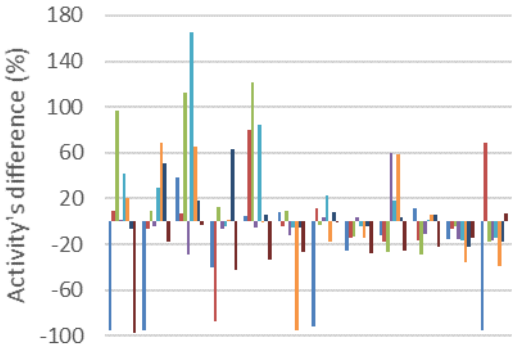

Activity assay of P110 library from plate 1 (A) and plate 2 (B) toward F6P. Average of activity of WT in plate 1 was 13.6±7.9% and in plate 2 was 12±6.9% ng/min. Mutation at 110 gave 39 variants (23.2%) that appeared to have increased activity and 84 variants (44.0%) that appeared to have decreased activity toward F6P.

C

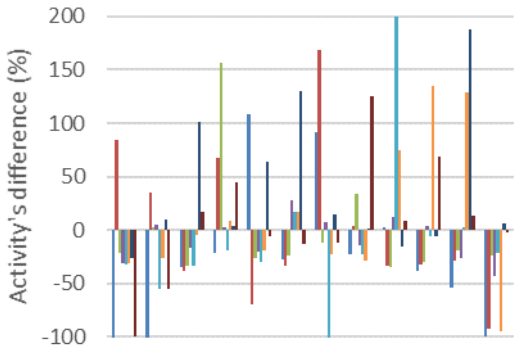

D

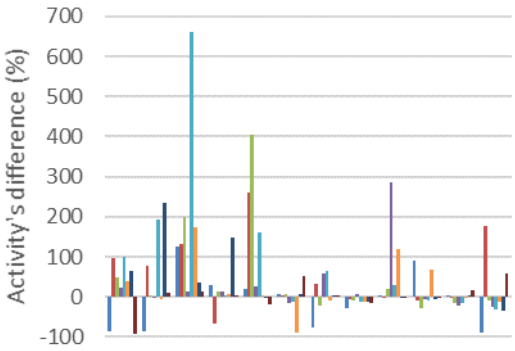

Activity assay of P110 library from plate 1 (C) and plate 2 (D) toward G6P. Average of activity of WT in plate 1 (C) was 4±11% and in plate 2 (D) was 3.0±5.8% ng/min. Different result was observed for activity toward G6P. There were more variants that appeared to have increased activity (64 variants or 38.1%) than decreased activity (55 variants or 29.2%).

E

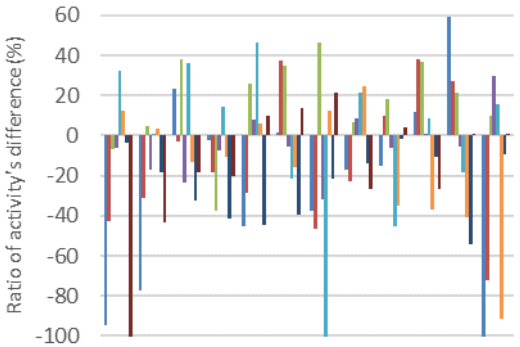

F

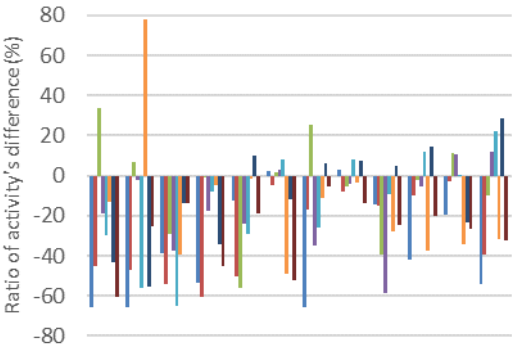

Ratio of activity assay (F6P/G6P) of P110NNK library from plate 1 (E) and plate 2 (F). Average of F/G ratio of WT in plate 1 (E) was 3.5±15.3% and in plate 2 (F) was 4±7.4% ng/min. The results (E and F) shows there were more variants (84 variants or 50%) that appeared to show lower F/G ratio than the variants (28 variants or 16.7%) that appeared to show higher F/G ratio. Lower F/G ration means the increased activity is better for G6P than F6P compared to each activity of WT enzyme. It could also mean the decreased activity is more severe for F6P than G6P.

In total only 4 variants were picked for second screening. Two of them appeared to belong to group A and the remaining appeared to belong to group B and C each. Subsequent analysis shows that there were 24 variants (14%) that appeared to belong to group D. These variants were not considered for further screening.

Appendix 3.2 Second screening

E47NNK

There were 18 variants were picked for this library. The result of the screening is presented in below

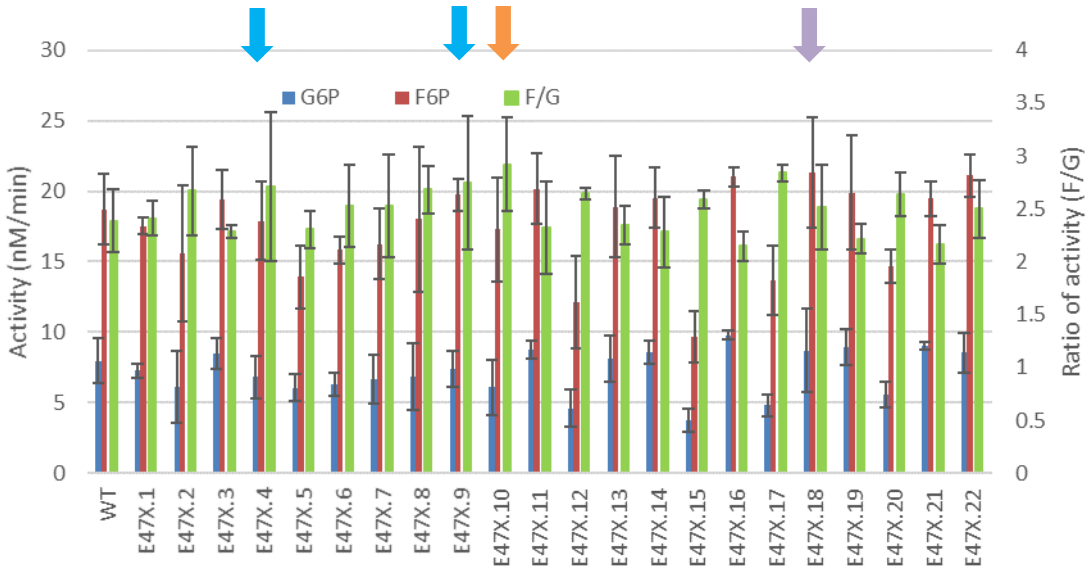

Result of second screening from variants picked from first screening of E47NNK library. Arrows represents variants that were picked for third screening. In general, result above shows there were no significant different based on F/G ratio amongst variants. E47X.17 variant showed slight increase in F/G ratio but its activity toward F6P decreased so this variant was not a good candidate for further screening. Analysis for second screening was then based on assumption that there is possibility if one colony that had been picked from first screening bearing more than one type of plasmid thus that colony would develop to more than one type of cell producing different kind of mutant enzymes. With this assumption, each replicate of each variant from this second screening could be different cells producing different mutant enzymes thus variants that showed high standard deviation were of interest. One replicate from E47X.4 and E47X.9 appeared to belong to group A. From previous screening E47X.4 appeared to belong to group B while E47X.9 appeared to belong to group A. Other replicate from E47X.10 and E47X.18 were of interest too as it appeared to belong to group B and C respectively. In previous screening, E47X.10 appeared to be in group B while E47X.18 appeared to be in group C. This result shows there was change between first and second screening.

Y19NNK, E47NNK & D14P

There were 22 variants from Y19NNK library and 3 variants from E47NNK & D14P were picked from first screening. The result of second screening is presented below

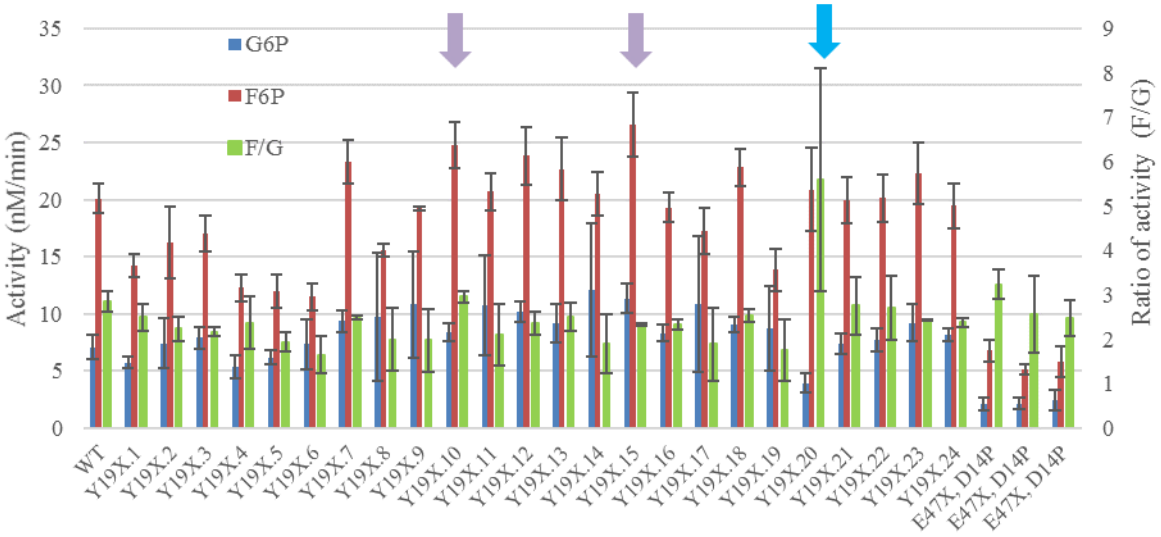

Result of second screening from variants picked from first screening of Y19NNK and E47NNK & D14P library. Arrows represents variants that were picked for third screening. Similar to previous library, there was no significant difference if F/G ratio was considered. The same assumption was used to choose variants for the next screening. Y19X.10 and Y19X.15 had shown activity that appeared to belong to group B but in second screening, their activity appeared to belong to group C. One replicate for each variant was chosen for third screening. Y19X.21 from result above showed very high standard deviation. One replicate of this variant showed activity that appeared to belong to group A. This variant had shown activity that appeared to belong to group A in the first screening.

R117NNK

There were 22 variants picked from first screening for this library. The result of second screening is presented below

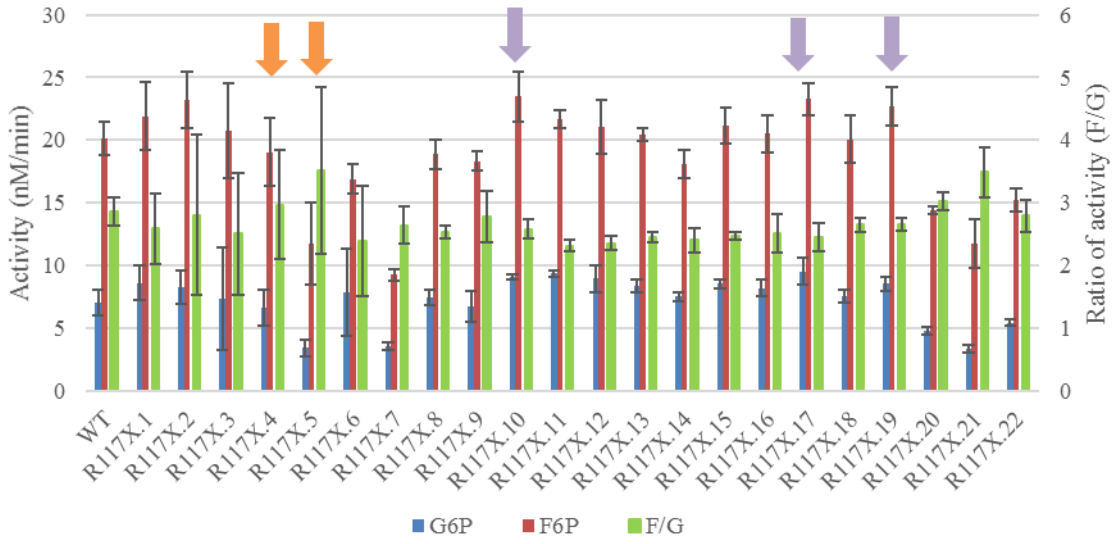

Result of second screening from variants picked from first screening of R117NNK library. Arrows represents variants that were picked for third screening. Based on the result above, variant R117.21 showed significantly higher F/G than wild type, but its activity toward F6P was very much decreased thus this variant was not considered for further screening. F/G ratio

of other variants seemed to not have significant difference with wildtype. As a result, the same assumption as mentioned earlier was used to pick promising variants for further screening. One replicate of R117X.4 and R117X.5 appeared to have activity that belongs to group B thus these variants were picked for further screening. All of them appeared to belong to group B in the first screening. One replicate from R117X.10, R117X.17, and R117.19 appeared to show activity that belong to group C. In the first screening each of them belong to group A, C, B respectively. Only the replicate from variant R117X.17 appeared to show constant behaviour.

M8NNK, P110NNK

There were 11 variants picked from first screening for M8NNK library and 4 variants from P110NNK library. The result is presented below

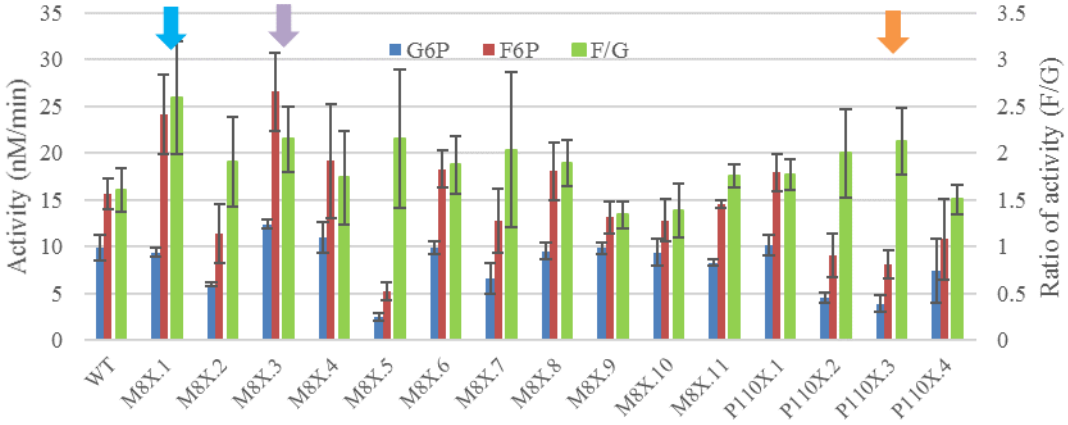

Result of second screening from variants picked from first screening of M8NNK and P110X library. Arrows represents variants that were picked for third screening. Variant M8X.1 and M8X.3 showed higher F/G ratio than wild type. Both of them also showed increased activity toward F6P thus they were of interest for further screening. In the first screening, both of them appeared to belong to group C. However, in the second screening, M8X.1 showed activity that appeared to belong to group A. P110X.3 variant showed slightly higher F/G ratio, this variant was chosen for the third screening although these variants showed decreased activity toward F6P.

Appendix 3.3 Third screening

This step was to make sure there were no either cells bearing more than one type of mutant enzymes or different cells observed as one activity in one well. This step included plasmid purification and transformation to eliminate those two possibilities.

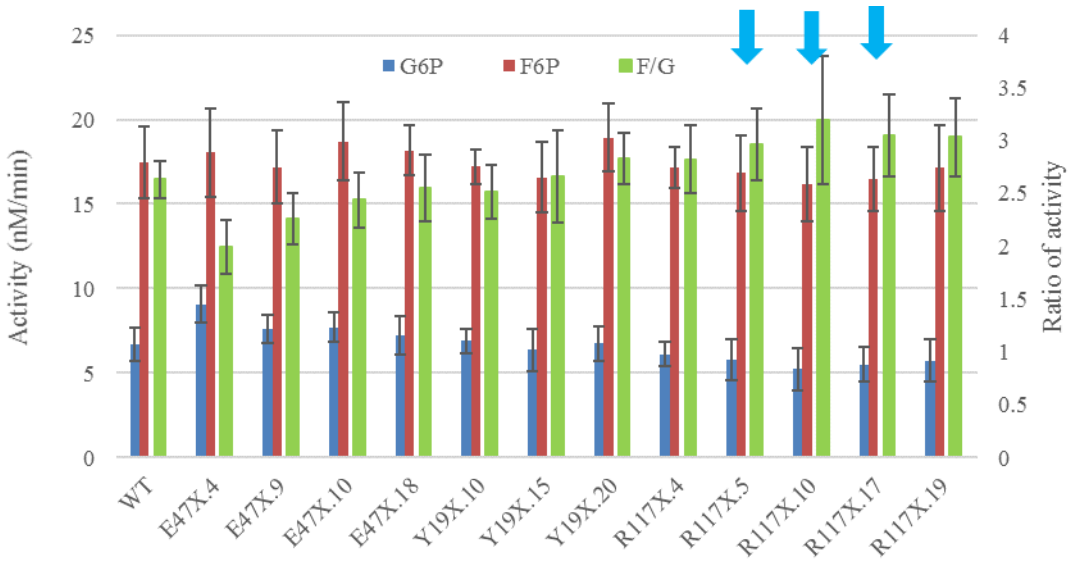

Result of third screening from second screening of E47NNK, Y19NNK, and R117NNK libraries. Arrow represents variants picked for sequencing. Third screening results showed no significance difference in F/G ratio. Then previous approach was used to decide variants that were sent for sequencings. One replicate from R117X.5 and R117X.17 showed higher F/G than wild type thus those replicates were inoculated in LB media for plasmid production. Three replicates out of six of R117X.10 showed higher F/G ratio and appeared to have increased activity toward F6P as a result one of them was also inoculated in LB for plasmid production. Sequencing result showed all of the variants sent were wild type.

Appendix 5 Biochemistry data

5.1 Standard curve for malachite green (P I assay)

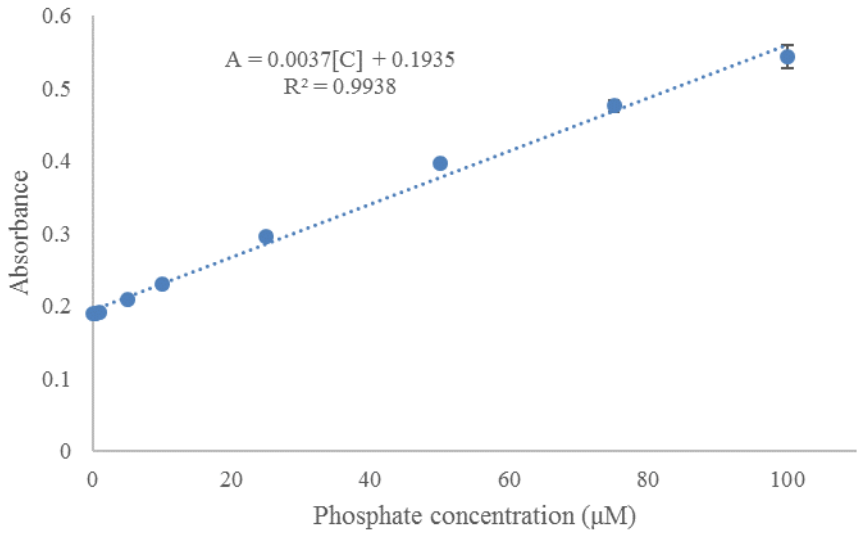

100 µM corresponds to 2 nmol (20 µl of sample used).

5.2 Standard curve for ascorbic acid based method (PII assay)

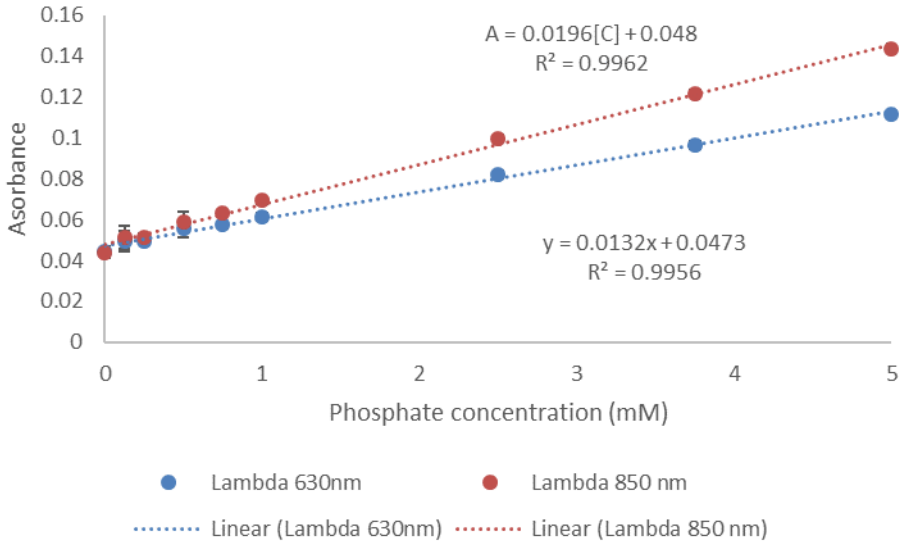

5 mM corresponds to 150 nmol (30 µl of sample used).

5.3 Standard curve for ascorbic acid pH 2.5 (P III assay)

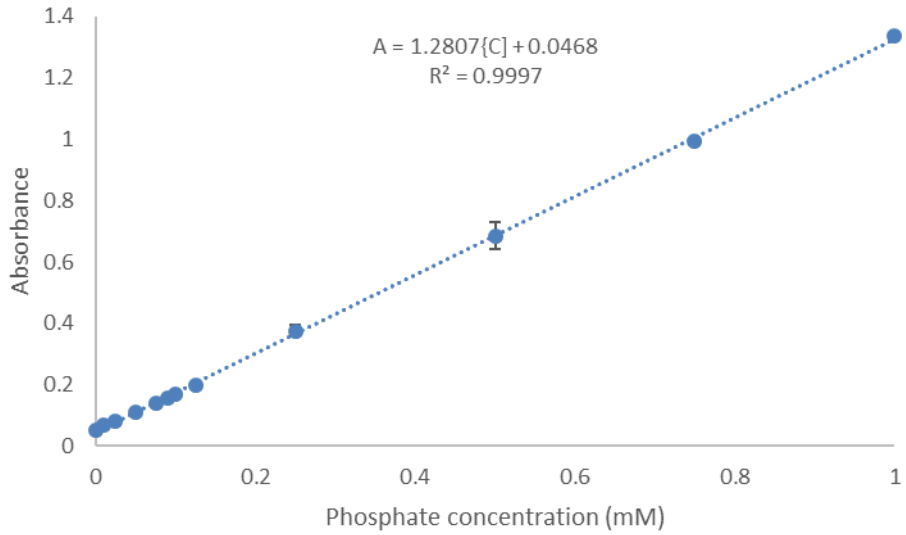

1 mM corresponds to 30 nmol (30 µl of sample used)

5.4 Standard curve for increased ions

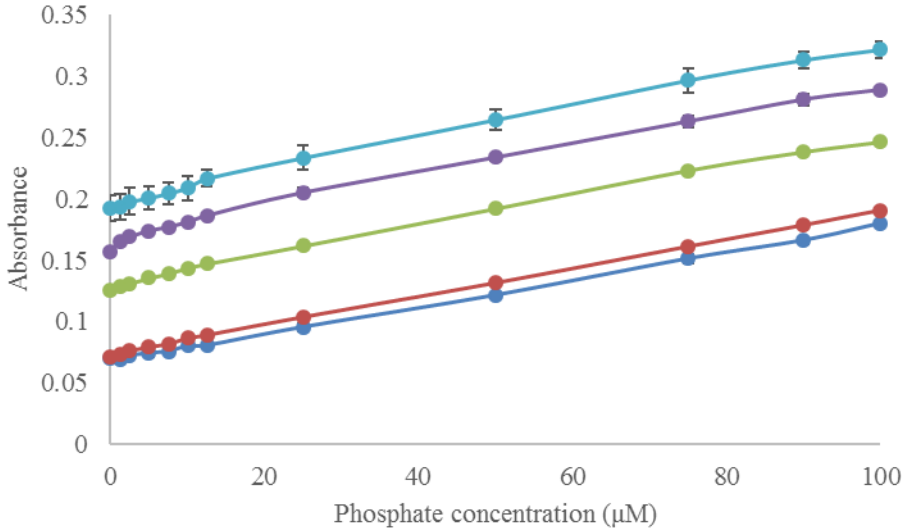

Line legend	Zn^{2+} (mM)	Mo^{6+} (mM)	R^2
Dark blue	30	20	0.9995
Red	60	40	0.9997
Green	90	60	0.9984
Purple	120	80	0.9960
Cyan	150	100	0.9977

100 µM corresponds to 3 nmol (30 µl of sample used).